Technical Report No. 32-700

Ranger VII

Part I. Mission Description and Performance

JET PROPULSION LABORATORY
CALIFORNIA INSTITUTE OF TECHNOLOGY
PASADENA, CALIFORNIA

December 15, 1964

Technical Report No. 32-700

Ranger VII

Part I. Mission Description and Performance

H. M. Schurmeier
Ranger *Project Manager*

JET PROPULSION LABORATORY
CALIFORNIA INSTITUTE OF TECHNOLOGY
PASADENA, CALIFORNIA

December 15, 1964

CONTENTS

CONTENTS (Cont'd)

FIGURES

FIGURES (Cont'd)

TABLES

PREFACE

This document constitutes the formal report of the *Ranger VII* mission, the second in the Block III series, whose flight phase lasted from July 28 to July 31, 1964.

Part I of the report is a technical description and an evaluation of the performance of the various systems and other elements comprising the *Ranger* project. Part II consists of the analyses and interpretations by the Experimenters of the photographic results of the mission.

Part I brings together the reports of a great number of individual efforts. Some of the content of the report was drawn from other published reports, a general list of which is given in the Bibliography. The greater portion, however, was prepared by the various cognizant engineers and other Jet Propulsion Laboratory members of the *Ranger* team. The report was compiled and edited under the direction of Mr. Gordon P. Kautz.

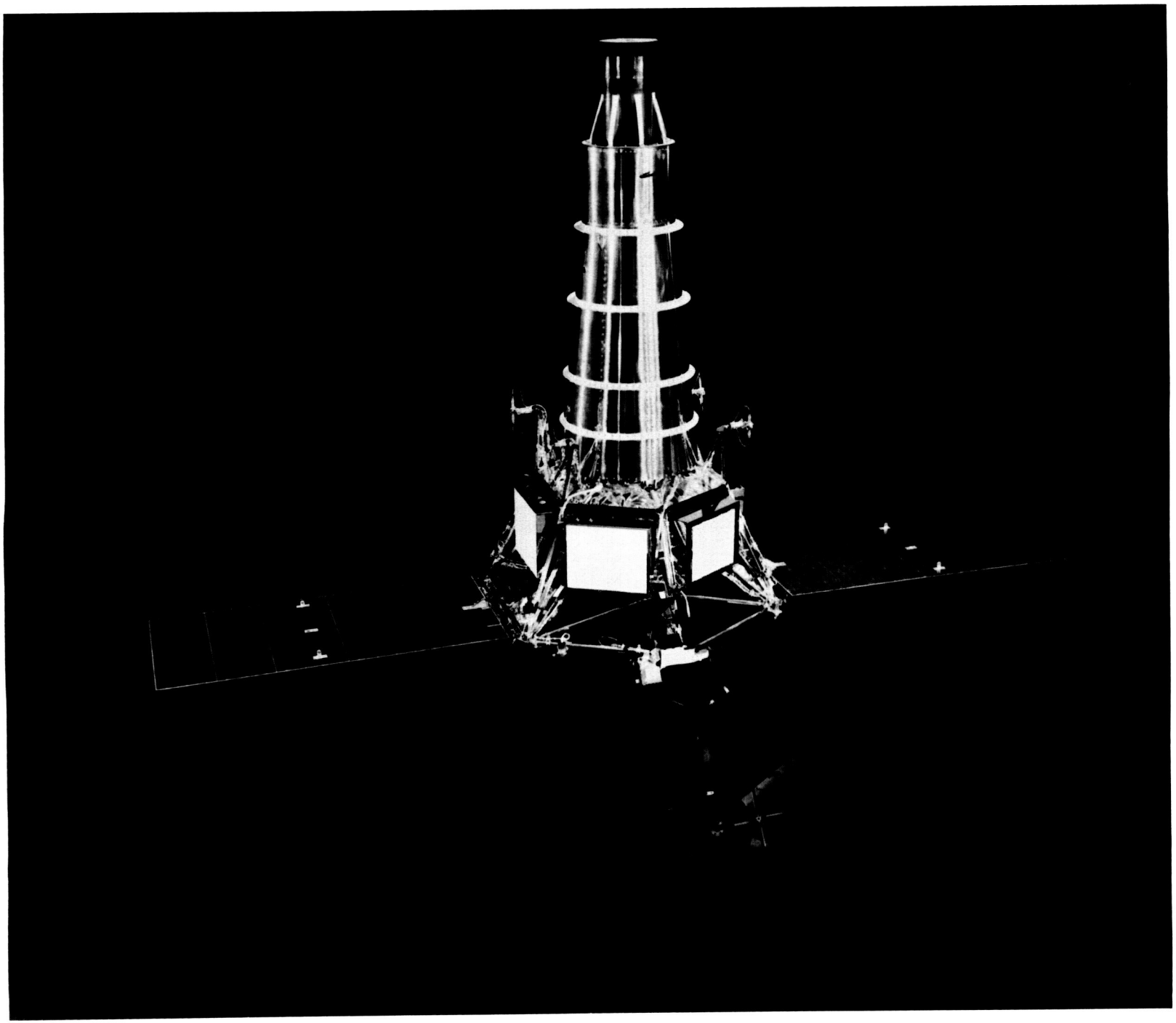

I. INTRODUCTION

Ranger VII was launched August 28, 1964 at 1650:08 GMT[1] from the Air Force Eastern Test Range, Cape Kennedy (ETR). The spacecraft was boosted by the vehicle combination of *Atlas* 250 D and *Agena B* 6009. The ETR downrange tracking and telemetry stations and computational facilities supported the early portion of the flight. DSIF stations 51 and 59 (Africa), 42 (Australia), and 11 and 12 (Goldstone, California) supported the space flight operations, which were conducted from the Space Flight Operations Facility at JPL.

The mission objective was to obtain television pictures of the lunar surface, of resolution at least an order of magnitude better than that of Earth-based photography, for the benefit of scientific knowledge and of the U.S. manned lunar program. This requirement was met.

A. Mission Events

The launch on July 28 was nominal after a countdown with no unscheduled holds. The *Atlas* and *Agena* vehicles performed within their tolerances and injected the spacecraft on a trajectory to impact the back side of the Moon.

[1]GMT times will be used in this report. For reference, liftoff occurred at 9:30 AM, PDT, or 11:50 AM, EST; impact occurred at 1325:49 GMT (also called "Z time") or 625:49 PDT.

Initial Sun acquisition occurred well within the nominal time even though the spacecraft was in the Earth's shadow when the CC&S initiated the Sun acquisition sequence. Earth acquisition required some 23 min after the sequence was initiated and was normal in all respects.

The largest rubble-free mare that was the proper distance from the terminator and reasonably close to the equator (the most preferred region for this day as designated by the Experimenters) was selected as the target area. The necessary midcourse maneuver sequence was performed over and commanded by the Goldstone Tracking Station. Both roll and pitch controlled-duration maneuver were as commanded, as was the midcourse-motor burn duration. Approximately half the spacecraft maneuver capability was employed, some 85% of the applied velocity impulse being used for flight-time correction. Impact data indicated the following comparisons:

Targeting Parameters	*Planned*	*Actual*
Impact time, GMT	1325:30	1325:49
Longitude, deg	−21.0	−20.67
Latitude, deg	−11.0	−10.70

The Sun and Earth reacquisition sequences following the midcourse maneuver also occurred well within the nominal times, with Earth reacquisition being accomplished almost instantly as predicted.

Due to the geometry of the trajectory at lunar encounter, a terminal maneuver was not required; however, to take advantage of an additional command to turn on the television cameras the terminal sequence counter was initiated. An inhibit command was transmitted to the spacecraft to prevent maneuver information from reaching the Attitude Control Subsystem.

The TV back-up clock, preprogrammed to turn on the F cameras in warmup at separation plus 67¾ hr, performed as designed, and the F chain went to full power some 17 min before impact, transmitting excellent video. Following this, the central computer and sequencer (CC&S) commanded P-camera warmup as programmed, and similarly at the designated time excellent P channel video was received, starting about 14 min before impact. After transmitting some 4304 pictures to Earth the *Ranger VII* spacecraft impacted the lunar surface at 1325:49 GMT on 31 July 1964.

Flight events are tabulated in Appendix A.

B. Project Background

Ranger VII was the second mission of Block III of the *Ranger* Project. Basic elements of the lunar impact mission include:

1. *Atlas/Agena* launch, using a parking-orbit ascent trajectory.
2. Attitude-stabilized spacecraft employing solar power, and capable of a midcourse maneuver and high-gain directional communications.
3. World-wide tracking, telemetry and command facility.
4. Integrated space-flight operational control, computation and data handling.

Block I consisted of two test missions which were designed as non-lunar-oriented engineering development flights for verification of the parking-orbit launch concept, and soundness of the spacecraft design. Both flights experienced launch-vehicle failures; the spacecraft remained in their parking orbits as low-altitude Earth satellites, which permitted the testing of some spacecraft design elements, and the obtainment of some scientific data, but the test objectives were not met.

In Block II, a lunar rough-landing capsule (incorporating a seismometer experiment) with its retro-propulsion system, and two lunar-approach scientific instruments were used in conjunction with the basic spacecraft bus. An approach television camera was included. The three Block II spacecraft were sterilized. Both spacecraft design adequacy and launch vehicle performance were successfully demonstrated, but, unfortunately, on separate attempts. The *Ranger III* mission demonstrated spacecraft midcourse maneuver, attitude control, and communications capabilities, but was unable to impact the Moon. Missions *IV* and *V* had satisfactory vehicle performance: *Ranger IV* impacted the Moon, but the spacecraft had failed early in the flight; the *Ranger V* spacecraft also malfunctioned early in the flight.

Ranger Block III consists of four missions, with a new payload comprised of a six-camera television subsystem for operation during the last 10 to 15 min before impact on the Moon. The first mission, *Ranger VI*, performed eminently satisfactorily throughout the flight up to the terminal phase, when the television system failed to operate. A number of minor spacecraft-bus and major TV-subsystem modifications were made (Appendix B). The second mission, *Ranger VII*, was successful.

C. Project Description

The effort in support of the *Ranger VII* mission was organized in four systems: Launch Vehicle (including launch facilities); Spacecraft; Space Flight Operations; and Deep Space Network.

1. Launch Vehicle System

The function of the Launch Vehicle System was to place the *Ranger* spacecraft on a prescribed lunar-transfer trajectory. Launch was conducted from the Air Force Eastern Test Range (ETR), Cape Kennedy, Florida, by Goddard Space Flight Center Launch Operations (GLO). The *Atlas D* first stage, No. 250 D, was manufactured by General Dynamics/Astronautics and procured by USAF Space Systems Division for the Lewis Research Center, the Launch Vehicle System Manager. The *Agena B* stage, No. 6009, was manufactured by Lockheed Missiles and Space Company, under contract to LeRC.

2. *Ranger* Spacecraft System

The requirement placed upon the spacecraft was to perform the functions necessary to deliver the cameras to the proper lunar encounter geometry with the necessary operating environment and transmit the required video. These spacecraft functions included the complex activities associated with launch, cruise, midcourse maneuver, and terminal maneuver. The TV subsystem was designed and manufactured under JPL contract by RCA's Astro-Electronics Division.

3. Space Flight Operations

The function of the Space Flight Operations system was to conduct and control the mission on Earth: to use the tracking and telemetry data in determining flight path and spacecraft performance, and to prepare the necessary commands for transmission to the spacecraft.

4. Deep Space Network

Consisting of a group of large tracking stations at Goldstone, California; Woomera, Australia; and Johannesburg, South Africa; the Space Flight Operations Facility at JPL, and the communication links binding these elements together, the Deep Space Network had the function of providing tracking of and communication with the spacecraft throughout the mission, and making original data recordings for analysis.

The relation of the various project elements supporting the *Ranger VII* mission is sketched in Fig. 1.

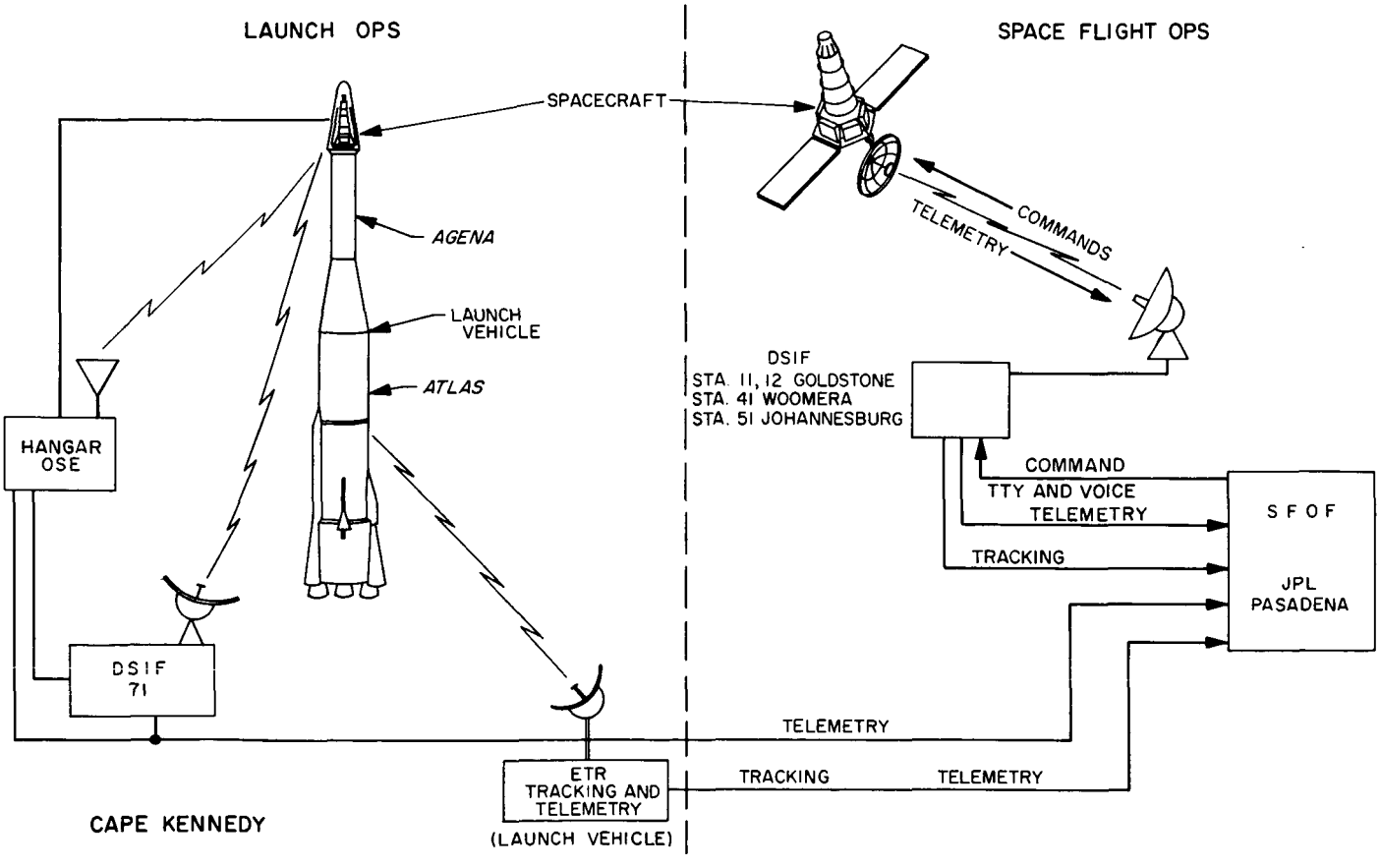

Fig. 1. *Ranger* system elements

II. LAUNCH PREPARATIONS AND OPERATIONS

A. Spacecraft Prelaunch

The *Ranger VII* spacecraft was assembled, tested, and inspected at JPL, Pasadena, and shipped to Cape Kennedy on January 29, 1964. Following the *Ranger VI* failure, the spacecraft bus was returned to JPL for minor rework, and the TV subsystem was sent to RCA and reworked. A summary of the redesign implemented at this phase is given in Appendix B.

Following the rework phase, assembly and system tests were reperformed at JPL. The microscopic inspection covered only selected areas. The spacecraft was then shipped to Cape Kennedy for final assembly, spacecraft system and integration testing, and launch.

1. System Testing

A mission verification test consisting of a preliminary run, a 66-hr high-temperature mission test, and a 66-hr low-temperature mission test, was accomplished at the JPL 25-ft space simulator.

A test using the RF link was then set up in the chamber. A non-vacuum pre-run showed that two TV cameras experienced a form of RF interference while radiating from the high-gain antenna. This was not expected to compromise the RF-link test, which was continued. The spacecraft was disconnected from ground control, the chamber door was sealed, and direct-access cables were removed from the spacecraft to simulate as near a flight condition as possible. All tests were satisfactorily conducted. The TV operation was normal throughout the maneuver sequence. The RF interference reported at ambient environment was also noted for this test phase.

The spacecraft was removed from the chamber and suspended from overhead cables, and the antenna was run from a nested position to about 150 deg with the TV subsystem in the full-power mode to ensure that the RF interference noted during the Space Simulator testing would not be a problem under free-space radiation conditions. Evaluation of the pictures which were recorded showed normal spacecraft operation throughout the expected range of high-gain antenna deployment.

Another new test, designed to examine the safety of operating the TV in full power in the Explosive Safe Area at ETR, was performed with the spacecraft mounted on a fixture with special RF monitor leads in the midcourse-motor squib locations. Measurements of the absorbed energy at the squib locations with the TV subsystem operating in the full-power mode showed results similar to those obtained with the Proof-Test-Model (PTM) spacecraft in the same test configuration. An evaluation of the test results indicated that it was safe to operate the TV in full power with live pyrotechnics in the midcourse location.

A backup functions test was performed; all spacecraft operations were normal. The attitude-control jet vane angles were recalibrated. An attitude-control-valve leak-rate test showed that one valve was leaking in excess of 150 cm^3/hr, and the valve was replaced.

The spacecraft was removed from the test stand and prepared for shipment. It was shipped June 17 and arrived at ETR on June 21.

2. ETR Operations

The spare TV subsystem was tested to verify proper functioning of the operational support equipment. The midcourse motor was tested in the explosive safe area for high-pressure leakage. A leak was detected at one of the valve seals at a pressure of 3300 psi; this seal was replaced. A backup functions system test on June 25 showed normal operation for all backup command functions. A system test indicated normal spacecraft operation. The only problems detected during these tests were found to originate in the operational support equipment. These problems were corrected.

A review of the computer/teletype data reduction showed that the outputs for the TV subsystem and the spacecraft low-rate telemetry measurements did not represent actual spacecraft performance. These data-handling problems were solved by cognizant personnel.

An RF link test was performed utilizing spacecraft batteries. All spacecraft direct-access connectors were removed in order to simulate flight operations. Commands furnished by space flight operations personnel were used for both the midcourse and terminal maneuvers. Spacecraft performance throughout the sequence was normal.

Results of testing the spacecraft in the Explosive Safe Area were satisfactory. A precountdown test run showed

a TV RFI problem and DSIF 71 reported discrepancies with the space loss measurements and varying signal strength. An RFI test was performed with all agencies participating. The results indicated that RFI would not be a problem during the launch countdown, and normal spacecraft performance was noted.

A countdown test to approximately T − 100 was run to verify that all equipment was ready for the joint flight acceptance composite test (J-FACT). Normal spacecraft operations were indicated. A record evaluation period on July 9 confirmed that all testing at Complex 12 was normal. The J-FACT testing started at T − 215 and ran through umbilical connector removal, which occurred at approximately T + 28. Spacecraft monitoring reported a power failure and transferred to the auxiliary generator at approximately T − 44. Spacecraft performance was normal.

TV subsystem calibrations were completed without any adjustment being required. Final flight assembly was completed and documented photographically. Spacecraft power was turned on for an attitude-control Sun-sensor test and a pyrotechnic midcourse-motor verification test. Results of the tests showed normal spacecraft operation.

The preflight system test indicated that the spacecraft was ready for flight. Then each solar panel was excited with the solar simulator, and proper operation was checked for all individual solar panel sections.

The autopilot, midcourse-motor transducer, and TV high-power tests were performed. An evaluation of the test results showed nominal spacecraft operation. Spacecraft weight and center-of-gravity measurements indicated that approximately 3 lb of weight would be required to properly locate the center of gravity upon the midcourse-motor thrust axis. The final flight weight was 809.57 lb.

The spacecraft was transferred to the *Agena* adapter for final flight mating. The pyrotechnics were installed, verified, and connected. The attitude-control gas system was charged to a flight pressure of 3600 psi. Spacecraft functions were verified with the *Agena* shroud installed.

The spacecraft participated in a combined simulated launch. On July 25 the test was run to T − 18 sec and then recycled to T − 7 min. It was concluded that spacecraft operation was normal.

B. Launch Vehicle

Atlas 250 D had originally arrived at ETR on January 15, 1964 to support a first-quarter CY 64 *Ranger* launch. It was subsequently erected on Launch Complex 12 on June 18 to support the *Ranger VII* July launch. *Agena* 6009 arrived at ETR on June 12, and, after hangar checkout, was mated to the *Atlas* for the first time on June 25. Both the *Atlas* and the *Agena* proceeded through preflight preparations and combined spacecraft/launch vehicle composite testing without major problems and were ready to support the launch on the initial day of the July launch period. Four attempts to perform the *Atlas* dual tanking test were required, however, before one successful test was completed, due in each case to a failure in a different component in the system. In addition, one command destruct receiver on the *Agena,* one Azusa beacon on the *Atlas,* and one klystron in the ground guidance station had to be replaced prior to the launch vehicle system successfully passing all the prelaunch tests and being declared ready to launch.

C. Countdown and Launch

The launch period for *Ranger VII* encompassed the period of July 27 through August 1. The launch window for July 27 was 1632-1842 GMT; for July 28 it was 1650-1858; and for each succeeding day of the period, it was a few minutes later, and about two hours in length.

The first launch attempt on July 27, initiated at 0847 GMT (T − 395), was cancelled after two problems had arisen during the countdown that took more time to resolve than the daily launch window would allow. At T − 57 min in the countdown a failure of the *Atlas* telemetry battery occurred. Seventy min were consumed in replacing the battery and neutralizing and cleaning the surfaces exposed to the battery fluid which escaped during the failure. At T − 22 min another hold was called to evaluate and correct the excessive noise evidenced in the ground guidance system. Immediate trouble-shooting did not isolate the problem such that resolution of the problem could not be confidently forecast within the remaining daily launch window. Therefore the launch attempt for this day was cancelled. Subsequently, several components of the ground guidance system were replaced, monitored for 10 hr for noise, and then declared operational to support the next launch attempt.

The second launch attempt, July 28, was successful, with liftoff occurring at 1650:08 GMT almost without incident during the countdown. Only one unforeseen problem was encountered. The *Agena* velocity meter

recorder in the blockhouse failed during the scheduled hold at T − 60 min in the countdown. It was replaced with the unit from Launch Complex 13 without the need for calling an unscheduled hold.

The weather during launch imposed no particular problems on the launch. There was a 2000-ft ceiling with 3/10 cloud cover, a 10-knot surface wind at 140 deg, and 86°F temperature, 68% humidity, no rain, and insignificant wind shears.

1. Vehicle Tracking

The Mark II Azusa system tracked the transponder in the *Atlas* booster from T + 5 sec to T + 410 sec. Reduced data indicated a dropout at booster staging.

Coverage by the ETR C-band radar systems was as given in Table 1.

Table 1. ETR C-band tracking coverage

Station	Type	Location	Coverage interval, range time, sec	Useful data interval, range time, sec
0	18	Cape Kennedy	24-484	23-473
1	16	Cape Kennedy	9-336	11-335
19	18	Cape Kennedy	8-310	—
3	16	Grand Bahama	67-495	70-495
5	16	San Salvador	124-565	125-565
7	18	Puerto Rico	225-595	—
91	18	Antigua	385-730	393-417; 418-692
12	16	Ascension	1243-1456	1244-1455
13	16	Pretoria	1860-2870	1845-2139; 2199-2297; 2428-2461; 2518-2528; 2640-2658; 2663-2772
		Bermuda	367-646	514-646
		Carnarvon	2461-3988	2704-3988

2. Range Telemetry Coverage

a. Atlas. Booster links at 229.9 and 232.4 mc were covered as follows (times in sec from launch):

Cape Kennedy	
Tel 2	− 420 to + 476
Tel 3	− 420 to + 491
Grand Bahama Island	+ 38 to + 500
San Salvador Island	
229.9	+ 119 to + 387
232.4	+ 330 to + 505

All *Atlas* events were confirmed by Cape Tel 2.

b. Agena. The Link at 244.3 mc was covered as follows (times in sec from launch):

Cape	− 420 to + 491
Grand Bahama Island	+ 38 to + 500
San Salvador Island	+ 119 to + 550
Antigua Island	+ 330 to + 738
Coastal Crusader[2]	+ 535 to + 940
Ascension Island	+ 1208 to + 1470
Ascension Island	+ 1539 to + 1551
Rose Knot[2]	+ 1450 to + 1875
Sword Knot[2]	+ 1604 to + 1885
Pretoria, S.A.	+ 1824 to + 3040

Agena discretes were covered in real time by the following stations:

Mark 7	Cape and Antigua
Mark 8	Cape and Antigua
Mark 9	*Sword Knot* and *Rose Knot*
Mark 10	*Sword Knot* and *Rose Knot*
Mark 11	(Exact time unconfirmed)
Mark 12	Pretoria
Mark 13	Pretoria

c. Spacecraft Coverage by ETR. The telemetry tapes provided by ETR were generally satisfactory with certain exceptions noted below. The telemetry coverage provided by these tapes is demonstrated in Fig. 2. It will be noted that *Agena* telemetry was very noisy at the time of electrical disconnect (Mark 11) and spacecraft/*Agena* separation (Mark 12); the latter was a Class I Requirement. As a result, the Mark 11 has not been verified and Mark 12 is uncertain, although the latter was observed on spacecraft gyro data recorded at DSIF 59.

As on all previous *Ranger* missions, better spacecraft telemetry data were recovered from the *Agena* telemetry-subcarrier Channel F (98 kc) than via the spacecraft L-band link, prior to electrical disconnect. The *Ranger VII* data which were retransmitted to the Cape Tel 2 station from downrange via single-sideband radio were much better than that on *Ranger VI*. The reason is that the *Agena* Channel F signal was used on *Ranger VII* while the L-band signal was used on *Ranger VI*. The best of these (from Ascension) had some frequency shift which caused the binary channels to be clipped off.

[2]Tracking ships, known formerly as *Whiskey*, *Victor*, and *Yankee*, respectively.

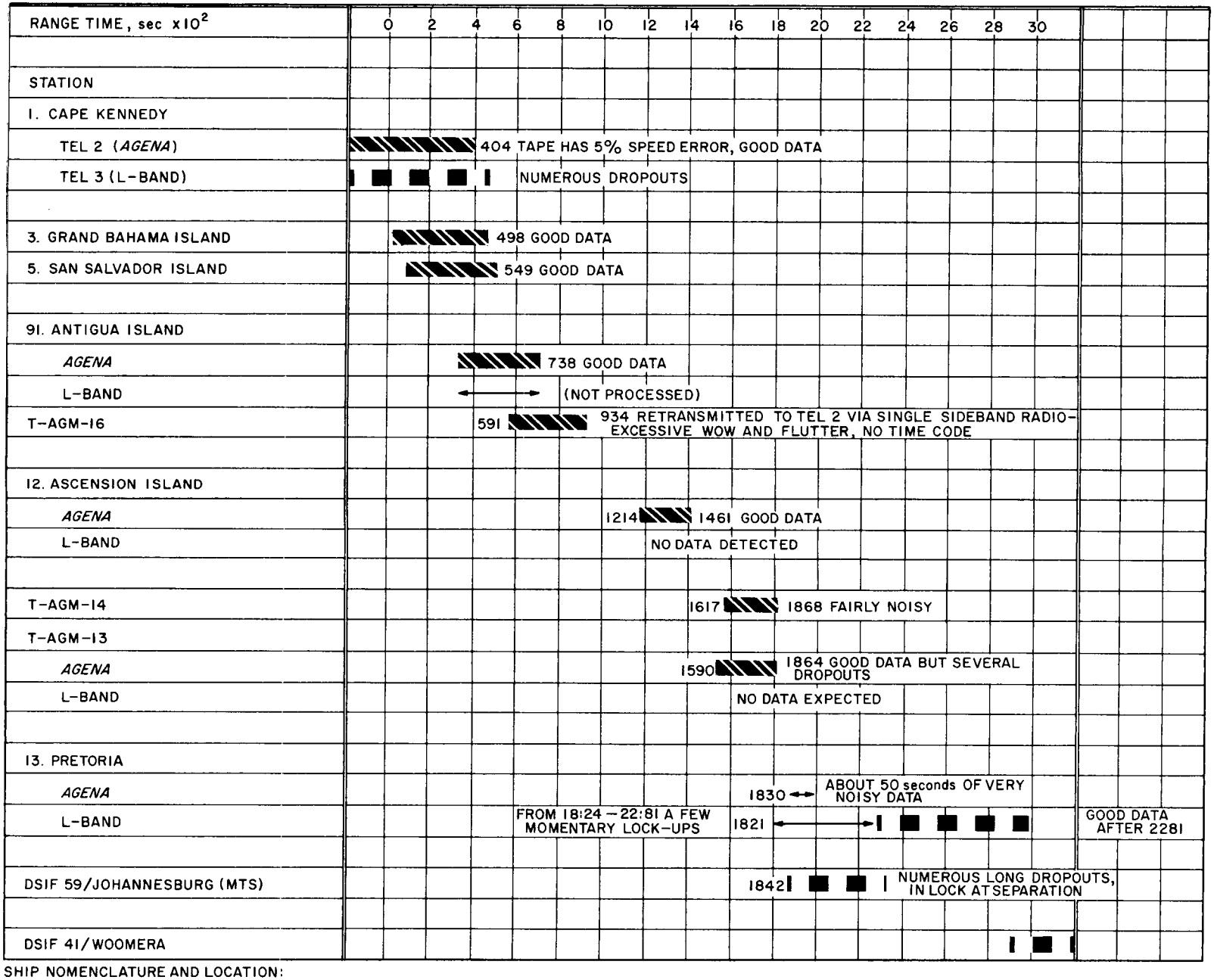

SHIP NOMENCLATURE AND LOCATION:

T-A6M-16 (COASTAL CRUSADER) = RIS 1851 (WHISKEY) AT 14°N 47°W

T-A6M-14 (ROSE KNOT) = RIS 1850 (VICTOR) AT 10°S, 6°E

T-A6M-13 (SWORD KNOT) = RIS 1852 (YANKEE) AT 20°S, 5°E

Fig. 2. *Ranger VII* launch telemetry coverage

The problem areas encountered during JPL processing of these telemetry tapes are summarized below:

1. Late acquisition by ETR Station 13 (Pretoria) for *Agena* was caused by the operator's tracking in a ground-antenna side lobe for approximately 6 min. L-band coverage by Station 13 was sporadic early in the pass, while DSIF-59 went in and out of two-way lock several times, each time causing ETR Station 13 to drop lock.
2. *Gemini* time code recorded on *Rose Knot* tape. (This is the only time code on the ship, and no other commitment was made.)
3. Tel-2 (*Launch*) tape had tape-speed error.
4. No data were detected on the retransmission tape from Antigua and Pretoria.
5. The retransmitted data tape from *Coastal Crusader* had excessive wow and flutter.
6. No data were detected on the L-band tape track from Ascension or *Sword Knot*. ETR reported that Ascension did track L-band but *Sword Knot* was not expected to track on the launch azimuth flown.

III. LAUNCH VEHICLE SYSTEM

An *Atlas D/Agena B* vehicle combination was utilized to accelerate the *Ranger* spacecraft to the required injection velocity and within the stringent guidance accuracy tolerances required to achieve the desired trajectory to the Moon. The vehicle was launched from Launch Complex 12 at the Kennedy Space Flight Center in Florida with powered flight telemetry, tracking, and other range support services supplied by the Air Force Eastern Test Range.

The *Atlas D/Agena B* is a 2½-stage vehicle in which all engines of the *Atlas* are ignited and stabilized prior to commitment to launch, while the single *Agena* engine is ignited in flight twice, first to accelerate the *Agena/* spacecraft combination to the velocity required to maintain a circular orbit about the Earth, and then, after a suitable coasting period in this "parking orbit," to accelerate the *Agena/*spacecraft combination to the required injection velocity necessary to escape the Earth's gravitational field and coast to the Moon.

A. Atlas 250 D

The *Atlas D* is a 1½-stage boost vehicle containing five rocket engines that utilize a kerosene-like hydrocarbon and liquid oxygen as propellants and at launch has a thrust-to-weight ratio of approximately 1.25. A modified version of the *Atlas* missile, it is shown in Fig. 3.

All five engines (the two boosters, the one sustainer, and the two vernier engines) were ignited on the ground prior to liftoff to ensure maximum reliability of this stage. After the majority of the *Atlas* propellants were consumed in flight, and prior to the time the vehicle acceleration attained 7 *g*, the two outboard booster engines were shut down and jettisoned, and the vehicle continued on, powered primarily by the sustainer engine. When the required velocity for the *Atlas* portion of the flight had been achieved, the sustainer engine was shut down and for a few seconds only the vernier engines provided thrust to stabilize the vehicle and to achieve the precise velocity desired. When this had been accomplished, the verniers were shut down, the *Agena/*spacecraft combination was separated from the *Atlas*, and the *Atlas* was backed away from the *Agena* by two small solid-propellant retro rockets.

The *Atlas* was guided during its flight first by an on-board programmer and autopilot and later by a radio guidance system that sent correction signals to the autopilot based on information obtained from a ground-based radar tracking station. The on-board programmer and autopilot guided the vehicle from liftoff through the jettisoning of the booster engines except for a brief 10-sec period when the radio guidance system was enabled to receive and steer in accordance with the radio signals from the ground. After the booster engines were jettisoned the radio guidance loop was enabled and the vehicle guided by the ground-based guidance and computer system for the rest of the *Atlas* portion of the powered flight.

B. Agena B 6009

The *Agena B* is a single-engine dual-start upper stage utilizing unsymmetrical di-methyl hydrazine as fuel and inhibited red fuming nitric acid as oxidizer and is depicted in Fig. 4. At first ignition it has a thrust-to-weight ratio of approximately unity. Its flight control system consists of a programmer, a reference gyro system, two horizon sensors and a velocity meter. Elements of the flight control system were preset on the ground prior to launch. Via the *Atlas* radio guidance system, a ground-calculated discrete command initiated the timing function for *Agena* second burn; the *Agena* received no further guidance or control signals from the ground subsequent to separation from the *Atlas*. The programmer and the gyro references provided the discrete events and the basic vehicle attitude information during coasting and powered flight phases. The horizon sensors viewed the Earth and updated the gyro information during the flight to compensate for gyro drift. The velocity meter was preset for the required velocity-to-be-gained by the *Agena* stage, and determined when the engine would be shut down. For *Ranger VII* the *Agena* engine was required to ignite twice in order to accelerate the spacecraft to the required injection conditions as will be described later. After attaining the required velocity the engine was shut down, the spacecraft separated from the *Agena*, and the *Agena* executed an almost-180-deg yaw maneuver and was decelerated by a small solid-propellant retro rocket to prevent it from impacting on the Moon.

C. Powered-Flight Sequence of Events

At liftoff the launch vehicle rose vertically for 15 sec while executing a roll maneuver to orient it for

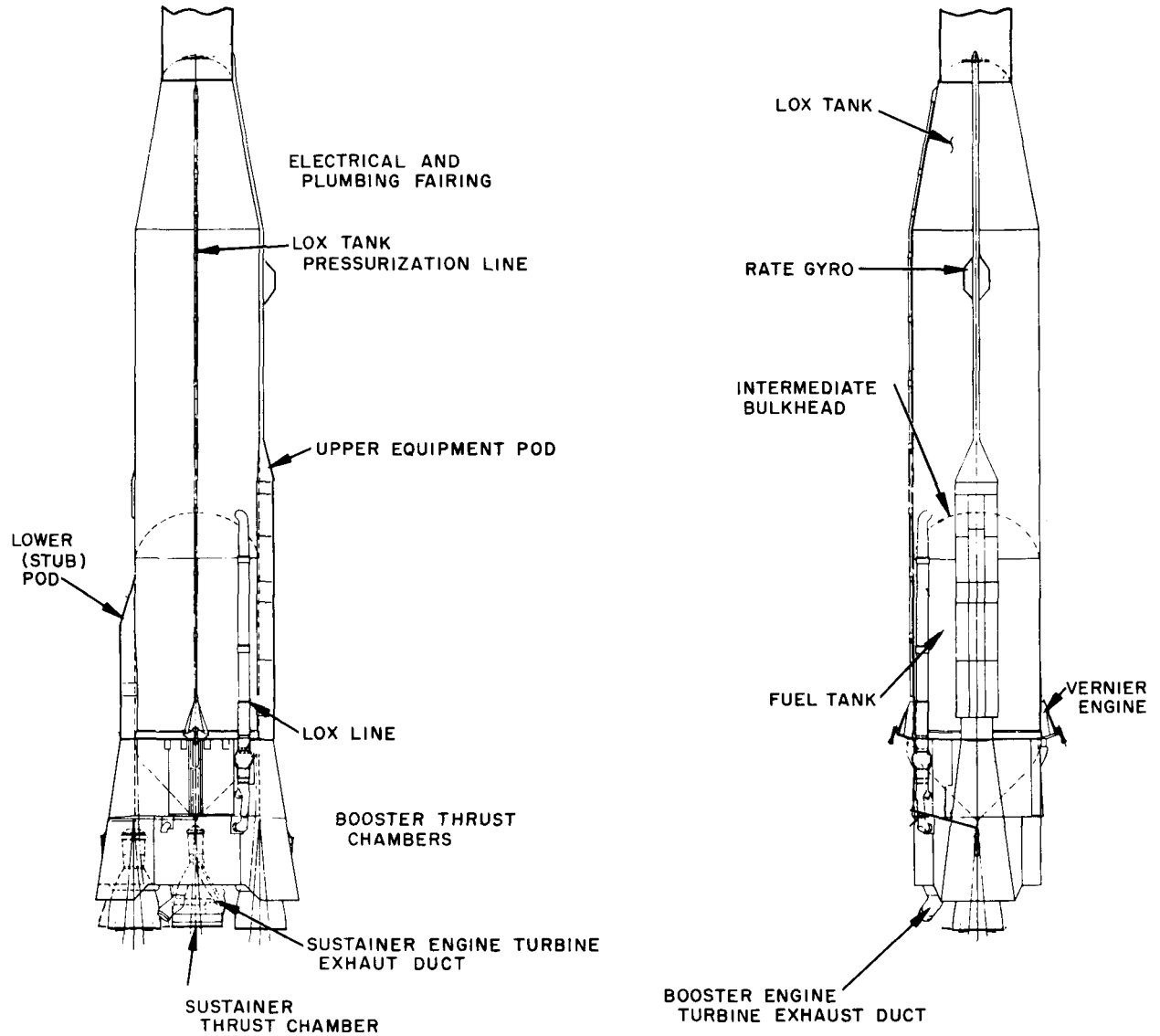

Fig. 3. *Atlas* launch vehicle

its subsequent flight down the Range on an azimuth of 97.1 deg E of N. After 15 sec the *Atlas* autopilot controlled the flight along a near-zero-gravity turn in the pitch plane. After about 136 sec of powered flight the booster engines were shut down and jettisoned, and the vehicle continued accelerating under the thrust of the sustainer engine and guided by the radio signals received from the ground tracking and computing station. Shortly after 6 min from liftoff, first the sustainer engine was shut down, next the vernier engines were shut down, then the aerodynamic shroud covering the spacecraft was separated from the vehicle, and finally the *Atlas* was retroed away from the *Agena*/spacecraft combination, all by radio command from the ground station. The *Atlas* portion of the trajectory was shaped to accelerate the *Agena*/spacecraft into an orbit whose apogee was approximately 100 nm, the altitude of the "parking orbit."

After separating from the *Atlas*, the *Agena* coasted for approximately one minute. Then its engine ignited upon command from its preset timer, and burned for about 2¾ min until it had been accelerated to that velocity required to maintain a circular orbit 100 nm above the Earth. The *Agena*/spacecraft combination then coasted in this "parking orbit" about 20 min until the proper position in space over the South Atlantic was reached for the spacecraft to be injected into its transit trajectory to the Moon. At that time the *Agena* was commanded to

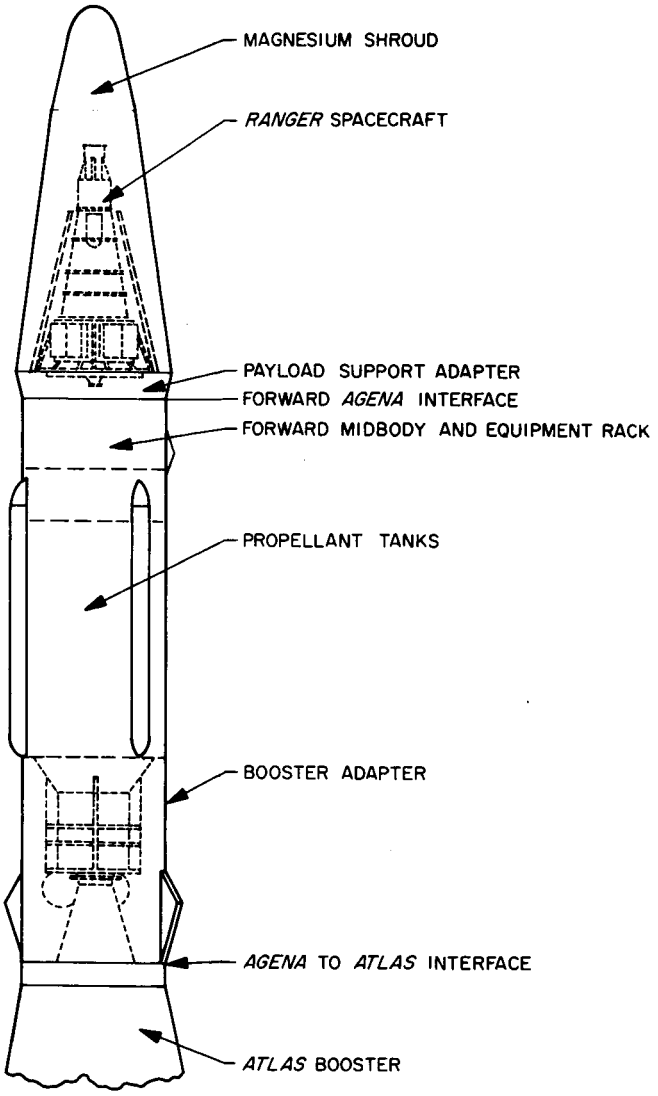

Fig. 4. *Agena* injection vehicle

re-ignite for approximately 1½ min and accelerated the spacecraft to the required injection velocity. After achieving this the *Agena* engine was shut down, the spacecraft was mechanically separated from the *Agena* by a spring push-off system and the spacecraft began its long coasting trajectory to the Moon. The *Agena* executed a yaw maneuver and was decelerated slightly by a solid propellant retro rocket to deviate it from the spacecraft trajectory and prevent it from impacting upon the Moon.

D. Launch Vehicle

The *Atlas* 250 D and *Agena* 6009 launch-vehicle combination, together with the radio guidance system, placed the spacecraft on a coasting trajectory well within the injection requirements. All vehicle subsystems performed within tolerance.

Radio-guidance steering of the *Atlas* during the boost-phase was effective for the first time on a NASA mission. Prior to the first steering signal the vehicle was traversing a 2.6-σ lofted trajectory. Steering commands were sent for three seconds during the booster-steering-enabled period of 100 to 110 sec to turn the vehicle a total of 1.68 deg down and back on course. At sustainer engine shutdown the *Atlas* contained enough propellants for 4.8 sec additional operation at rated thrust.

The *Agena* performed satisfactorily throughout both coasting and thrusting phases, delivering the spacecraft to the injection point with 35 ft/sec excess velocity. This, however, is within the capability of the spacecraft mid-course system to correct the trajectory to that desired. At injection the *Agena* contained enough propellants for 2.3 sec additional operation at rated thrust.

IV. SPACECRAFT SYSTEM

The *Ranger VII* spacecraft system performed successfully and well within all design tolerances throughout the mission. A general tabulation of spacecraft flight events is given in Appendix A.

The spacecraft configuration, coordinate system, and functional diagram are given in Appendix C.

The spacecraft is made up of twelve basic subsystems, whose gross relationships are given in Fig. 5. Each subsystem is treated separately below, and the general approach attempted is to cover the following material:

1. The function of the subsystem.
2. The subsystem mechanization to perform the function.
3. The subsystem performance.
4. An explanation of any anomalies.

A. Radio Subsystem

The spacecraft L-band radio subsystem is composed of five major elements: omnidirectional antenna, high-gain antenna, receiver, transmitter, and auxiliary oscillator (see Fig. 6). The subsystem is designed to receive signals and commands via the omnidirectional antenna. The omniantenna is also used to transmit signals when the spacecraft is solar-oriented or non-oriented. The high-gain antenna is used to transmit signals when the spacecraft is Earth-oriented. The transmitter-receiver combination is designed to transmit a phase-modulated signal which is phase-coherent with the received signal. When no signal is received by the spacecraft, a non-coherent signal is provided to the transmitter by an auxiliary oscillator.

Operation of the transmitter is monitored by three telemetered measurements. Two antenna-drive measurements indicate the amount of power supplied to each antenna and a 250-v monitor indicates the amount of plate voltage on the RF power amplifiers.

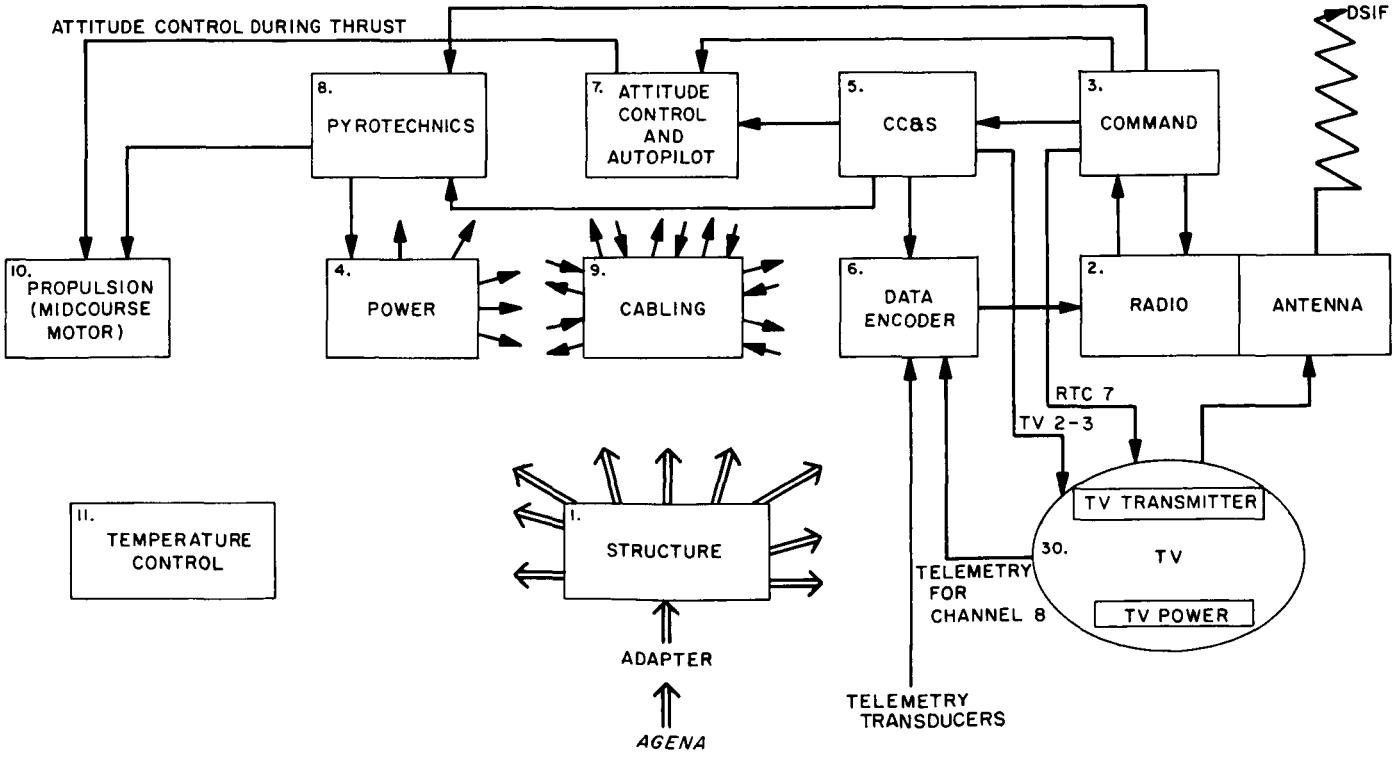

Fig. 5. *Ranger* Block III spacecraft Subsystems

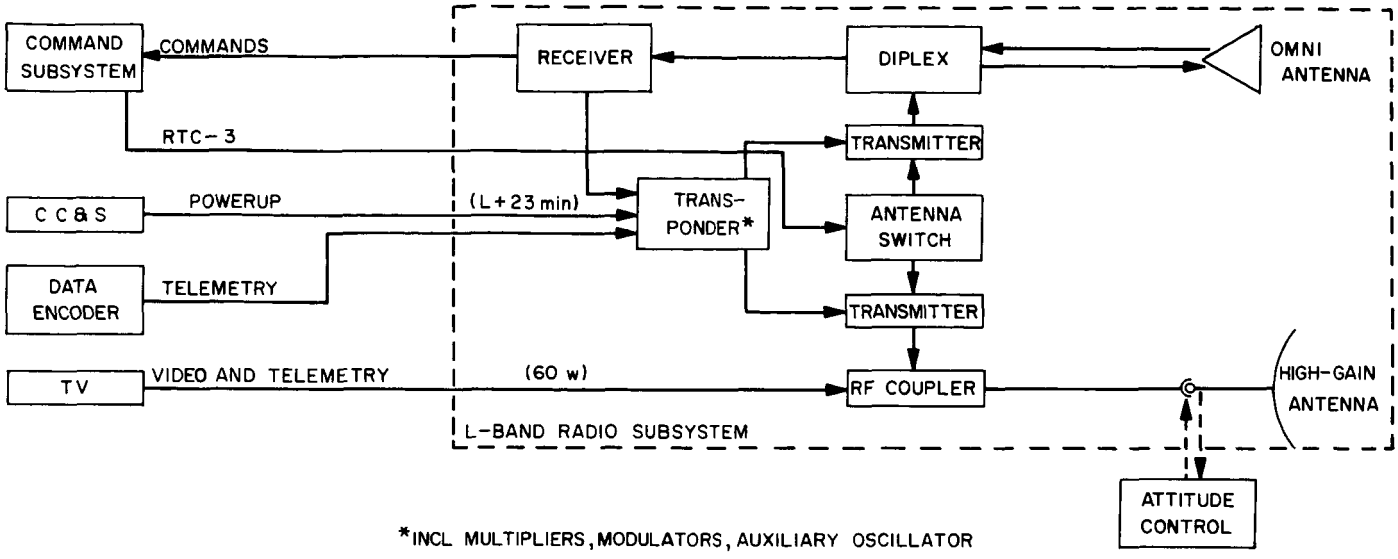

Fig. 6. L-band radio Subsystem

The receiver operation is monitored by means of five telemetered measurements. Two measurements of receiver AGC voltage with coarse and fine resolution indicate the spacecraft received signal strength, and a local-oscillator-drive measurement indicates the amount of power supplied by the receiver local oscillator. Two other measurements, coarse and fine static phase error, indicate the DC correction voltage resulting from the frequency difference between the up-link signal and the receiver VCO. These measurements are generally zeroed for the transmission of a command and thus become operational aids for ground stations.

The spacecraft and DSIF 71 were in two-way lock prior to launch to permit the sending of a command immediately after launch if necessary. Although the Cape station, DSIF 71, momentarily lost lock at liftoff, telemetry indicated that the spacecraft receiver maintained lock with the DSIF 71 transmitted signal until the spacecraft went over the horizon. Thus a command could have been sent if warranted.

Power-up was scheduled to occur at L + 23 min, and the CC&S event was telemetered and received by ETR. Normal power-up operation was not confirmed by spacecraft data, however, until DSIF 51 acquired at L + 31 min. At this time, the 250-v monitor measurement (see Fig. 7) indicated 252 v and the low-gain antenna drive indicated 34.5 dbm, corresponding to the normal power-up operation.

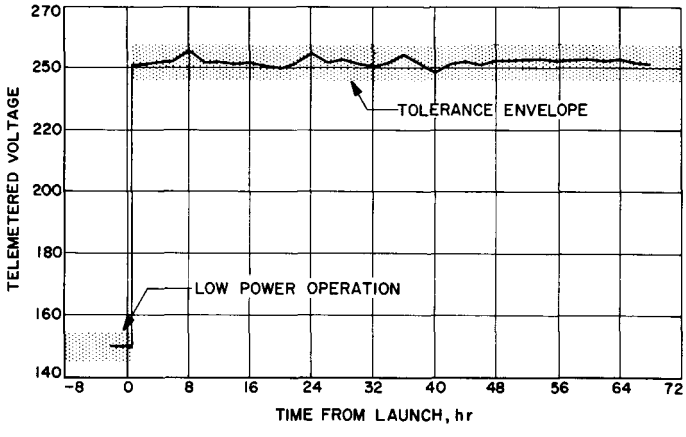

Fig. 7. Radio transmitter "250-volt" monitor

During the initial rise over DSIF 51 and DSIF 59, the spacecraft appeared to be tumbling and DSIF 59 experienced difficulty in maintaining two-way lock. Stable two-way lock did not occur until L + 52 min when DSIF 41 acquired the spacecraft. At this time, since the spacecraft was tumbling, the spacecraft AGC coarse and fine measurements exhibited large excursions. The spacecraft received signal strength values, however, appeared to fall within predicted tolerances.

Solar acquisition was completed at L + 75 min and was reflected in smaller variations in the spacecraft receiver AGC telemetry. Since the spacecraft was rolling, these variations were due simply to differences in the omni-

antenna gain for different clock angles. Again the values fell within predicted tolerances.

Earth acquisition was completed at L + 234 min; again, the receiver AGC measurements showed an improvement in stability. For the remainder of the mission the spacecraft received signal strength measurements generally fell within 1.5 db of predicted values. Figure 8 shows a typical plot of measured values during a pass over DSIF 51.

At L + 265 min, an RTC-3 command was transmitted to the spacecraft to initiate the switchover to the high-gain antenna. The switchover was confirmed by the antenna drive power measurements (Fig. 9). After switchover the high-gain antenna drive indicated 23.75 dbm, normal power output. The switchover was also confirmed by the DSIF-received signal strength which increased by approximately 10 db.

Throughout the cruise phase preceding the midcourse maneuver, all of the measurements fell within predicted tolerances.

Prior to the midcourse maneuver the planned maneuver was analyzed in terms of its effect on signal strength. Since the omni-antenna pattern contains numerous nulls in the direction of the roll axis, the spacecraft or the DSIF-received signal strengths can fall below threshold

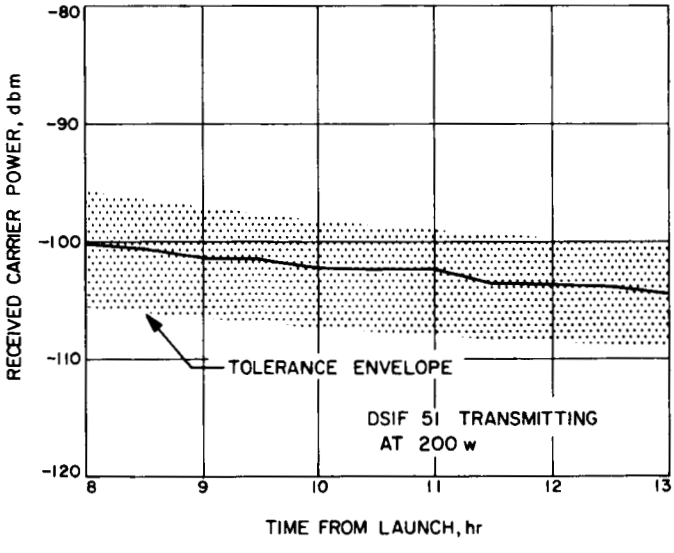

Fig. 8. Spacecraft received carrier power, second pass over Johannesburg

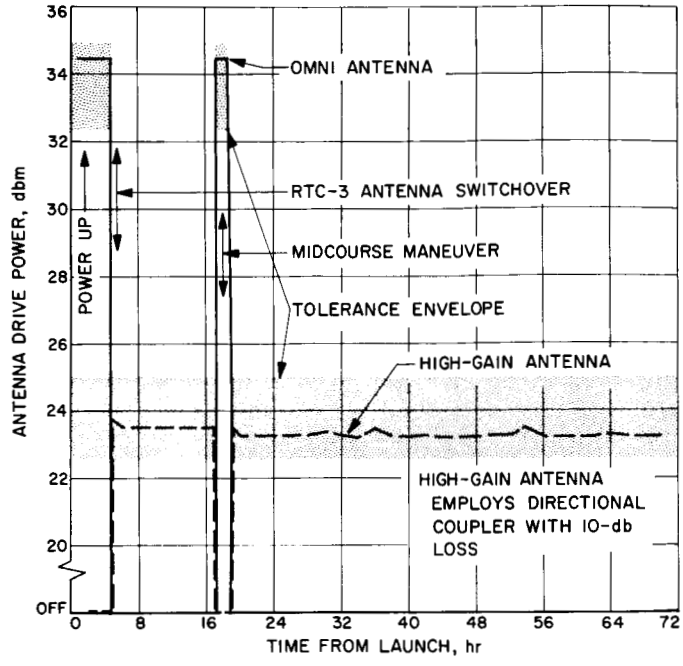

Fig. 9. Antenna drive power

for some maneuvers. Figure 10 shows a plot of calculated received signal strength at DSIF 12 incorporating all adverse tolerances together with approximate values measured during the maneuver. It can be seen that the critical region occurred near the end of the pitch turn when several of the channels fell below threshold. However, as predicted by the analysis there was never any loss of lock with the carrier.

Antenna-power switchover to the omni antenna 10 min before the maneuver started, and back to the high-gain antenna 81 min after, were commanded, executed, and observed in the antenna power measurements.

Solar reacquisition and Earth reacquisition occurred within nominal expected times and were again evidenced by the spacecraft receiver AGC measurements which slowly settled down as attitude stabilization was achieved.

Throughout the post-midcourse phase, and until impact, all the measurements indicated normal values; no discrepancies were noted in telemetered data. There were, furthermore, no times of flight at which ground stations indicated any difficulty in transmitting to or receiving from the spacecraft. On the basis of these facts, the spacecraft radio system appeared to function normally in all respects during all phases of the mission.

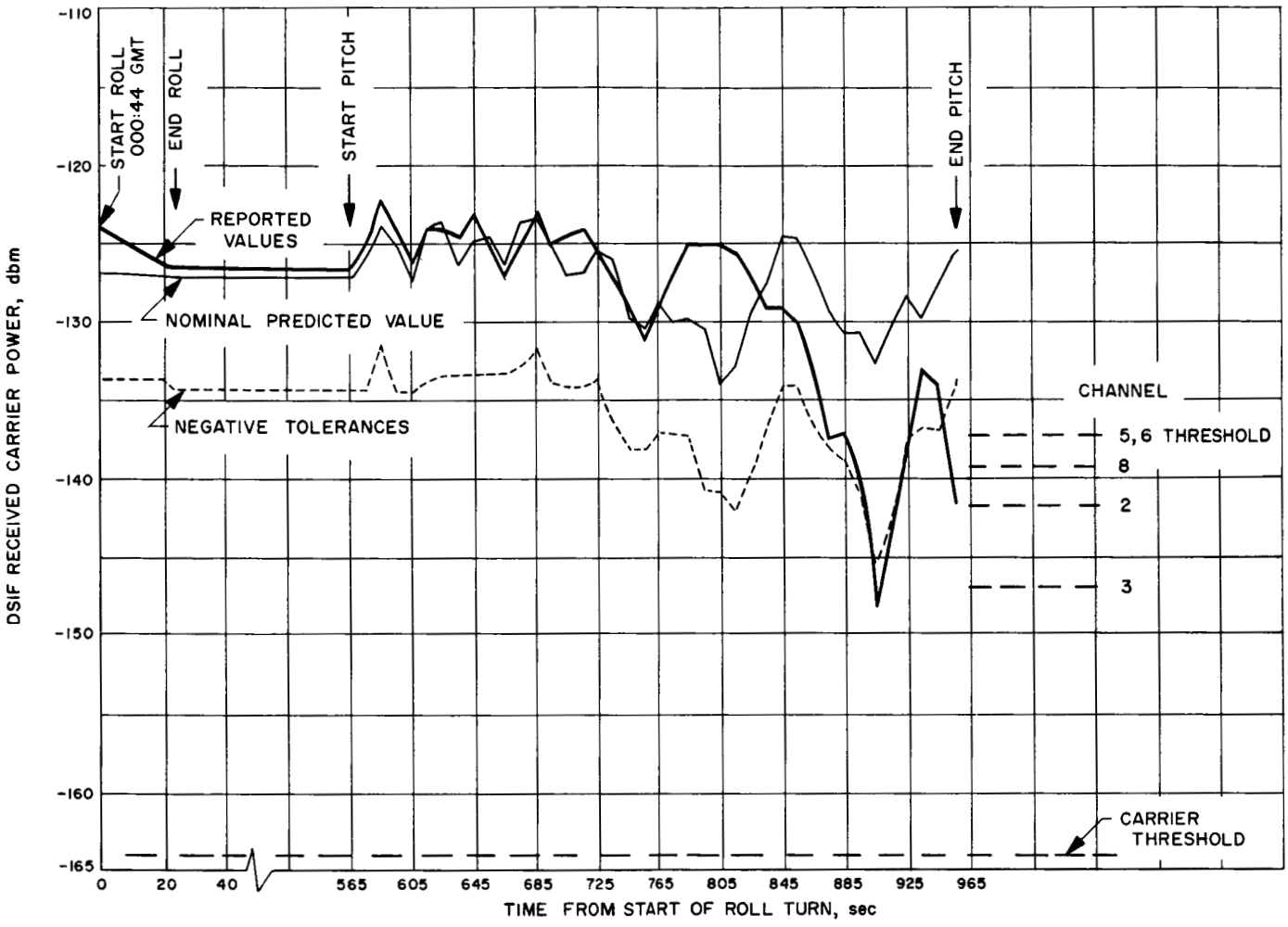

Fig. 10. Goldstone received carrier power during midcourse maneuver

B. Command Subsystem

The spacecraft Command Subsystem consists of a command detector and a command decoder (Fig. 11). Commands are sent to the spacecraft over the radio link by means of a frequency-shift-keyed (FSK) subcarrier signal that is recovered in the spacecraft radio receiver. The command detector performs the functions of detecting the FSK signals provided by the spacecraft radio receiver, determining whether a command is being sent, converting the detected FSK signals into a serial sequence of binary ones and zeros (which comprise the code), generating various clocking signals for code processing both in the detector and the decoder, and routing these binary and clocking signals to the command decoder. The command decoder receives the serial sequence of binary ones and zeros from the command detector, forms the data into command words and determines

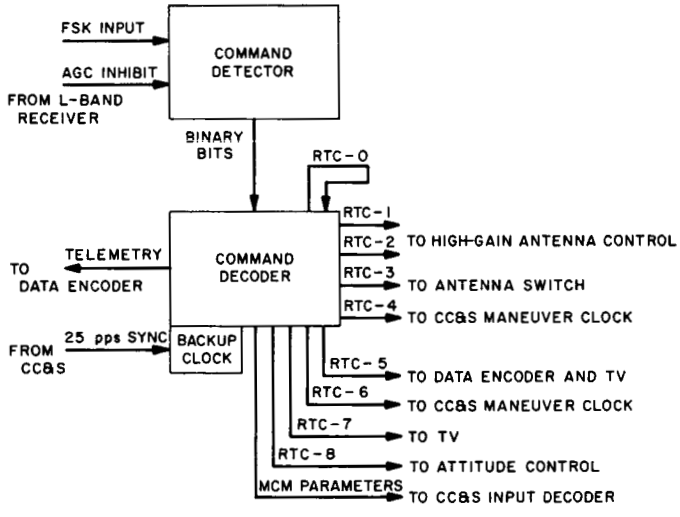

Fig. 11. Command Subsystem

whether the command is a real-time command (RTC) or a stored command (SC). If the command is a RTC, it is decoded to determine which RTC has been transmitted and the appropriate relay is closed to inform the corresponding addressee (CC&S, Attitude Control, etc.). If the received command is a SC, the data are clocked serially into the CC&S for further processing.

Verification that the decoder has received and acted on a command is telemetered in the form of FM pulses on a subcarrier (B-20) which in turn phase-modulates the RF carrier transmitted from the spacecraft; RTC verification is of a form indicating that some relay closed while a SC is verified by telemetering each data bit as it is transferred to CC&S. Additional verification of the commands is accomplished by the action noted on the other subsystems via telemetry. Since noise inherent in transmitting and receiving a command can modify the command itself — the probability of a bit error is $\leq 10^{-5}$ — the reaction of each command is watched closely.

In every case in which a command was transmitted to *Ranger VII*, a verification of action was indicated on telemetry in the form of the proper pulses; in addition, all reactions of the spacecraft were correct for every command. On the basis of these facts the Command Subsystem appeared to function normally in all respects throughout the mission.

A summary of the commands received by the Command Subsystem is given in Table 2.

Table 2. Commands received during flight

Command	Received, (date/GMT)	Station sending	Telemetry event blips
RTC-0	28/2115:38	41	—
RTC-0	28/2116:38	41	—
RTC-3	28/2119:38	41	CH B-20 at 2119:38
RTC-0	29/0850:39	12	—
RTC-0	29/0852:39	12	—
SC-1	29/0854:40	12	CH B-20 at 0854:41
SC-2	29/0856:41	12	CH B-20 at 0856:42
SC-3	29/0858:41	12	CH B-20 at 0858:42
RTC-0	29/0936:38	12	—
RTC-0	29/0938:39	12	—
RTC-3	29/0940:39	12	CH B-20 at 0940:41
RTC-4	29/1000:38	12	CH B-20 at 1000:40
RTC-0	29/1121:38	12	—
RTC-0	29/1123:39	12	—
RTC-3	29/1125:41	12	CH B-20 at 1125:43
RTC-0	31/1116:08	12	—
RTC-0	31/1116:09	12	—
SC-4	31/1120:11	12	CH B-20 at 1120:13
SC-5	31/1122:10	12	CH B-20 at 1122:12
SC-6	31/1124:11	12	CH B-20 at 1124:13
RTC-0	31/1151:38	12	—
RTC-0	31/1153:39	12	—
RTC-8	31/1155:52	12	CH B-20 at 1155:54
RTC-6	31/1225:52	12	CH B-20 at 1225:54

The commands used are defined as follows:

RTC-0: Clear spacecraft command subsystem

RTC-1: Roll override

RTC-2: Antenna hinge-angle change

RTC-3: Antenna switchover

RTC-4: Initiate midcourse maneuver sequence

RTC-5: Television off, clock inhibit

RTC-6: Initiate terminal maneuver sequence

RTC-7: Television warmup backup (not used)

RTC-8: Maneuver override (used prior to RTC-6 because no terminal attitude maneuver was necessary, but CC&S commands to the TV Subsystem for both turn-on and switching to full power were desired).

SC-1: Midcourse maneuver roll duration

SC-2: Midcourse maneuver pitch duration

SC-3: Midcourse maneuver velocity increment

SC-4: Terminal maneuver first pitch duration

SC-5: Terminal maneuver yaw duration

SC-6: Terminal maneuver second pitch duration

RTC-0 is a clear command whose sole function is to cycle the logic of the Command Subsystem to make sure it is in a state wherein it can receive a command; there are no telemetered data to assure that it was in fact received.

C. Power Subsystem

The Power Subsystem of the *Ranger VII* spacecraft consisted of three major elements—batteries, solar-cell panels, and conversion equipment—as shown in Fig. 12. Two silver-zinc batteries provided raw power during those phases of the flight in which the spacecraft was not Sun-oriented. The total battery capacity at launch was 84 amp-hr. The two solar panels satisfied all raw power requirements while the spacecraft was Sun-

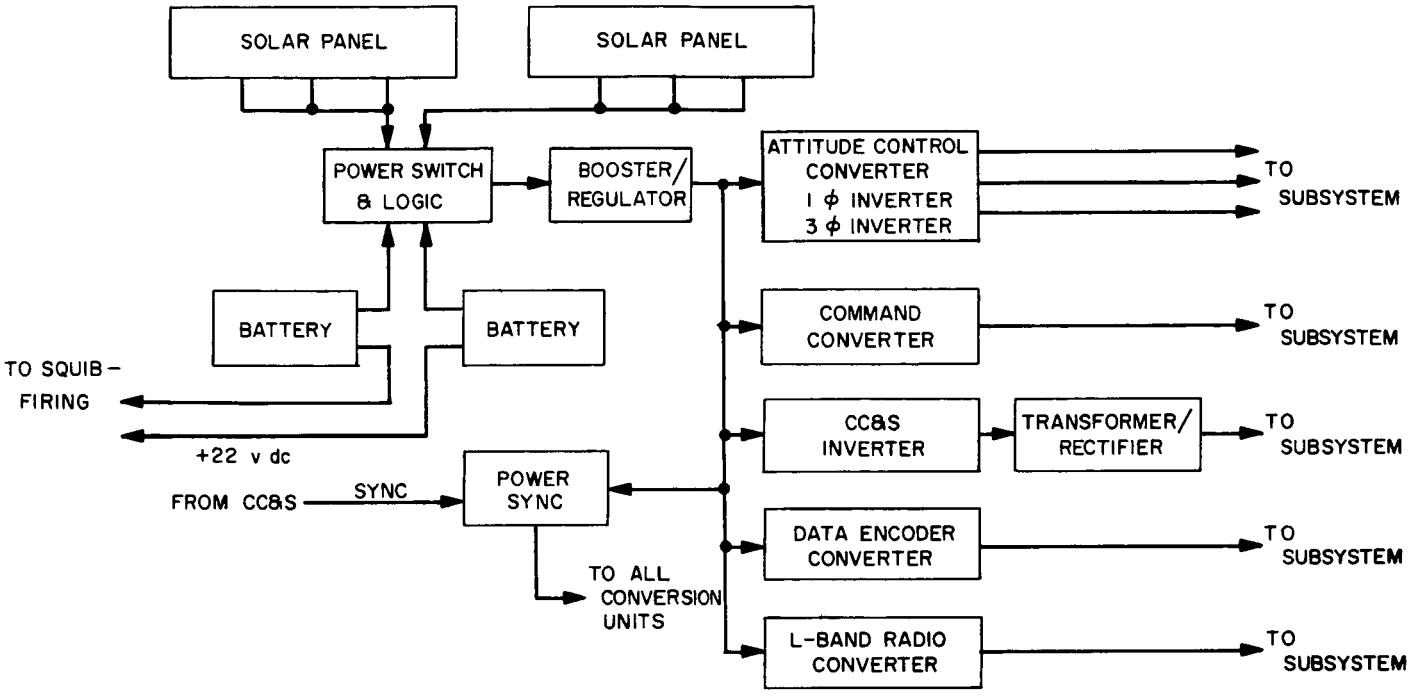

Fig. 12. Power Subsystem

oriented. Each panel employs 4896 *p*-on-*n*-type silicon solar cells. The power conversion equipment selected the appropriate raw power source, provided a regulated bus voltage, and converted the bus voltage to the voltage and current level requirements of the individual subsystem users. System power, voltage and current are shown in Fig. 13.

The solar panels operated within their expected limits during the entire flight as shown in the real-time-data plots in Fig. 14. During Sun acquisition, as well as immediately following, the $-X$ panel supplied more current than the $+X$ panel. This was because the $-X$ panel was illuminated first, allowing it to supply current and warm up faster than the $+X$ panel. The faster warmup of the $-X$ panel was indicated in the solar panel temperature measurements. With the $-X$ panel at a higher temperature, the shunt regulators located on the back of the panel operated at a higher voltage at any given current than those on the $+X$ panel, accounting for the larger current from the $-X$ panel just after Sun acquisition.

As the temperatures stabilized on both panels, the current sharing became equal. During this time the panel voltages increased as the panel temperatures increased owing to the increase in the shunt regulator voltage. When thermal equilibrium was achieved, the voltage stabilized at equal values.

During the pitch-turn portion of the midcourse maneuver, the solar panels were able to supply the raw power load of approximately 145 w out to a pitch angle of 48 deg (approximately L + 17 hr, Fig. 12). At this point the panels began to share the load with the battery. During the Sun acquisition after the midcourse motor burn, the panels were able to supply the total raw power load of about 120 w at a pitch angle of 58 deg.

During the cruise mode of flight, the solar panel front temperature transducer measurements (Fig. 15) indicated 132°F and 129°F for the $+X$ and $-X$ panels respectively. Converting these to solar cell temperatures, the $+X$ and $-X$ panels were 116°F (47°C) and 113°F (45°C) respectively. The back temperature transducer on the $+X$ panel indicated a temperature of about 112-114°F during cruise-mode flight.

Approximately 68 min before impact, the solar panel temperatures began to increase due to intercepted radiant energy from the Moon. At the last reading prior to termination, the front temperatures had increased 13°F and the back temperature had increased 16°F over the cruise temperatures.

The solar panels supplied a continuous raw power load of about 120 w throughout the flight, with the exception of the launch and midcourse maneuver periods.

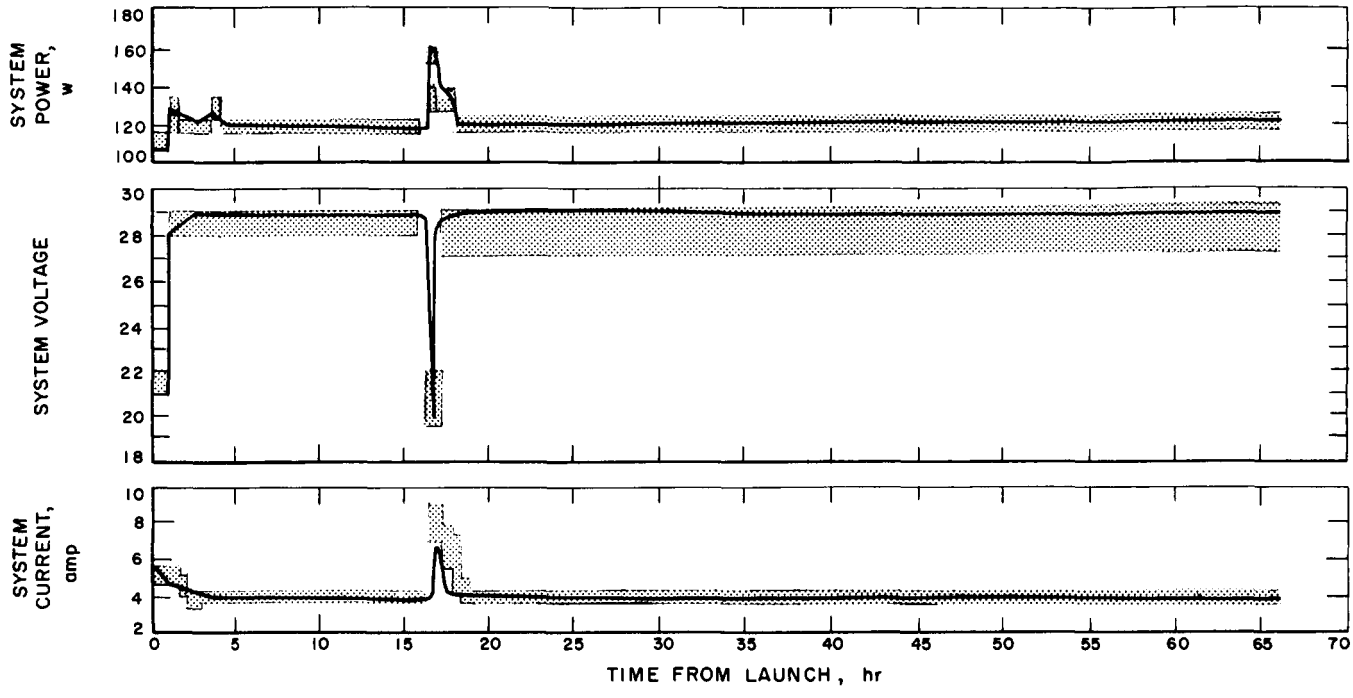

Fig. 13. Power Subsystem performance

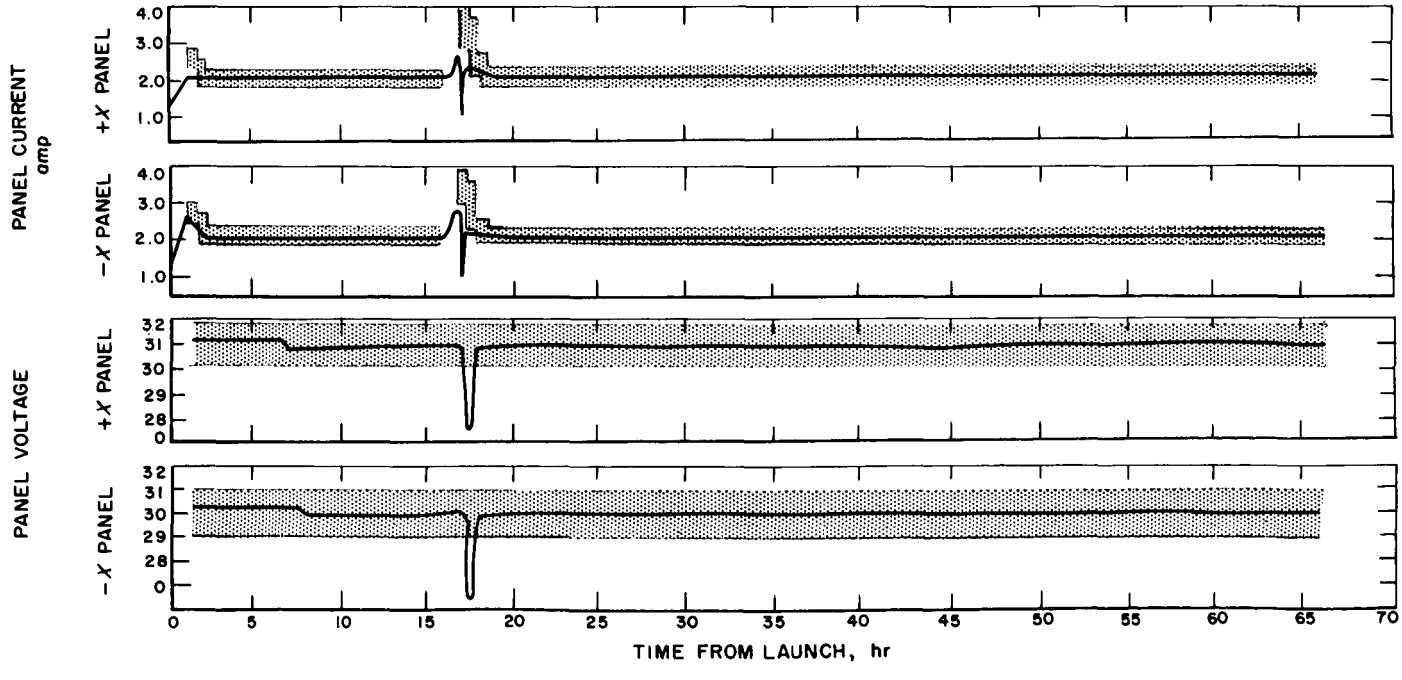

Fig. 14. Solar-panel performance

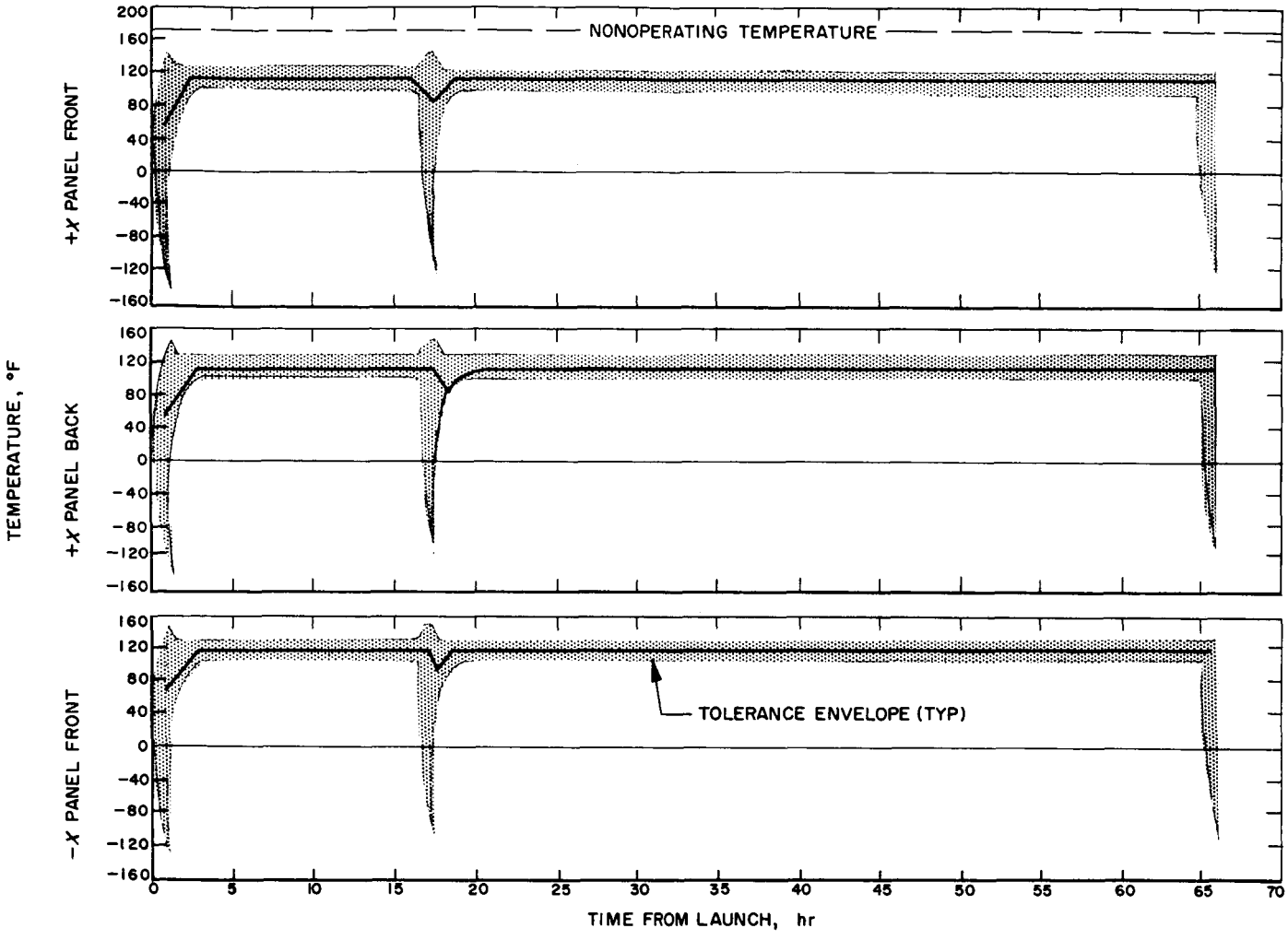

Fig. 15. Solar-panel temperatures

During the mission, the spacecraft operated on battery power from five minutes prior to liftoff until initial Sun acquisition, and during the midcourse maneuver. The total battery usage time was approximately 1.7 hr. The total battery capacity utilized was 10 amp-hr.

Battery operation during the flight was within the specified limits for both voltage and temperature as shown in Fig. 16. The loading was not sufficient to determine capacity. The load voltages were the same as for *Ranger VI* within the resolution and accuracy of the telemetry. The open circuit voltage characteristics of the *Ranger VII* batteries showed a difference in that parameter with respect to *Ranger VI*. The difference is not considered cause for concern as it had little effect on the load voltage or capacity of the battery.

Differences in leakage current parameters of the blocking diodes in the Power Switch and Logic module may have caused the difference due to differences in "charge" currents available to the batteries associated with them. The battery in Case VI of the *Ranger VII* spacecraft (Fig. 16) appeared to rise to the plateau voltage sooner than the other. This could also be explained by differences in "charge" currents, or it may only have been caused by slight differences in battery pre-flight environments.

Performance of the conversion modules is given in Fig. 17 and 18. The individual voltage-monitor data (Fig. 17) indicate typically nominal performance of the units, and the voltage averages between units are an indication of the stability of the booster/regulator 31.5-v output. Temperature curves (Fig. 18) verify that operating efficiencies were normal.

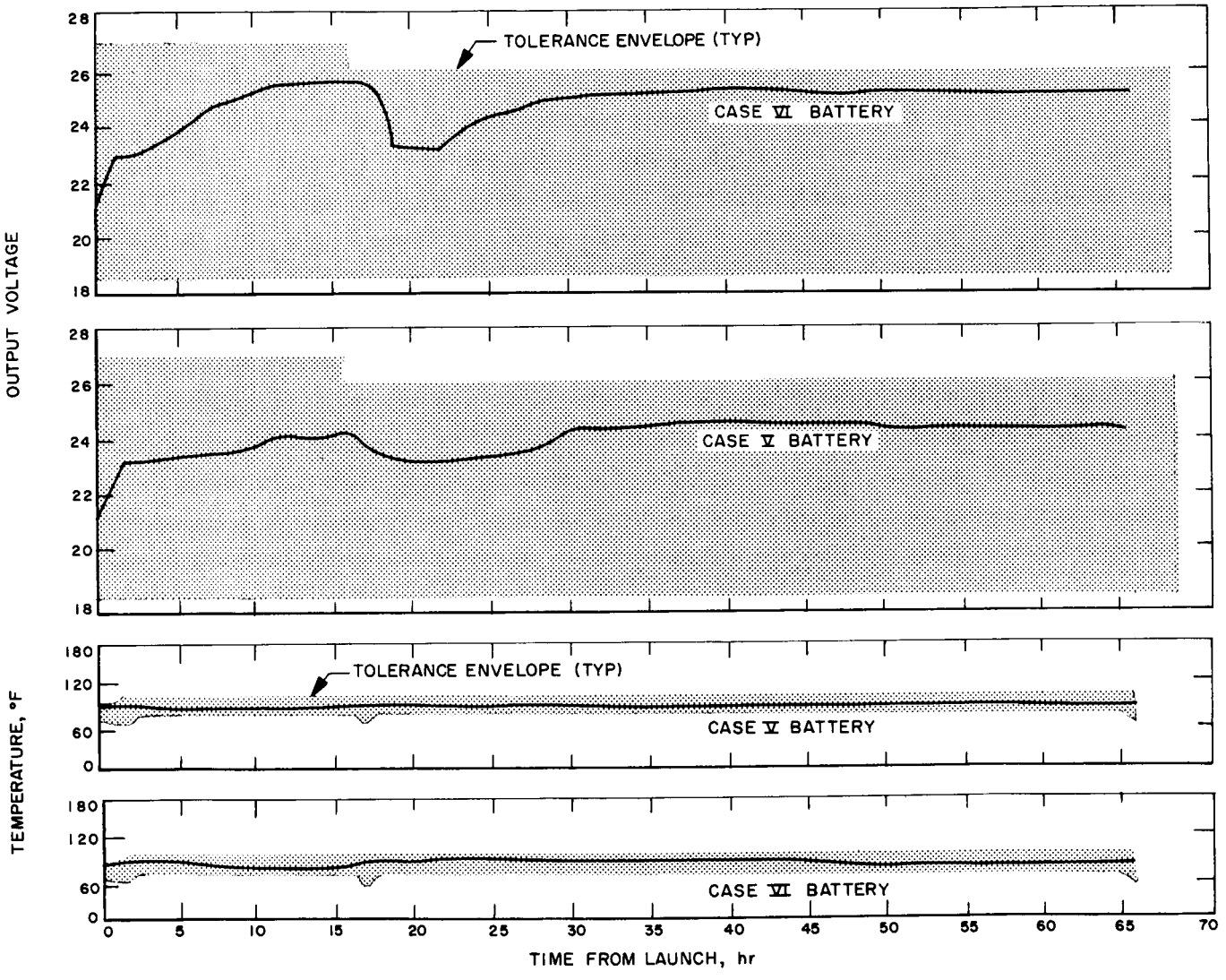

Fig. 16. Battery performance and temperatures

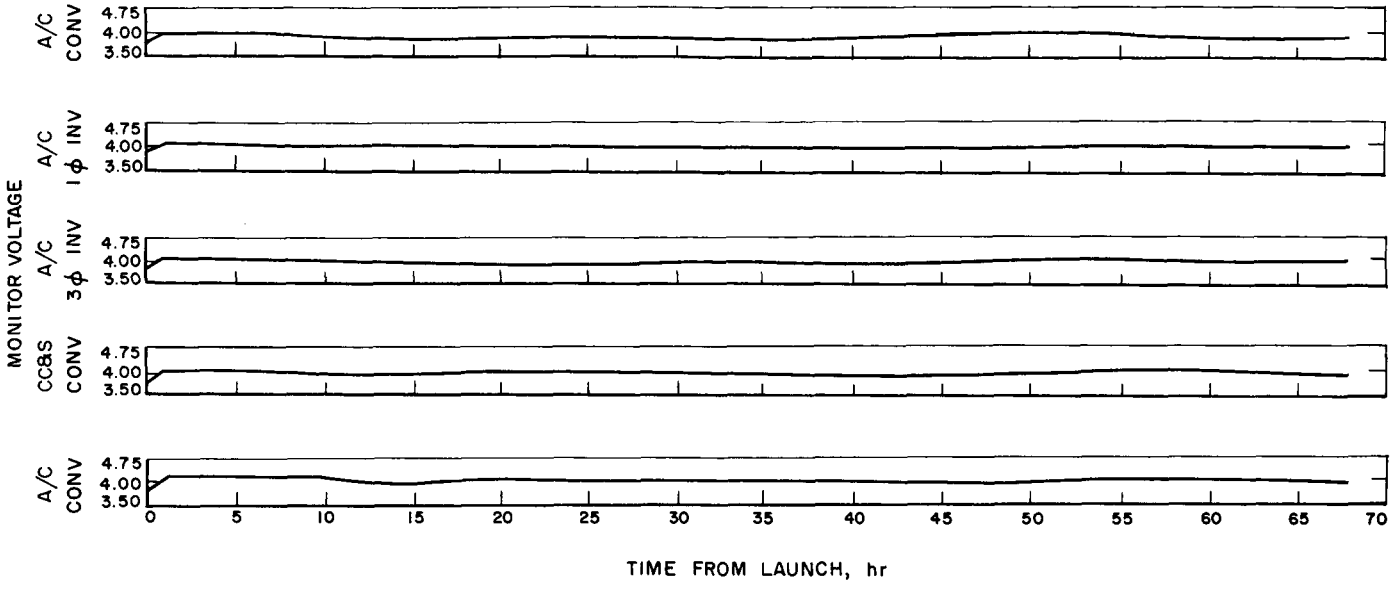

Fig. 17. Power conversion "4-volt" monitors

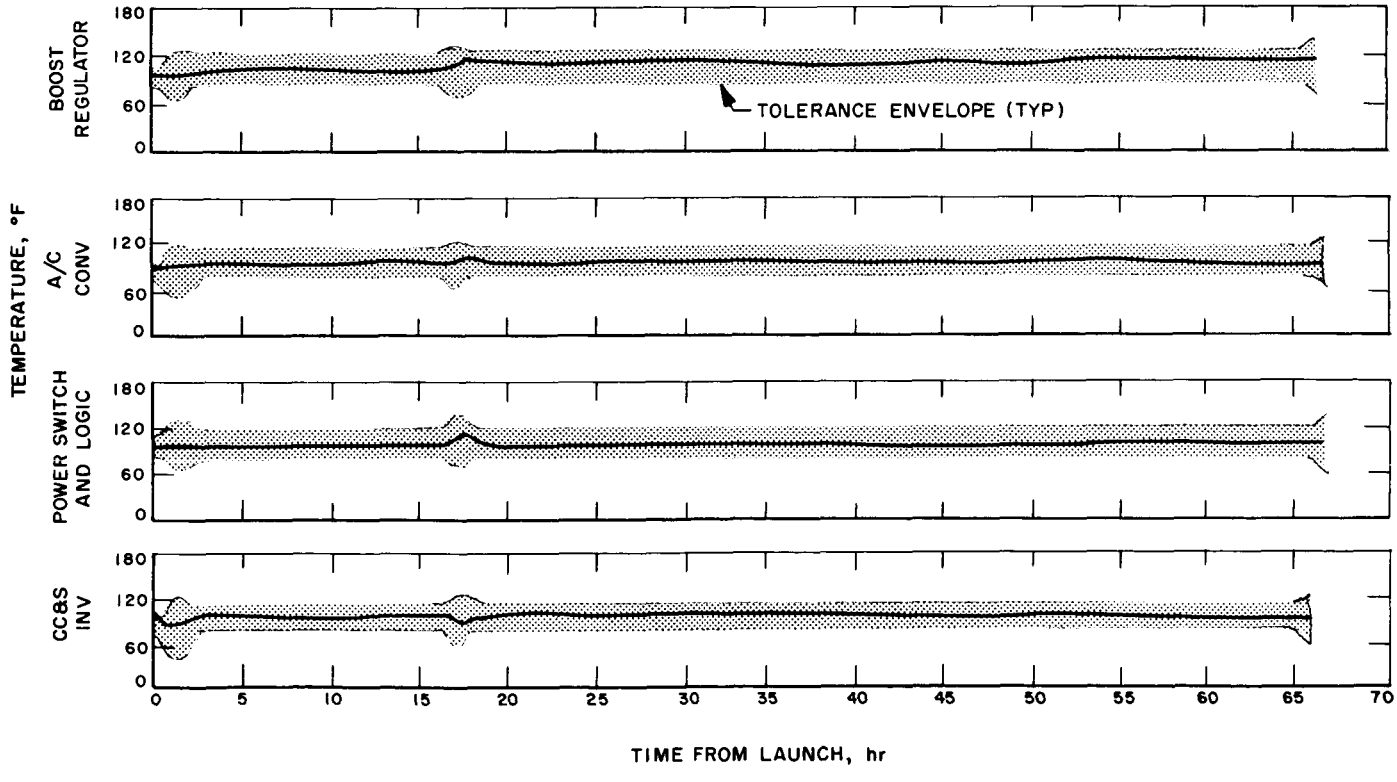

Fig. 18. Power conversion temperatures

D. Central Computer and Sequencer (CC&S)

The Central Computer and Sequencer (Fig. 19) is the control center of the spacecraft, acting upon commands sent from the ground or upon the settings of its internal counters to activate various other subsystems. The spacecraft responds to several types of ground commands: Real Time Commands (RTC) which initiate immediate action (such as RTC-3, antenna switchover), those which start a sequence of actions governed by the CC&S (such as RTC-4, start midcourse maneuver), and the Stored Commands (SC), which transmit magnitude information for storage and subsequent use by the CC&S in controlling the maneuvers. The CC&S in addition provides internal commands (which are established prior to launch) from the diode matrices associated with its counters.

For the CC&S, the flight mission is divided into three phases of major activity: launch, midcourse, and terminal. The launch phase consists of the first few hours of flight, until the spacecraft is in a cruise or coasting mode. The midcourse phase begins with the receipt of the first midcourse maneuver commands and lasts until the spacecraft returns to cruise mode. Similarly, the terminal phase is concerned with the terminal maneuver and subsequent operations. In addition, there are continuing CC&S functions which prevail throughout the mission.

The *Ranger VII* CC&S had power turned on at L − 280 min on July 28, 1964. There were no anomalies during any phase of the mission.

1. Continuing CC&S Functions

During certain portions of the flight it is desirable to have particular engineering measurements, indicating spacecraft performance, telemetered back to Earth. During other portions of the flight, different engineering measurements are desired. For this reason, four different telemetry modes are used. The CC&S issues commands at the proper times to change from one telemetry mode to another.

All spacecraft subsystems requiring time synchronization are referenced to a central clock within the CC&S. The central clock provides the output pulses used for synchronization of other subsystems as well as providing pulses necessary for proper operation of the CC&S. Synchronization pulse trains include a 38.4 kc pulse train to the spacecraft power subsystem, 400 pps and 25 pps to the Data Encoder Subsystem, and 25 pps to the Command Decoder Subsystem. One pulse per second is provided as an input to the launch counter, maneuver clock, and maneuver duration subassemblies of the CC&S. The central clock output pulses are derived from a 307.2-kc

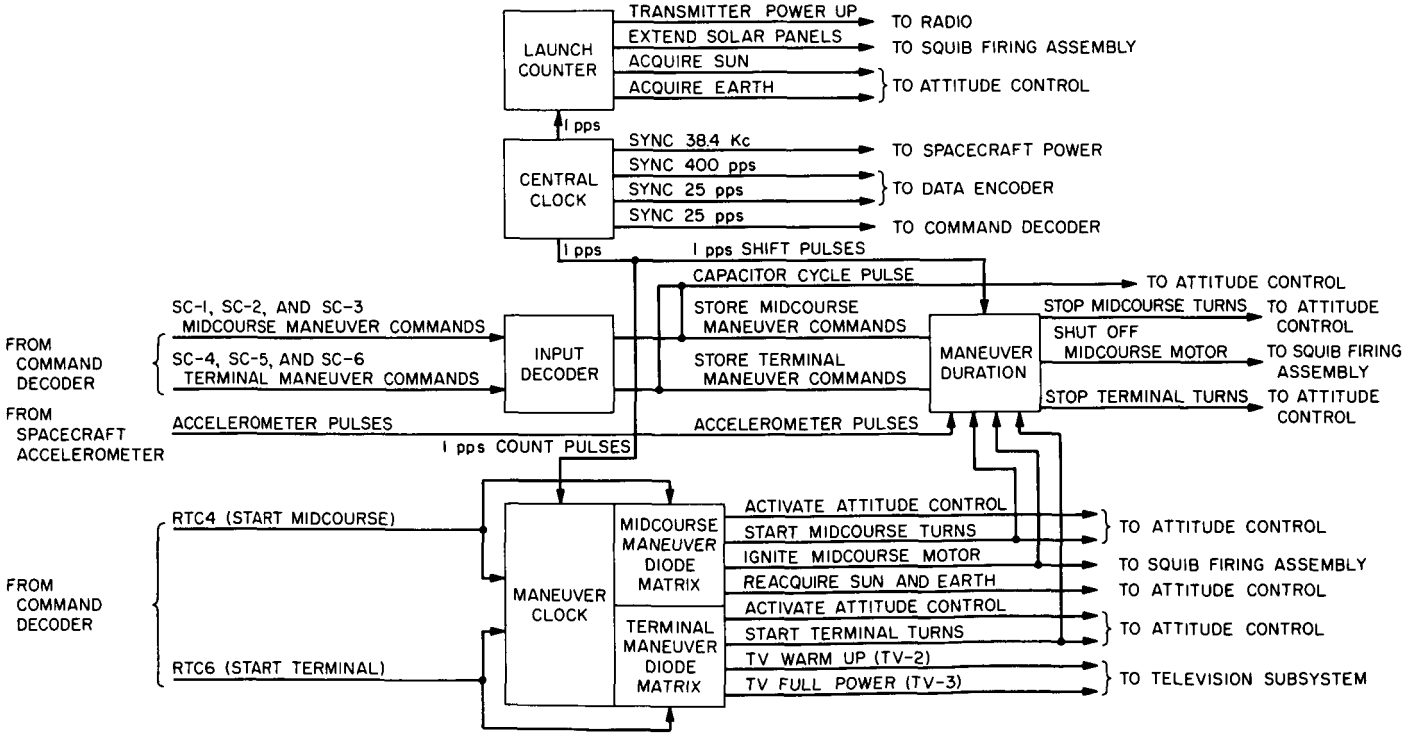

Fig. 19. Central Computer and Sequencer

crystal controlled oscillator (±0.01% design accuracy) that is divided down from the basic 307.2 kc to 1 pps. Transistorized binary flip-flops and ferromagnetic-core divider chains are used to obtain the 1-pps output.

The synchronization pulse frequencies from the central clock, the telemetry mode change signal, and a capacitor cycle pulse (AC1) to the Attitude Control Subsystem are all electron (transistor) switch outputs. All other CC&S outputs are in the form of relay closures. The accuracy of the central clock was better than one part in 250,000 for the 68-hr-plus mission (well within design requirements).

All output pulses (synchronization pulse frequencies, capacitor cycle pulse to Attitude Control, and telemetry mode change pulses) were observed at their nominal times.

2. Launch Phase

The launch counter consists of a transistorized ferromagnetic-core ÷60 circuit which reduces the 1-pps input from the central clock to 1 ppm, and three transistorized ferromagnetic-core, decade counter stages. The result is a binary counter that counts from zero to one thousand in one-minute increments. The counter is inhibited from counting until two minutes prior to launch. An output diode matrix associated with the counter made it possible to preselect a launch phase command time at any one-minute increment from zero to one thousand. The preselection of launch phase command times is accomplished through the proper placement of diodes within the matrix; times can be changed by removing or adding diodes (normally these command times remain fixed for a given mission, and need not be changed).

Ranger VII had four launch phase commands preselected. These consisted of a command to increase spacecraft transmitter power at L + 23 min, extend the solar panels at L + 60 min, acquire the Sun at L + 63 min, and acquire the Earth at L + 211 min. Upon issuance of the acquire Earth command, the launch counter had completed its function. The CC&S continued to count, but issued no more commands until the midcourse maneuver. It was verified that all launch phase commands occurred at their nominal preprogrammed times.

3. Midcourse Phase

The midcourse phase begins when the maneuver information is received from ground and stored in the CC&S. The information is in the form of three binary commands: A roll turn (duration), a pitch turn (duration), and a velocity change. The roll-turn command (SC-1), is sent from the ground, received by the spacecraft Command Decoder Subsystem, checked for accuracy, and then fed to the CC&S, where it goes to the input decoder subassembly and thence to one of three magnetic-core shift registers in the maneuver duration subassembly where it is stored. In addition, on receipt of this, the first of the three stored commands, the input decoder sends a capacitor cycle pulse to the attitude control autopilot which is used during motor burn. The pitch-turn command (SC-2) and motor-burn command (SC-3) are similarly routed to the maneuver duration subassembly and stored in the second and third shift registers respectively.

The midcourse maneuver sequence is initiated on receipt of the real-time ground command (RTC-4). The maneuver clock subassembly begins counting at a 1-pps rate and the midcourse maneuver matrix is energized. The maneuver clock is similar to the launch counter in mechanization and operation. The first command, initiated five seconds after the start of the midcourse sequence (M + 5 sec), activates the maneuver portion of the Attitude Control Subsystem and starts the roll turn. The shift register containing the roll-turn duration starts counting at a constant 1-pps rate; when it overflows it initiates a command to stop the roll turn.

At M + 9.5 min another command from the maneuver clock diode matrix starts the spacecraft into a pitch turn, which is mechanized similarly to the roll turn. Register overflow also changes the telemetry from mode 1 to 2.

At M + 26.5 min, another command from the maneuver clock ignites the midcourse rocket motor; the third shift register receives shift pulses from an accelerometer mounted on the spacecraft and when the desired velocity increment has been achieved, register overflow sends a signal for motor shutoff.

At M + 30 min, a command from the maneuver clock diode matrix initiates the reacquisition of the Sun, and changes the telemetry mode from 2 to 3. At M + 58 min a command is given to reacquire the Earth. At M + 10,000 sec, the maneuver clock has counted to its capacity and it overflows and shuts off, ready to count the terminal sequence when commanded.

Midcourse turn commands, motor burn duration, and reacquisition commands all occurred at the correct times. The desired change in velocity and direction was achieved, resulting in a satisfactory lunar impact trajectory.

4. Terminal Phase

The CC&S has the capability of performing a terminal maneuver in which the CC&S operation, like the midcourse phase, begins with the receipt of the maneuver information in the form of three commands: a first pitch-turn, a yaw-turn, and a second pitch-turn. This sequence of turns is necessary to maintain the high-gain antenna pointed at the Earth throughout the maneuver. Stored commands SC-4, SC-5, and SC-6 containing the maneuver information can be sent, stored, and acted on in a manner similar to the midcourse maneuver, and the same clock and shift registers used. A Real Time Command (RTC-6) initiates the maneuver; however, there is no motor burn and the autopilot is not turned on. The end of the second pitch turn initiates a transfer to telemetry mode 4.

In addition, two commands are furnished to the Television Subsystem while the CC&S is counting the terminal maneuver. Forty-five minutes after the terminal maneuver is started (T + 45 min) an output from the diode matrix of the maneuver clock commands both the F and P channels into warmup. After an 80-sec warmup period, a timer in the TV Subsystem commands them to full-power operation. As a backup to the full-power sequencing command within the TV Subsystem, the CC&S issues a full-power command to both channels about four minutes later at T + 50 min.

Ranger VII required no terminal orientation (or attitude) maneuver since the alignment of the television cameras in the cruise- or Sun-oriented attitude was acceptable. In order to use the TV turn-on capability of the CC&S it was necessary to initiate the terminal sequence. Minimum turn durations (1 sec) were sent and stored in the CC&S in case the RTC-8 (see below) malfunctioned. Prior to initiating the sequence, a ground command (RTC-8) was sent to the spacecraft Attitude Control Subsystem to disregard all forthcoming CC&S commands except for the TV turn-on commands, essentially by "disconnecting" it. The terminal sequence was then initiated. The 1-sec-duration, first-pitch, yaw, and second-pitch turns were properly commanded by the CC&S, and as planned, the spacecraft did not react to them. The television warmup (TV-2) and full-power (TV-3) commands were issued at the proper times by the CC&S.

E. Data Encoder

This subsystem is required to accept, encode, and prepare for radio transmission signals corresponding to voltages, temperatures, pressures and other normally telemetered variables. The block diagram of the Data Encoder shown in Fig. 20 lists all of the telemetered measurements. The Data Encoder uses semi-conductor circuitry and relay commutators. The unit consumes approximately 10 w of power, weighs 27 lb, and occupies about 0.9 ft^3.

Because of the limited bandwidth and signal power available, both time division and frequency division multiplexing methods are employed. Time division multiplexing is obtained by commutation and sub-commutation. Frequency multiplexing is accomplished by the use of ten subcarrier frequencies which are linearly summed for direct modulation of the flight transmitter. The ten channels consist of one channel for the reference timing frequency, three binary subcarrier channels, and six conventional, voltage-controlled-oscillator channels.

The major elements employed to perform this function are: temperature and pressure transducers to convert physical parameters to electrical signals; signal conditioning networks to tailor measurement ranges to the proper levels; commutators to perform measurement selection; rate-limited amplifiers to limit the rate of change of sampled signals to a value consistent with the communication system design; voltage-controlled oscillators (VCO's) and binary oscillators; and modulation mixing networks. Also included as major elements are the data selector or programmer, the event coder and the auxiliary clock.

1. Element Description

To evaluate the Data Encoder it is necessary to observe the performance of certain major elements. These are briefly described below.

Temperature bridges using dc-to-dc converters are employed to convert resistance temperature measurements to dc voltages. Included in the temperature measurements are bridge calibration points to detect possible variations in the supply voltages and changes in the values of the fixed resistors which will affect the temperature measurements.

Voltage-dividing networks, bucking voltage circuits, and amplifiers are used as signal-conditioning devices to tailor measurements to the desired voltage levels. Reference calibration points are included as part of the signal-conditioning network to indicate zero shifts and sensitivity shifts of dc amplifiers, rate limiters, and VCO's.

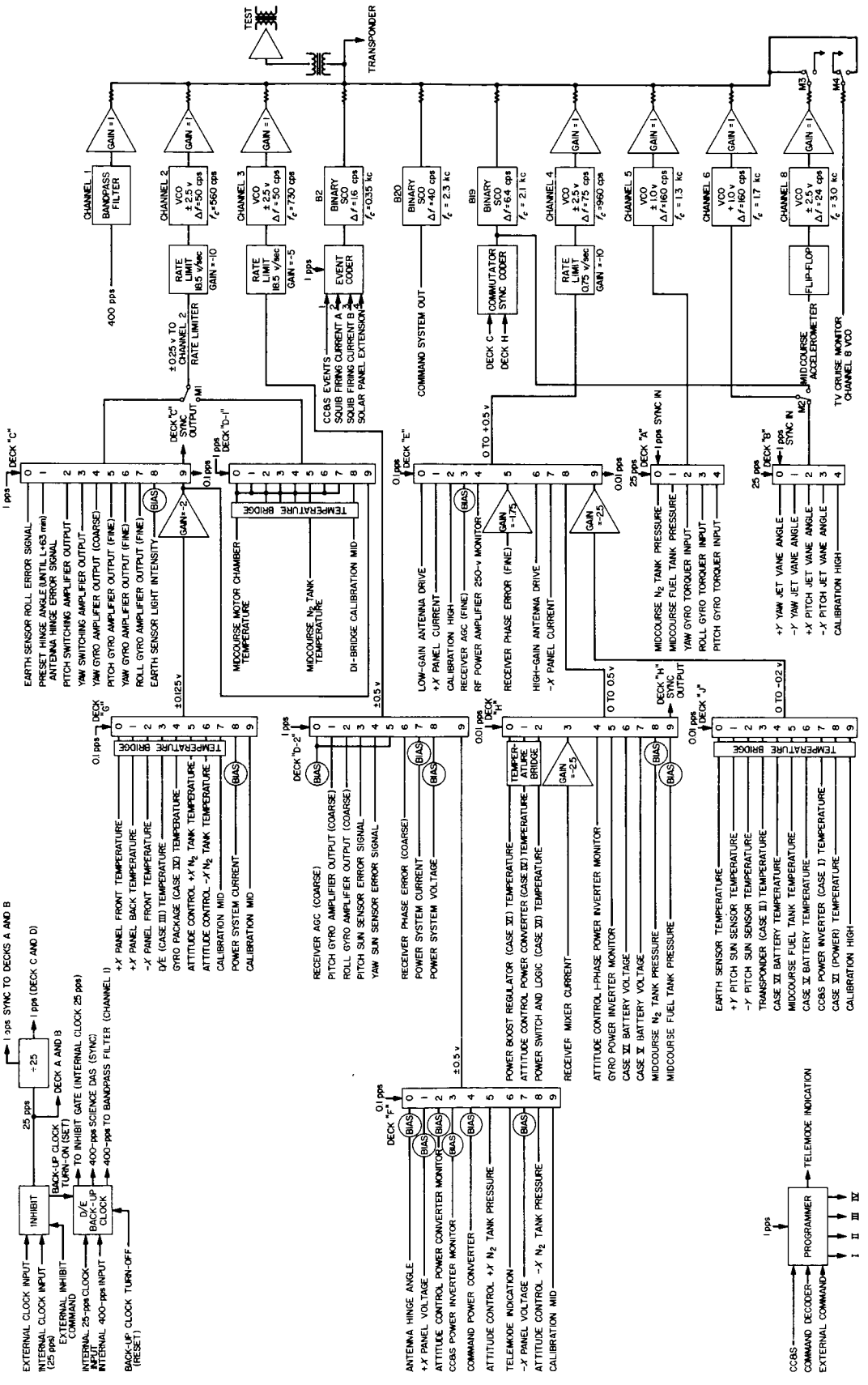

Fig. 20. Data Encoder functions

Both solid-state switches and magnetic latching relays are used as time-division multiplexers to increase the information capability of the telemetry system. These commutators must operate properly so that sequence of measurement selection will be maintained.

Phase-lock-loop discriminators are used in the ground telemetry subsystem to utilize fully the limited power, and therefore, the limited information bandwidth available on the spacecraft. The magnitude of the phase error in the ground phase-lock-loop discriminators is directly proportional to the rate of change of the input frequency and inversely proportional to some power of the loop bandwidth. Since the available power is limited it is impossible to increase the loop bandwidth and maintain the desired threshold performance. In order to maintain a phase error of 30 deg or less for Channels 2, 3, and 4 ground discriminators, it is necessary to control the rate of change of their input frequencies. The rate-limited amplifiers are used to provide the required rate of input voltage to the VCO's. The maximum allowable rate of change of frequency for Channels 2 and 3 is 185 cps/sec and for Channel 4 it is 11.2 cps/sec.

Ten subcarriers are used to perform frequency-division multiplexing. Channels 2, 3, 4, 5, 6, and 8 are conventional VCO's; Channel 1 is a band-pass filter; and Channels B2, B19, and B20 are binary oscillators. Engineering measurement voltages are impressed upon the VCO's. The Channel 1 band-pass filter produces a 400-cps sine wave from a 400-pps rectangular wave provided by the CC&S. Since the 400-pps rectangular wave is the basic clock for the Data Encoder, this information along with the synchronization information discussed below is required by the ground telemetry system to perform automatic data reduction.

Channels B2, B19, and B20 are narrow-band oscillators to transmit binary or two-state information. Channel B2 along with the event coder transmit binary coded information to indicate the occurrence of spacecraft events. The events are listed elsewhere in Appendix A. Channel B19 is used to transmit a time reference (frame synchronization) to indicate the completion of a cycle of the commutator. This information is used by the ground telemetry station to identify the 80 or so commutated measurements. Channel B20 is used for command verification.

The event coder encodes the occurrence of spacecraft events into four codes. Four one-second bit codes are used to identify specific events. The events are read into the event coder in parallel fashion and read out in serial fashion. A priority system is incorporated such that should different events occur simultaneously, the event with the highest priority is read out first.

The Programmer changes the telemetry mode to meet the information requirement of the different phases of Spacecraft operation. The telemetered information on Channels 6 and 8 are changed during the midcourse maneuver mode. Except during this mode, TV telemetry and redundant synchronization information are transmitted via Channels 8 and 6 respectively. During the midcourse maneuver Channel 8 transmits midcourse acceleration information, and Channel 6 transmits attitude-control jet-vane information.

2. Performance of the Data Encoder

The Data Encoder performed to meet all of the design requirements. The commutators, the synchronization signals on Channel B-19, and the basic Encoder timing information on Channel 1 all functioned perfectly, permitting continuous automatic data reduction. No loss of data could be attributed to a malfunction in the Data Encoder.

The performances of the Event Coder and Channel B-2 provided information to indicate the proper sequence and duration of events, and also provided the CC&S subsystem with information to evaluate properly its performance. In all, the occurrences of about 22 events were telemetered. The Programmer performed its function of switching telemetry modes in response to the preprogrammed command from the CC&S.

The successful performance of the Data Encoder is evidenced by the fact that the evaluation of the spacecraft was possible throughout the entire mission. The final test rests with the data users. Except for Channels 5, 6, and 8, the accuracy of the Data Encoder is $\pm 5\%$ of full scale from input to frequency readout. The evaluation of all subsystems by telemetry data indicated their performances have been nominal or as predicted. This leads to the conclusion that the Data Encoder met the design requirements of providing data of sufficient accuracy and fidelity.

The stability of the Data Encoder is indicated by Fig. 21 and 22. The 1-cps variations shown are primarily

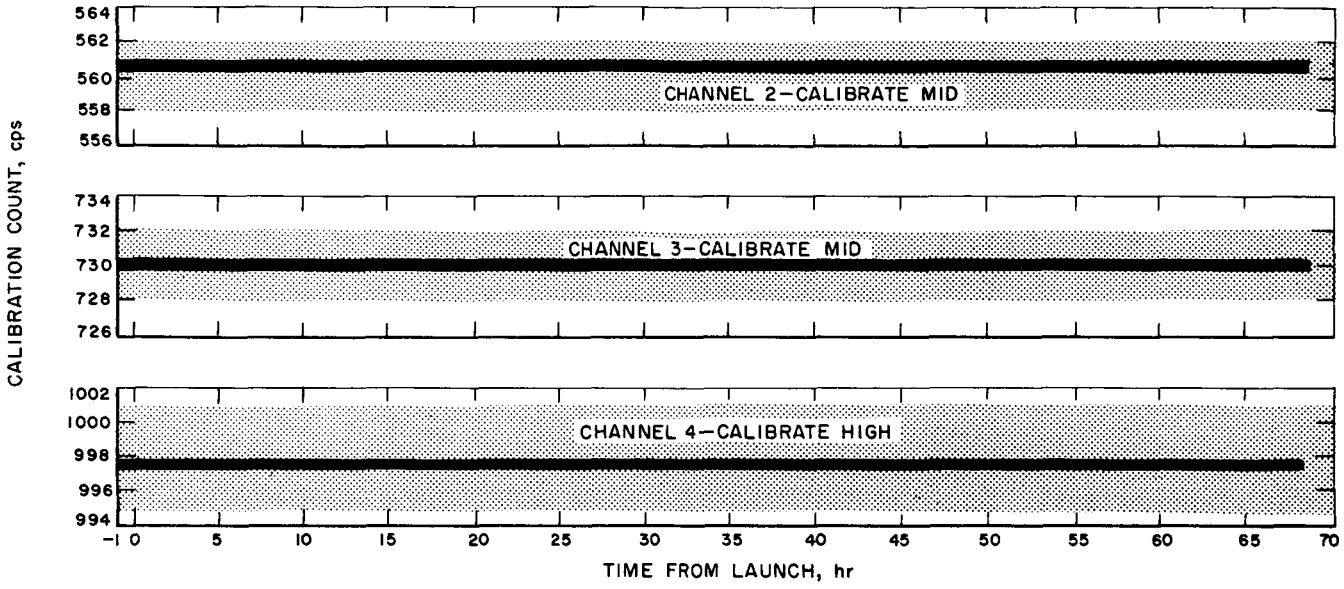

Fig. 21. Data Encoder VCO calibrations

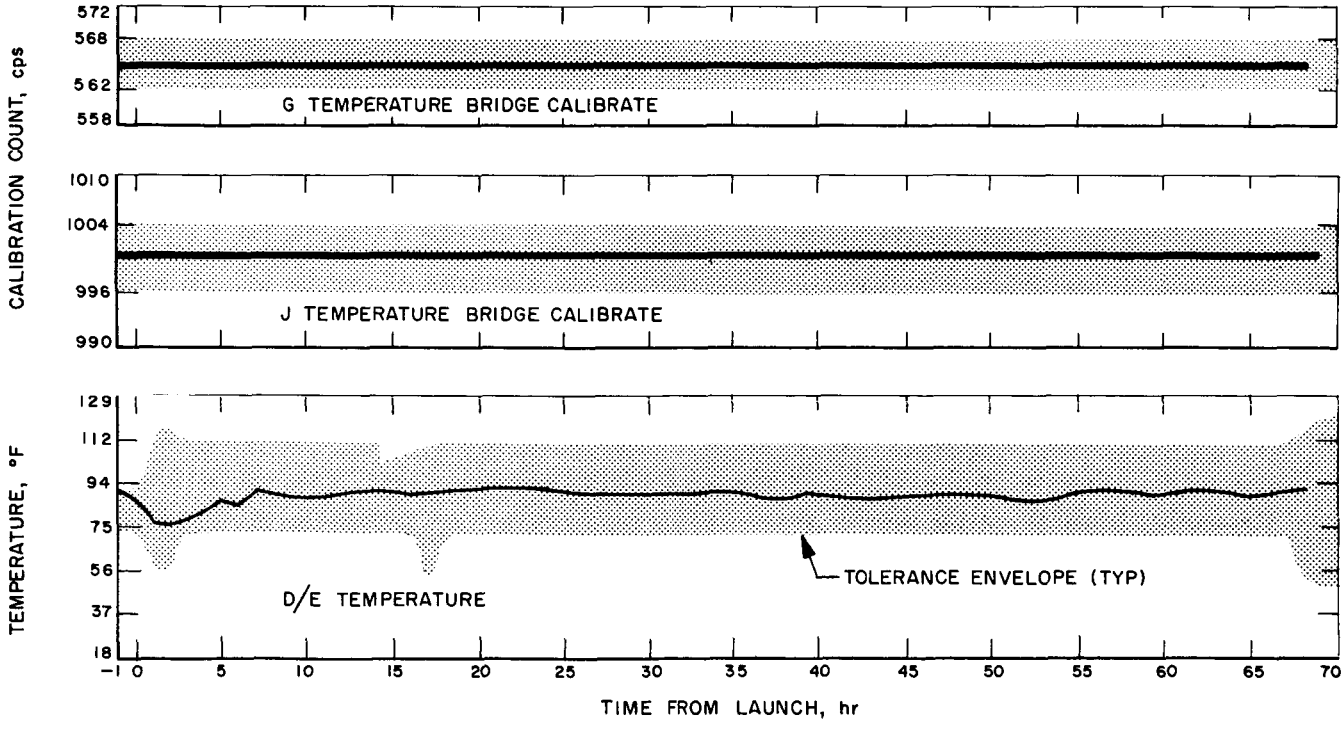

Fig. 22. Data Encoder temperature-bridge calibrations

a result of the ground data handling system and not necessarily indicative of spacecraft drift. Both the VCO calibration measurements (Fig. 21) and the temperature bridge calibration measurements (Fig. 22) for the entire mission show that drift and sensitivity shifts were well within design tolerances.

F. Attitude Control Subsystem

The attitude control subsystem is designed to maintain spacecraft orientation with respect to Sun and Earth, and to control the pointing of the high-gain antenna. Position error signals are obtained from Sun sensors and the Earth sensor, and rate signals are obtained from three single-axis gyros. Control torques about the spacecraft axes are produced by a nitrogen-gas expulsion system. A midcourse autopilot provides vehicle stability during the midcourse motor firing by jet-vane control of thrust direction. System elements are shown spatially in Fig. 23, and functionally in Fig. 24.

1. Prelaunch Conditions

The gas system was pressurized to 3650 psi at 91°F for flight on 21 July. The total gas stored was 4.24 lb. High accuracy (10-sec frequency count) telemetry data indicated 4.24 lb prior to launch on 28 July. The gyro output voltages measured in the blockhouse were very close (within 5 mv) to the levels computed from gyro laboratory readings. Two RTC-2's were transmitted to select the 122-deg antenna preset angle required for the particular launch day.

2. Separation

The earliest data available after spacecraft separation indicates the pitch and roll rates were +2.0 and +0.4 mrad/sec at 1746 GMT. The yaw rate was beyond the −10 mrad/sec saturation limit of the gyro. Since the

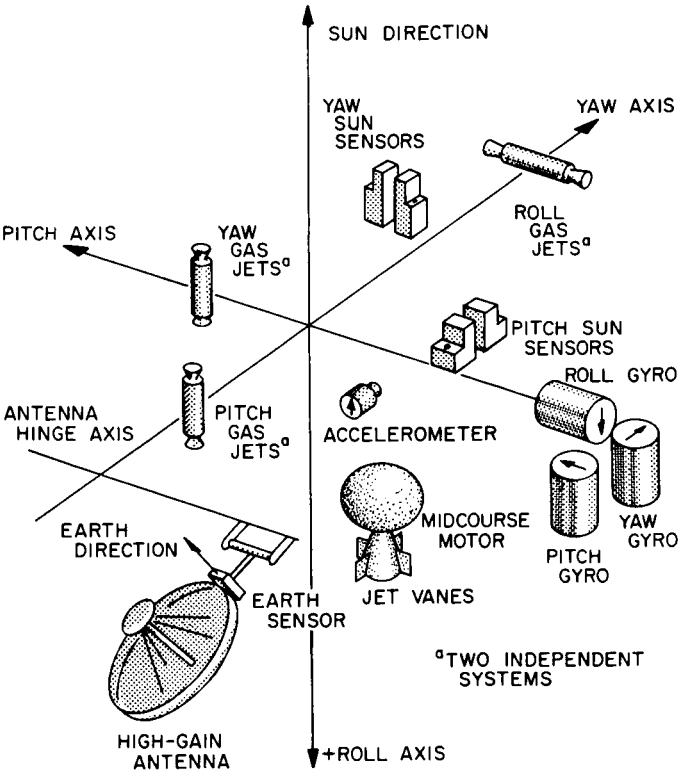

Fig. 23. Attitude Control elements

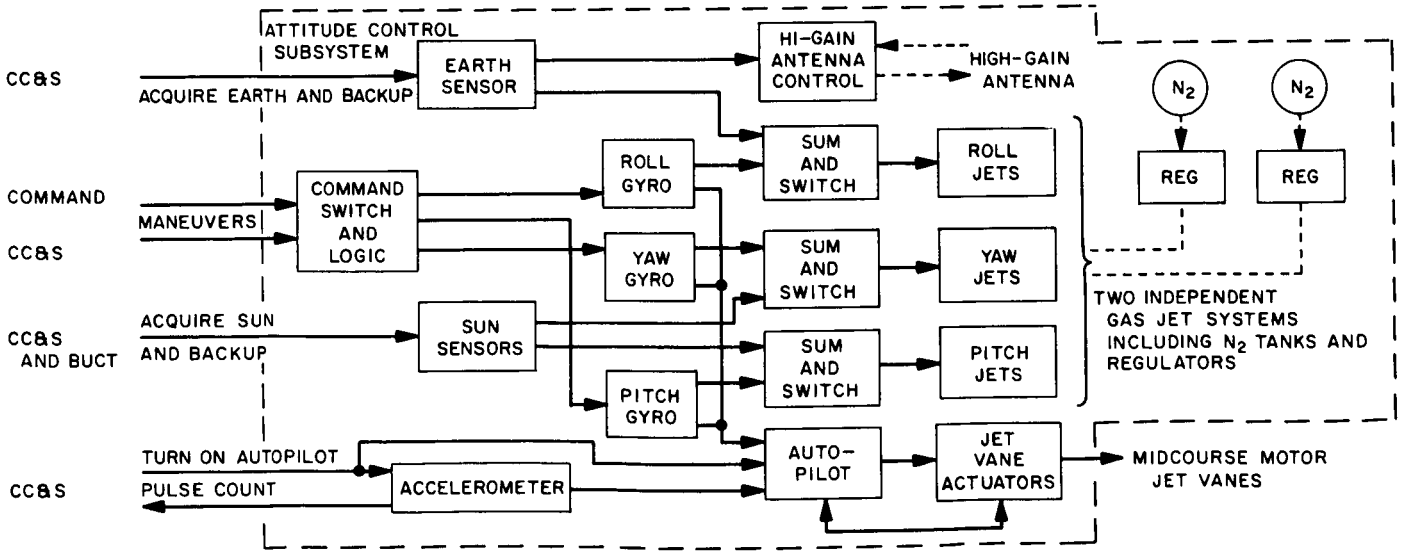

Fig. 24. Attitude Control Subsystem

pitch and roll rates were so small compared to yaw, it may be assumed that cyclic rate variations were negligible, and the above rates were the same as the separation rates. The yaw rate reduced to −7.0 mrad/sec over a 90-sec interval at the time of solar-panel opening.

3. Sun Acquisition

The spacecraft was still in the Earth's shadow at the time of the Sun-acquisition command so that no position error signals were available from the Sun sensors. Under this condition, the only control on the spacecraft attitude is to maintain the pitch, yaw, and roll rates within the rate deadband of ±0.90 mrad/sec. The yaw rate was thus reduced to −0.90 mrad/sec within 16 sec from the Sun-acquire command. When the spacecraft emerged from the Earth shadow the spacecraft began turning toward the Sun at the rate of +5 mrad/sec in yaw and +2 mrad/sec in pitch. The acquisition was completed within 6.5 min after emergence from the Earth shadow. Integration of the acquisition rates indicates the spacecraft rotated approximately 105 deg in yaw and 27 deg in pitch.

4. Earth Acquisition

The Earth-probe-Sun angle at the time of acquisition was 55 deg. The antenna angle (and thus the angle of the Earth sensor to the −Z axis) had been preset to 122 deg to bring the Earth into the sensor field of view. The Moon was not in the sensor's field on this launch day.

Upon receipt of the Earth-acquire command, the spacecraft roll rate increased from an initial +0.9 mrad/sec to the search rate of −4.0 mrad/sec. After a 21-min roll search, during which time the spacecraft rolled through an angle of 310 deg, the Earth sensor detected earthlight and the acquisition was completed within 23 min after the command.

5. Cruise

The system maintained the spacecraft position within the nominal ±2.8 mrad deadband in pitch and yaw. Roll orientation was within the normal deadband limits which vary with the spacecraft-Earth distance. The average limit cycle velocity increment was 60×10^{-6} rad/sec in pitch and 55×10^{-6} rad/sec in yaw which compare well with the design maximum of 90. The external pitch-axis torque varied from −370 dyne-cm at launch + 5 hr to −160 dyne-cm at launch + 20 hr. This compares well with the −170 dyne-cm measured on *Ranger VI*.

6. Midcourse Maneuver

The midcourse parameters were: roll turn, 5.56 deg (24-sec duration); pitch turn, −86.8 deg (392-sec duration); and motor burn, 29.89 meters/sec velocity change. The commanded turns were executed in a normal manner and the gyro transients compared well with results from analog computer simulations. At the time of the start-roll-turn, the roll limit-cycle position was +1.8 mrad which is well within the normal deadband of ±7.0 mrad. This fortuitous circumstance greatly increased the midcourse system accuracy since the initial roll-position error is the predominant error in the system. The pitch and yaw limit-cycle positions at the start of the pitch turn were +2.2 and −1.6 mrad respectively. Their contribution to system error is insignificant. The midcourse autopilot performance was normal in all respects. A more detailed analysis of autopilot performance will be undertaken as better data become available.

7. Reacquisition

Upon receipt of the Sun-acquisition signal from the CC&S the spacecraft accelerated to an acquisition rate of +4 mrad/sec and reacquired the Sun in 5 min 10 sec. The yaw rate and position remained nulled during the reacquisition.

At the end of the motor burn, the residual roll rate had been 0.11 mrad/sec. This rate reduced the roll-position error relative to the Earth from +5.56 deg (introduced by the midcourse roll turn) to −2.0 deg at the time of Earth acquisition. The Earth sensor detected earthlight as soon as it was turned on and acquired instantaneously.

8. Gas System

Preliminary data indicate that spacecraft acceleration by the gas system was 0.46 to 0.50 mrad/sec^2, which is less than the lower design limit of 0.54 mrad/sec^2. The gas jets which provide rotation about each spacecraft axis are fabricated with a nozzle-throat size matched to the moment of inertia about that axis. Uncertainties in matching the thrust to the actual in-flight moments, and changes in the moments with high-gain-antenna hinging, are believed to account for the low-acceleration condition noted. This abnormality had no effect on the system performance since the system is not degraded until the acceleration drops to 0.24 mrad/sec^2, corresponding to the loss of one of the redundant gas-jet systems.

Based on the limit cycle performance the expected gas usage was 0.10 to 0.30 lb. The pressure/temperature telemetry data indicate a usage of 0.16 ±0.06 lb.

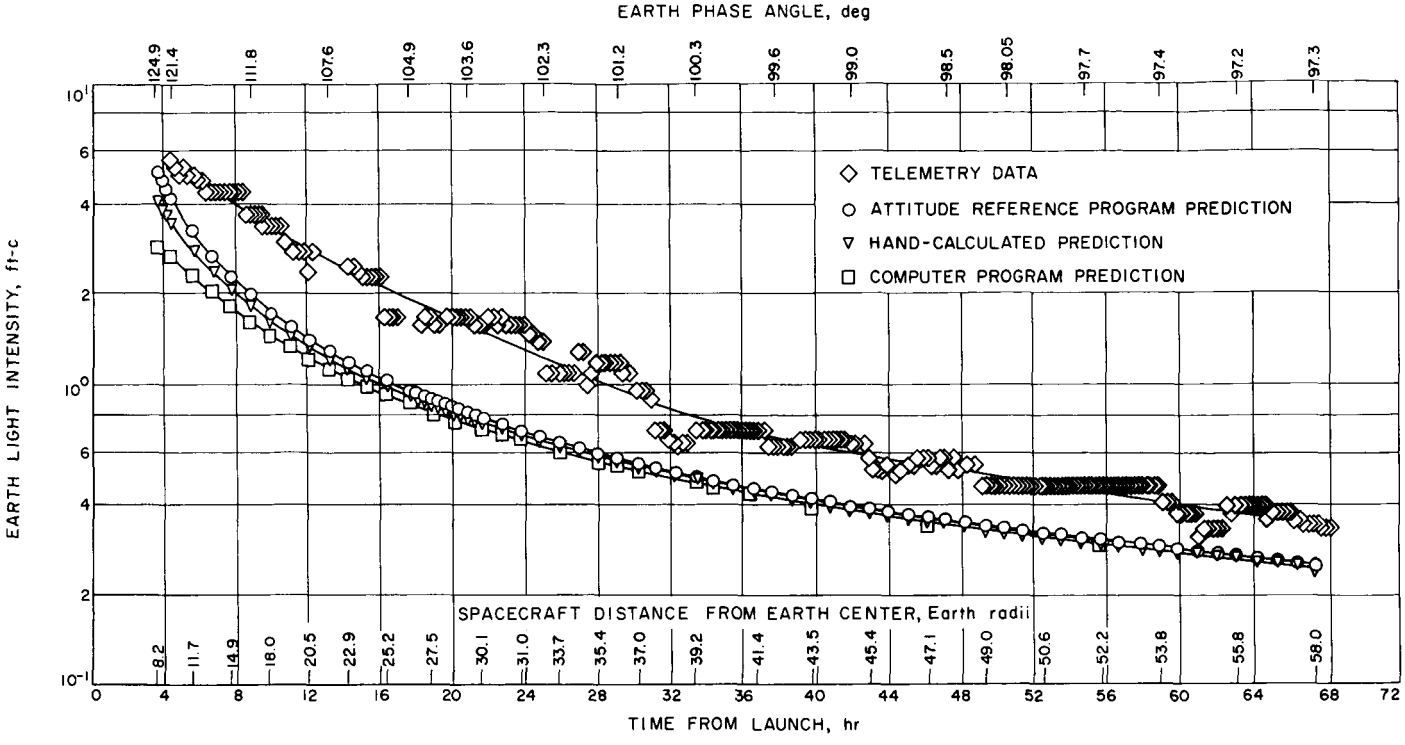

Fig. 25. Earth Sensor Earthlight intensity

9. Antenna Hinge Control

The hinge system tracked the Earth within the 1.25-deg deadband of the hinge servo during the cruise operation. During Sun acquisition, the antenna extended to the 122-deg preset angle inserted before launch. During the midcourse maneuver it moved to the 180-deg exit angle and then to the 109-deg reacquire angle at Sun acquisition. In all cases the slewing rate was well above the 0.30-deg/sec minimum requirement.

10. Earth Sensor

The telemetered earthlight intensity from the Earth sensor was 1.6 to 1.4 times the expected value. This is explained in part by uncertainties of the Earth's albedo and by telemetry system accuracy. Since the characteristic of the measurement is logarithmic, a telemetry subcarrier-frequency error of 0.5 cps multiplies the measurement by a factor of about 1.3. A plot of measured and predicted earthlight intensity is given in Fig. 25.

G. Midcourse Propulsion Subsystem

Successful accomplishment of the *Ranger VII* mission requires the spacecraft to be capable of undergoing a single midcourse propulsion maneuver to remove or reduce vehicle injection-dispersion errors. This maneuver is accomplished through the use of a small, monopropellant-hydrazine propulsion system delivering 50 lb thrust to the spacecraft. This midcourse propulsion system is capable of delivering a variable total impulse in response to signals from an integrating accelerometer circuit. It is functionally a regulated-gas-pressure-fed constant-thrust rocket. Principal system components consist of a high-pressure gas reservoir, a gas-pressure regulator, a propellant tank and bladder, a rocket engine and an ignition cartridge containing a small amount of nitrogen tetroxide to initiate propellant decomposition (Fig. 26 and 27).

The flight performance of the propulsion subsystem was normal. The premidcourse normalized pressures were approximately 3300 psia in the high-pressure nitrogen reservoir and 266 psia in the fuel tank. These pressures remained constant until the motor-burn period, indicating no leakage from either tank. A normal motor burn was accomplished at 1027:09 GMT on 29 July 1964. A velocity increment of 29.89 meters/sec (approximately 50% of the system capability) was commanded, and involved a motor burn time of approximately 49 sec. Regulated fuel-tank pressure was 301 psia and final nitrogen-reservoir pressure was approximately 1700 psia. Both of these values were near those predicted. A positive shutoff was obtained at the end of motor burn; the pressures remained stable until lunar impact.

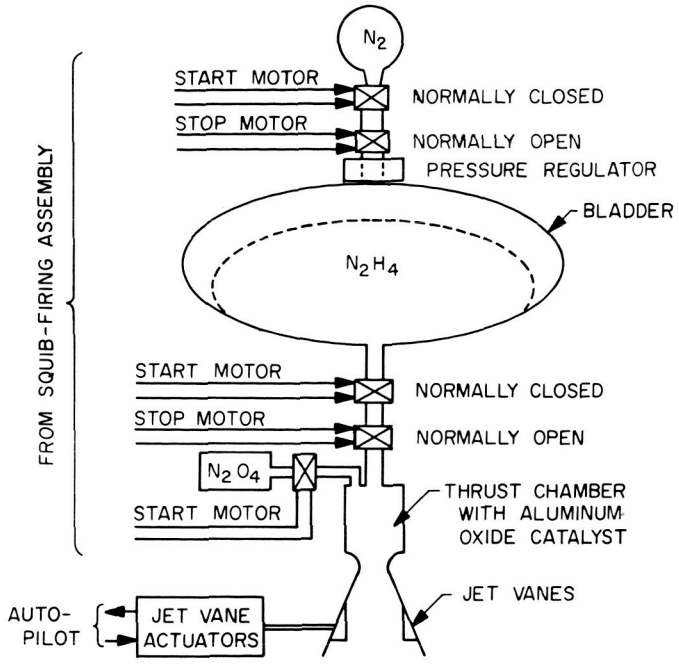

Fig. 26. Midcourse Propulsion Subsystem

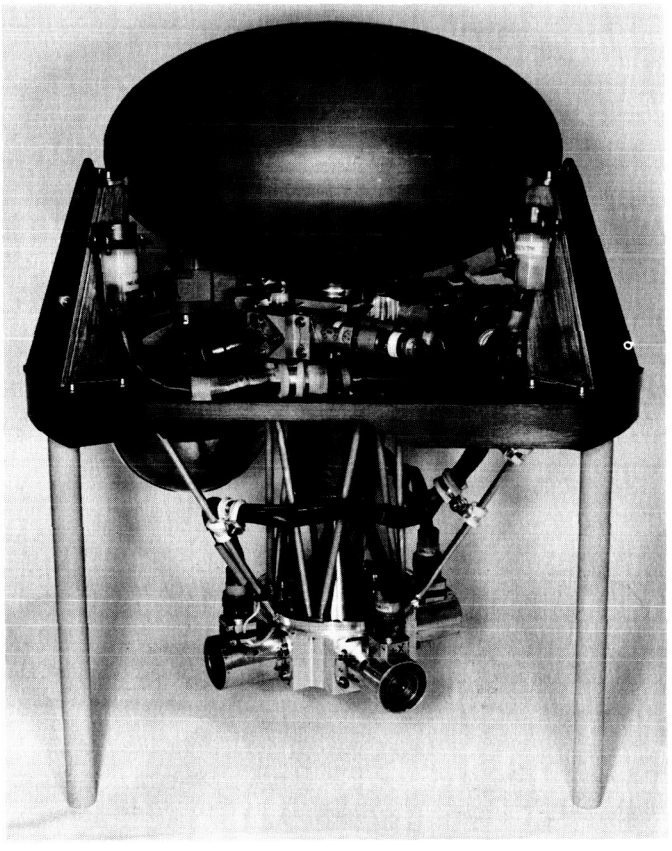

Fig. 27. Midcourse motor

H. Spacecraft Structure

The spacecraft bus structure is a redundant truss-type design of aluminum and magnesium alloys. In configuration, it appears as a series of concentric hexagons, the lower and larger of which comprises the attachment and separation plane from the *Agena* adapter. This plane or base is surmounted by a smaller double-walled hexagonal structure which houses and supports the electronics cases around its outer periphery, and the midcourse propulsion system within its inner periphery. Appendix C includes drawings which show structural details. The structure provides stable reference for the Sun sensor units, the TV subsystem, directional antenna—Earth sensor system, the midcourse propulsion system, and the attitude control system.

During the *Ranger VII* mission, the structure performed its required functions satisfactorily and with no known anomalies.

The high-gain antenna is a circular dish-shaped structure constructed of fabricated sheet aluminum-alloy ribs emanating radially from the center and supported at midpoint and the outer diameter by sheet-metal rings. The dish surface is covered by a black anodized aluminum mesh, held in conformation by the radial ribs and the mid and outer rings. The antenna feed is mounted at the center of the concave side of the dish, supported by four fiberglass, tubular struts. The antenna is driven and maintained at the required attitude by the antenna gearbox through a yoke and arm attached to the convex side of the antenna. In its retracted position, the antenna nests in the rearward end of the spacecraft, just above the separation plane. During ascent, the antenna is protected from vibration effects by snubbing elements provided in the *Agena* adapter.

From a structural and mechanical standpoint, the high-gain antenna performed satisfactorily during the *Ranger VII* mission. There were no known anomalies.

The solar panel substrates are fabricated of spot- and seam-welded aluminum-alloy sheets, providing structural support and protection for the solar cells. The cells are mounted on a flat, rectangular aluminum-alloy sheet, whose flatness and rigidity are maintained by corrugated aluminum-alloy sheets in the longitudinal direction and by cross-bracing in the transverse direction. The cross braces also provide the mounting and the heat sink for the zener diodes of the power system.

During the *Ranger VII* mission, the solar panel substrates performed satisfactorily. There were no known anomalies.

I. Temperature Control Subsystem

The purpose of the temperature control subsystem is to provide a spacecraft temperature environment which is within the operating limits of the spacecraft hardware and electronic components. This environment is to be provided for all spacecraft attitudes and conditions except when an Earth shadow or non-Sun-oriented attitude of greater than 60-min duration is experienced by the spacecraft. Violation of these constraints on the trajectory will, in general, result in an overcooling of some components and, perhaps, an overheating of others.

The Thermal Control Subsystem on *Ranger* Block III is a passive system with no moving parts. Through precise regulation of the radiating characteristics of the external surfaces, the relationship between the input energy and the energy lost to space is regulated to yield the proper spacecraft temperatures.

The philosophical approach taken on *Ranger* is the result of several years of flight and test experience with similar spacecraft criteria (i.e., Sun-oriented, constant power dissipation, short-transit-time flight profile).

One of the major problem areas encountered has been the effects of reflected solar energy. The *Ranger* Block III design is aimed at eliminating or minimizing solar reflections as much as possible. Black paint or black cloth are used on surfaces which might reflect to the spacecraft; polished surfaces are used where practical to direct the reflected energy away from the spacecraft.

There are uncertainties and unaccountable variations in both directly absorbed solar energy and in internal power dissipation. Since these are the only sources of input energy, an attempt is made to have each source account for approximately half of the total. This way uncertainties and variations in either source produce minimum variations in spacecraft temperatures.

A side product of the use of significant amounts of solar energy is that a relatively larger amount of energy must be radiated to space which in turn dictates higher average emittance on the radiating surface. Since uncertainties in emittance measurements seem to be a fixed increment regardless of the absolute magnitude of the emittance, these uncertainties are reflected in smaller temperature uncertainties with increasing average emittance.

Another effect of a higher average emittance is the possibility of using a low absorptance-high emittance surface on the large radiating area to minimize the change in solar load when the spacecraft is in a non-Sun-oriented maneuver.

Space simulators are at best rather inexact duplication of the space environment. One area of difference is the spectrum of the solar simulator, which in general is very different from the actual spectrum of the Sun. However, by use of surfaces which exhibit similar properties regardless of spectrum, the validity of solar simulator tests is greatly enhanced. Such surfaces are called Thermally Grey, and black paint is one of them. In addition, black absorbs almost all of the incident energy, leading to very little reflected solar energy. For these reasons, *Ranger* uses black paint on most of the sunlit areas where energy input and/or solar reflections are important.

Thermal shields (good insulators) are used over large areas of the spacecraft to control the amount of solar energy absorbed and to close off openings in order to help raise the remaining average emittance.

The *Ranger VII* thermal control subsystem maintained the temperatures within the predicted bands at all times. The telemetry measurements indicated that the majority of the measured temperatures were close to the mid-band or predicted nominal temperatures. The exceptionally good performance of the thermal control subsystem on *Ranger VII* compared to *Ranger VI* (which was quite satisfactory) is due to several factors:

a. The solar intensity was less at this time of year.

b. Emitting areas of some cases were increased.

c. The absorptance of the TV subsystem painted surfaces was decreased, resulting in lower temperatures in that subsystem, allowing heat transfer from the bus to the TV tower, resulting in lower temperatures in the bus.

d. A new thermal shield was designed for the high-gain antenna yoke which effected a reduction of the Earth-sensor temperature.

Ranger VII was in Earth's shadow for 39 min. Because of the cooling expected during the Earth-shadow phase,

Table 3. *Ranger VII* flight temperature summary

Location	Temperatures, °F				Predicted limits, °F	Operating limits, °F
	Launch	Pre-M/C	Post-M/C	Pre-impact		
+X solar panel (front)	75	130±	130±	146±	105-131	112-131
+X solar panel (back)	75	114	114	132	105-131	112-131
−X solar panel (front)	73	130±	130±	146±	105-131	112-131
Data encoder	87	87	89	87	70-110	32-131
Gyro package	91	91	96	92	75-115	40-131
+X A/C N_2 bottle	75	75	77	81	65-105	32-148
−X A/C N_2 bottle	75	74	74	77	65-105	32-148
Booster regulator	101	104	109	109	80-125	32-131
A/C Inverter	93	95	95	93	75-115	32-131
Power switch & logic	94	96	104	100	75-120	32-131
Earth sensor	75	61	59	65	20-90	14-94
+Y pitch sensor	73	71	77	78	65-110	40-140
−Y pitch sensor	70	75	76	78	65-110	40-140
Transponder	86	89	92	93	70-110	32-148
Case V battery	82	82	90	85	65-105	50-130
M/C fuel tank	78	81	94	89	70-105	32-148
Case VI battery	78	77	85	80	65-105	50-130
CC&S inverter	95	100	105	103	80-110	32-131
Case VI chassis	94	91	96	100	75-110	32-148

±Temperature transducers have a correction of 16°F less.

the launch temperatures were elevated a few degrees compared to previous *Rangers*.

Tables 3 and 4 show the indicated temperatures of the various components as received from telemetry and reduced by the PDP-1 computer. Table 3 compares the temperatures at the critical phases of the flight with the predicted temperatures and the component temperature limits. Table 4 summarizes the temperatures experienced during the time in the Earth's shadow.

The solar panels indicated temperatures that were within the predicted bands at all times. The front sides indicated temperatures of 130 to 132°F for the cruise equilibrium temperature, which because of the transducer thermal finish is believed to be 16° higher than the actual panel temperature. The solar panel temperature readouts during the Earth-shadow and midcourse phases of flight were at the lower limit imposed by the data encoder and do not represent true temperatures. It is estimated that the panel temperatures did not exceed −100°F during the Earth's shadow and −20°F during the midcourse maneuver. During the last hour of flight the solar panel temperature was greatly influenced by the lunar albedo and infrared radiation. Both the $+X$ and $-X$ front temperatures increased by 14°F and the $+X$ back temperature increased 16°F.

The internal temperatures were within the predicted cruise temperature range at all times. During the period that the spacecraft was in Earth's shadow, the internal temperatures decreased. The change in temperature varied, but the variation was between 2 to 13°F. The batteries, which were well insulated and massive, showed the least variation, as expected, and the data encoder had the greatest change.

During the midcourse maneuver, the attitude of the vehicle was such that the face of electronic assembly VI was approximately broadside to the Sun and electronic assembly III was on the shaded side of the spacecraft.[3]

The temperatures of the booster regulator, the power switch and logic and the case VI chassis increased, while the data encoder temperature dropped about 7°F. The electronic assemblies adjacent to VI-A did not show a very large change but the electronic assemblies adjacent to III did. The gyros increased approximately 3°F due more to the increased electrical power dissipation than to the attitude, while the power inverter remained relatively constant. Electronic assembly II, the transponder, showed some shading effect also.

[3]See Appendix C for configuration and location of assemblies.

Table 4. Earth-shadow temperatures

Location	Measured temperature, °F					
	Launch	Enter shadow	10 min after enter shadow	20 min after enter shadow	38 min after enter shadow (exit shadow)	16 hr after enter shadow
+X solar panel (front)	75	—	—	—	—	130[a]
+X solar panel (back)	75	—	—	—	—	114
−X solar panel (front)	73	—	—	—	—	130[a]
Data encoder	87	86	83	79	73	89
Gyro package	91	91	91	90	89	96
+X A/C N_2 bottle	75	75	73	72	72	77
−X A/C N_2 bottle	75	78	76	74	72	74
Booster regulator	101	108	107	106	103	109
A/C inverter	93	93	90	87	85	95
Power switch & logic	94	97	96	96	94	104
Earth sensor	75	64	59	56	55	59
+X pitch sensor	73	66	62	56	45	77
−Y pitch sensor	70	66	59	50	42	76
Transponder	86	86	85	77	72	92
Case V battery	82	86	86	86	85	90
M/C fuel tank	78	80	80	80	78	94
Case VI battery	78	83	83	83	82	85
CC&S inverter	95	95	95	95	95	105
Case VI chassis	94	91	89	87	82	96

[a] Temperature transducers have a correction of 16°F less.
— Not available.

After the midcourse motor fired, a portion of the heat it generated was distributed to the internal components and increased their temperatures. After the vehicle was returned to its cruise attitude the components dissipated the excess energy and achieved equilibrium temperatures not very different from pre-midcourse values.

As was the case on *Ranger VI,* electronic assembly VI-A was the only assembly whose internal temperature was affected by the lunar albedo and IR radiation. The booster regulator, power switch and logic and the case chassis all showed increasing temperatures during the last half hour of flight.

The majority of the external components, like the solar panels, did not operate within the cruise predicted band at all times. Despite the fact that the attitude control nitrogen bottles had a good shield, the long Earth-shadow period caused the bottles to drop approximately 12°F. During the midcourse maneuver, they were not affected to a very large degree.

The Sun-sensor temperatures during the Earth-shadow phase dropped approximately 28°F and were approaching 40°F, their lower operating limit, when Sun acquisition was completed. These temperatures were well within the predicted bands for this transient region. After Sun acquisition the sensors started increasing in temperature and achieved a steady-state temperature within three hours.

The *Ranger VI* Earth sensor operated at a temperature which was somewhat higher than desired. A better conduction path existed between the Earth sensor and the yoke than had been believed. A shield was added to the yoke on *Ranger VII* to minimize the change in solar input with hinge angle. The shield also reduced the radiating area of the yoke, and, therefore, the net result was a more uniform operating temperature for all antenna hinge angles. This modification to the yoke and its consequence on the yoke temperature had a direct influence on the Earth-sensor temperature.

During the Earth-shadow phase the sensor dropped from approximately 74°F to 54°F. These temperatures were within the predicted cruise band at all times. Shortly before the Earth-acquisition command was given, the sensor had risen to approximately 62°F, where it remained until the midcourse maneuver. During the maneuver, it was on the shaded side of the spacecraft,

but it only cooled 2°F; apparently, it and the yoke were receiving solar radiation while the antenna was at the exit angle. The Earth sensor temperature was slightly influenced by the lunar albedo and IR radiation.

J. Solar Panel Extension and Support System

The solar-panel hinge, latch-support structure, pyrotechnic pin-puller, point damper, and actuator have the required function of supporting the solar panels in a manner to avoid high dynamic loads during the launch and deploying the panels in approximately one minute after the squib-firing current is supplied.

The solar-panel actuators were predicted to open 142 sec nominal (163 sec maximum) after the B-2-1 indication of CC&S solar-panel extension command. The B-2-1 blip occurred at 1750:00 GMT. The B-2-4 blip indicating that the $+X$ panel was deployed occurred at 1751:17 (77 sec after the CC&S command). This was 65 sec faster than predicted. Satisfactory currents and voltages indicating solar power from both panels showed that both panels opened as designed.

The most probable conclusion that can be drawn from this fast opening is that the solar-panel actuators were actually warmer than was predicted from the temperature time-in-Earth-shadow curves. These curves were based on tests in which the actuators were cooled in a simulated Earth shadow with the panels open. In actual flight the panels were closed during flight through the Earth shadow, so that the actuators lost less heat and thereby were warmer at the time of solar-panel extension. Based on the actual opening time of 77 sec the actuators were 54°F.

The nominal deployment time and proper solar-panel performance throughout the flight indicate normal performance of the equipment during the flight.

K. Miscellaneous Timing and Arming Functions

1. Backup Command Timer (BUCT)

The BUCT is a hydraulic device which, through mechanical linkage, actuates a switch assembly to complete a common circuit. It provides spacecraft on-board command-signal redundancy for four crucial commands. The BUCT is installed between the spacecraft and the *Agena* adapter and is set into operation by the removal, at spacecraft separation, of the restraint provided by the *Agena* adapter.

The command sequencing and nominal times with respect to spacecraft/*Agena* separation are as follows:

1. Arm the squib firing assembly (SFA) at 2.5 min (Backup)
2. Release inhibit of TV subsystem at 30 min (Backup)
3. Deploy solar panels command at 45 min (Backup)
4. Initiate Sun acquisition command at 60 min (Backup)

These functions were successfully accomplished, presumably by primary command.

2. TV System Arming Switch

The primary function of releasing inhibit of the TV subsystem is accomplished by a solar-panel actuated microswitch located at foot *E* of the spacecraft. The indications are that this function was satisfactorily performed during the *Ranger VII* mission.

3. TV Backup Clock Turn-On Switch

A microswitch located at the base of the spacecraft and actuated by spacecraft/*Agena* separation, causes turn-on of the TV backup clock. This function was satisfactorily performed during this mission.

L. Pyrotechnics Subsystem

The pyrotechnic subsystem (Fig. 28) consists of four squib-actuated pin pullers, three squib-actuated valves, and a squib-firing assembly (SFA). The SFA is a redundant unit employing separate battery sources, armed by separate g-switches during the boost phase, and fires redundant squibs upon command from the CC&S. The arming of the unit is backed up by the BUCT, and in the event of a CC&S failure the BUCT will command the SFA to fire the solar-panel squibs.

The arming of the SFA was accomplished as attested by the fact that the squib firing events did occur. Whether the g-switches or the BUCT armed the SFA is not known since no telemetry gives this information.

The predicted time for command of solar-panel extension was 1750:00 (62 min after CC&S inhibit release). B-2-1, B-2-2, and B-2-3 event blips observed at the time indicate that the CC&S sent the command to the SFA, which in turn, sent the current to the A and B redundant squib circuits.

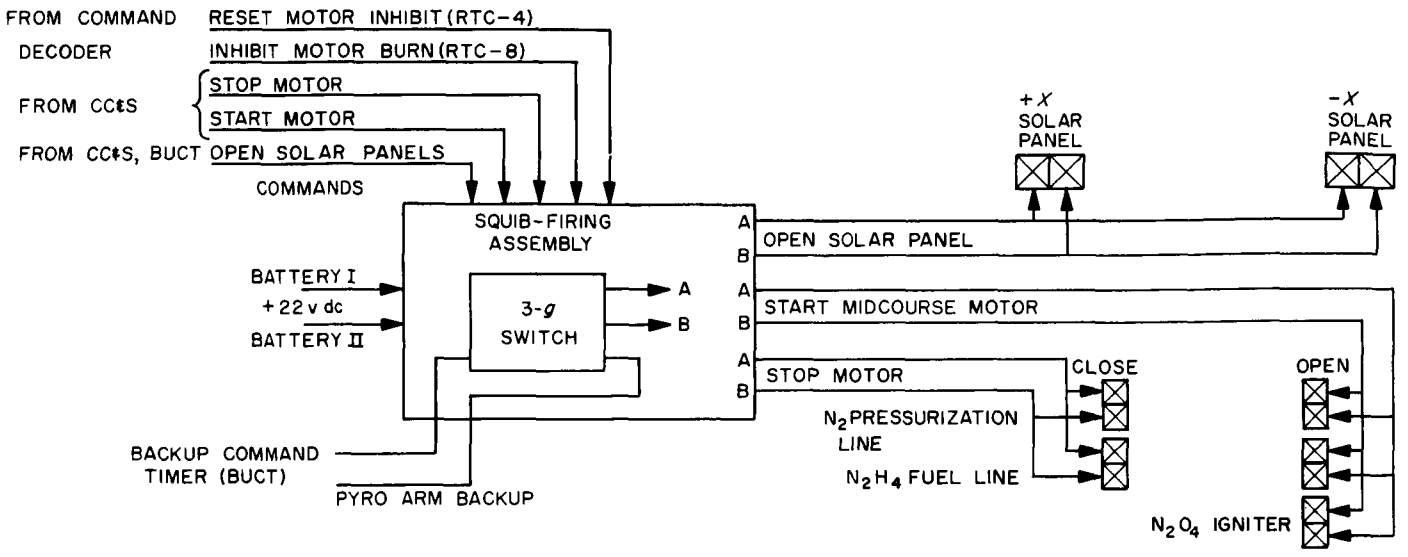

Fig. 28. Pyrotechnics Subsystem

Nominally, the nitrogen, fuel and oxidizer valves on the midcourse motor are opened by redundant squib firings on command from the CC&S at 26.5 min after maneuver initiation. The nitrogen and fuel shut-off valves are closed by redundant squib firings on command from the CC&S when the accelerometer pulse count reaches the stored value. The B-2-1, B-2-2 and B-2-3 blips at 1027:09 and 1027:59 GMT indicate that both A and B squib circuits fired for both motor ignition and cutoff. The start and stop of accelerometer pulses at these times verify that the pyrotechnic subsystem performed its designed task.

M. Electronic Packaging and Cabling

The electronic assemblies for *Ranger VII* provided conservative mechanical support for electronic components in order to ensure proper operation throughout the various environmental exposures. The assemblies consisted of structural units which were integrated into the spacecraft by bolting to the six bays of the structure. Each electronic assembly consisted of one or more functional subsystems consisting of subassemblies of various widths and standard cross section, bolted into a metal chassis and interconnected by pigtailed cable harnesses which were connected into the system "ring" harness. The subassemblies were designed to perform as an integral part of the spacecraft structure and to provide a high conductive thermal path from the components to the primary thermal-control surfaces.

By means of Electronic Packaging Specifications, the following system goals were achieved:

1. Materials were restricted to a few whose space-environment behavior had been evaluated and understood.
2. Hard-mounted circuit boards were employed for added structural strength and to minimize temperature gradients from components to temperature control surfaces. This technique provided an operating margin in the dynamic and temperature environments without weight penalty. Further, the circuit-board design permitted optimum maintainability and modification without reducing subassembly integrity, and provided for simple and unlimited replacement.
3. Since a standard subassembly cross section and a defined chassis mounting were used, the requirements for the thermal and dynamic environments could be evaluated and understood prior to subassembly layout and design, resulting in improved end reliability.
4. Conformal coating was employed to obtain an assured complete insulation of all electrical conductors, which reduced the hazards from peripatetic space trash.
5. Hidden solder joints and trapped air voids were eliminated.
6. Connector pin retention tests were used to obtain interconnection integrity.
7. Test-equipment connections were provided on the assemblies to permit electrical testing without hardware degradation.

The function of the cabling system was to interconnect the various assemblies. The cables were built in accordance with a JPL specification and properly fitted; samples of wire were tested environmentally prior to final assembly. The spacecraft cabling was divided into three groups: the subsystem interconnection harness usually referred to as the "ring harness," the squib harness, and the assembly harness or case harness. The ring harness separated the wires into two bundles for "clean" and "dirty" signal characteristics to eliminate or minimize noise pickup. The squib harnesses were physically separated from other harnesses to prevent impulse signals from affecting squibs. The assembly harnesses allowed environmental and functional testing as well as checkout of the assemblies prior to incorporation into the total spacecraft system.

During the *Ranger VII* mission, the spacecraft electronic packaging and cabling areas performed within their design expectations and no anomalies were recorded.

N. Television Subsystem

The TV Subsystem was designed to provide the equipment to fulfill the mission objectives of obtaining high-resolution video pictures of the lunar surface. The design objective was to have a system capable of a resolution of 0.5 to 5 m in the final picture.

Two separate chains of equipment comprised the subsystem in order to give increased reliability. Each chain contained slow-scan video cameras, camera electronics, sequencing circuits, transmitters, power supplies and control circuitry. The two chains were essentially similar with the exception of the camera configurations. The F chain contained two fully-scanned ("F") one-inch-vidicons, while the P chain contained four partially scanned one-inch-vidicons. The cameras of each chain were exposed and read out in sequence, with the two chains operating simultaneously. The video output was utilized to modulate the FM transmitters for transmission of the signal to the Earth-based receiving stations. For utilization in real-time subsystem performance analysis, diagnostic telemetry was: transmitted through the bus telemetry system by the bus transponder, and also combined with the video signal for transmission by the TV transmitters.

The TV Subsystem is electrically complete and independent of the spacecraft bus with three exceptions: commands are received from the spacecraft command receiver and the on-board computer and sequencer (CC&S); the spacecraft data encoder receives and passes on TV-Subsystem diagnostic telemetry; and the spacecraft's directional antenna is used by the TV transmitters.

1. Subsystem description

The major assemblies of the Subsystem are: cameras, camera and control sequencer, telecommunications, electrical power, command and control, back-up clock, and structure with associated passive thermal control. The electrical block diagram is shown in Fig. 29.

a. Cameras. The camera system is composed of six vidicons which operate in a slow-scan mode. The "F" channel has two fully-scanned cameras (400 optical line pairs) F_a and F_b, and the "P" channel has four partially-scanned cameras (100 o. l. p.) P_1, P_2, P_3, and P_4. The camera tube is an electrostatically focused and deflected one-inch-diameter vidicon with an ASOS photoconductor target.

Each camera consists of a camera head assembly (vidicon, shutter, lens, preamplifier and housing) and its individual camera electronics assembly. The received image is focused on the vidicon photoconductor target by the lens and exposed by the shutter. The shutter utilized is an electromagnetically-driven, linearly-actuated slit, located in front of the vidicon focal plane. The image formed on the photoconductor causes target resistance variations equivalent to the image brightness. After exposure, a high-frequency electron-beam signal scans the target and restores the charges on the target. During the beam scan the charge current is conducted off the target as video signal and coupled to a preamplifier. The signal is passed through the preamplifier and a video amplifier and gated in a video combiner, then sent to the respective transmitter. The associated camera electronics supplies the necessary operating voltage, sweep signals, focus signals and shutter pulses for the camera head assembly. The nominal camera fields of view are indicated in Fig. 30.

The dynamic ranges of the cameras were set to cover a possible lunar-luminance range from 20 to 2700 ft-lamberts. Cameras F_a, P_3 and P_4 cover 20 to 650 ft-lamberts, and cameras F_b, P_1 and P_2 cover 80 to 2700 ft-lamberts. The F type cameras had a 5-msec shutter-exposure time; F_a had a 25-mm-focal-length lens and F_b a 75-mm lens. The P cameras had a 2-msec shutter-exposure time; P_1 and P_2 had 75-mm lenses, and P_3 and P_4 had 25-mm lenses.

The F-type camera utilizes 1152 active horizontal scan lines over a vidicon faceplate area of 0.44 × 0.44 in. The

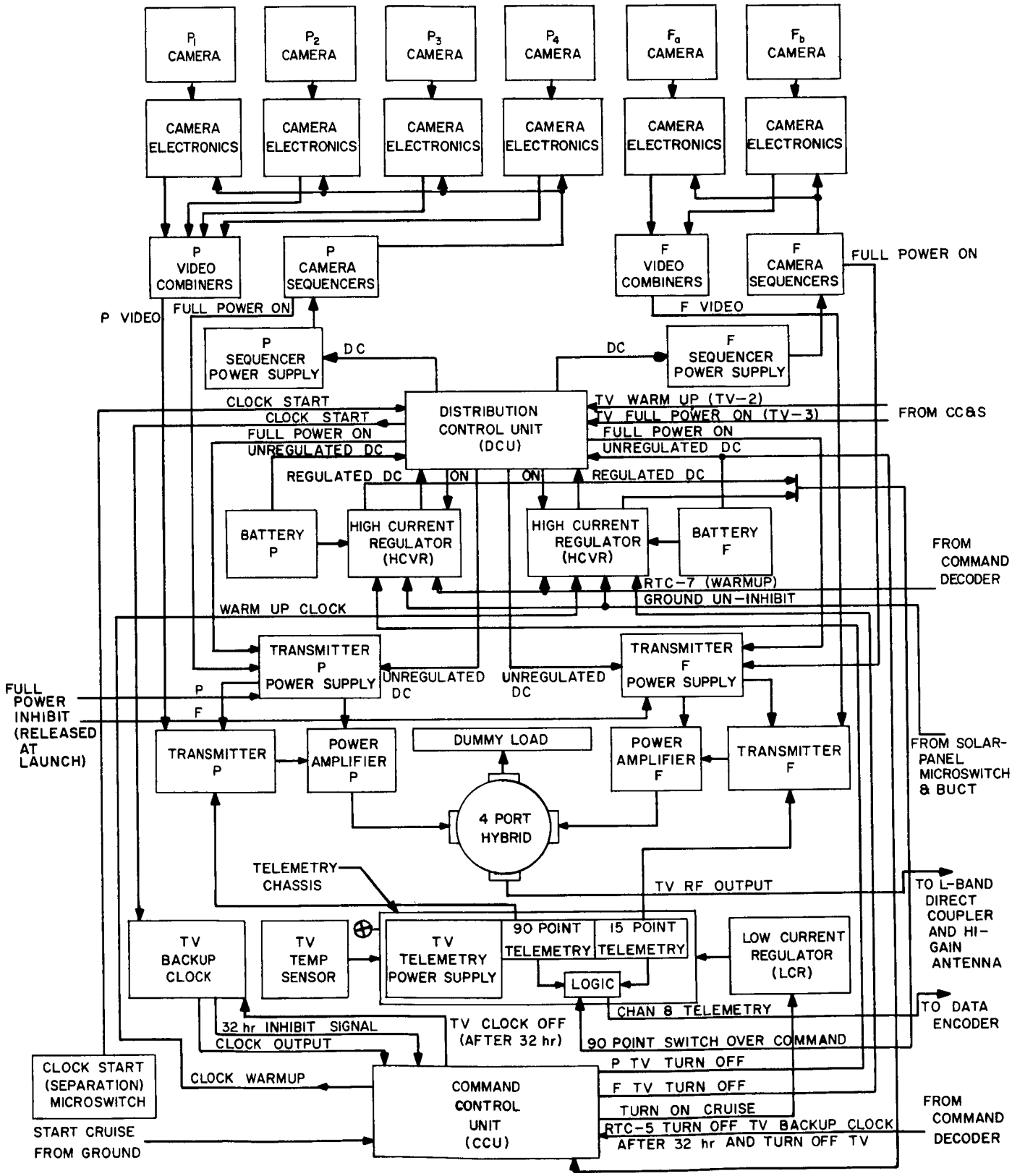

Fig. 29. Television Subsystem

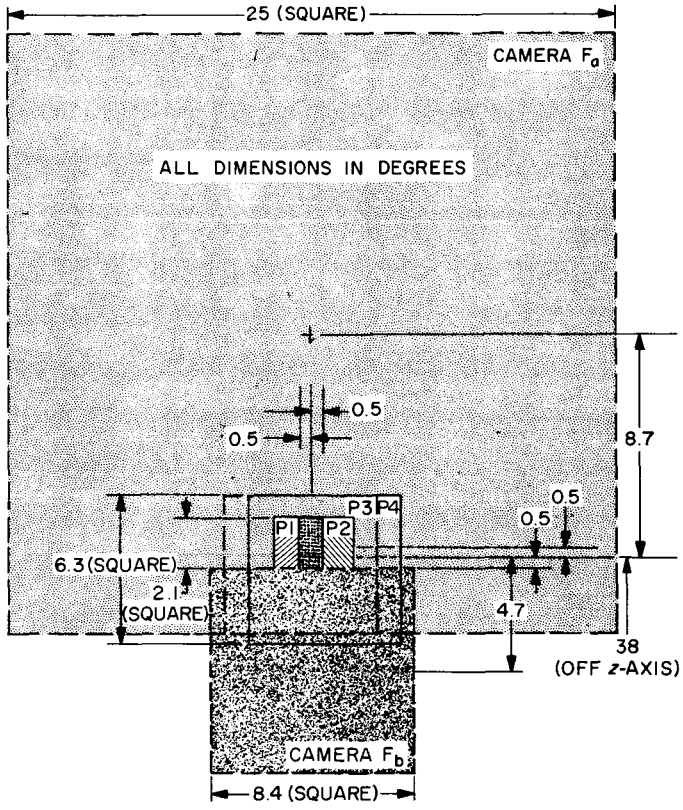

Fig. 30. TV camera fields of view

horizontal scan rate was 450 cps, with 0.22 msec apportioned to horizontal blanking. The active scan lines, plus 46.6 msec for vertical blanking, add up to a 2.56-sec frame rate. At the end of the active scan, the camera enters an erase cycle to prepare the target for the next exposure. The two F cameras are alternately scanned and erased, so that while one is being scanned and read out, the other is being erased and prepared for the next exposure.

The P-type camera utilizes 300 horizontal scan lines over a vidicon faceplate area of 0.11 × 0.11 in. The horizontal line rate is 1500 cps, with 111.1 msec allocated to horizontal blanking. The vertical scan and a 6.6-msec blanking period occupy 0.2 sec. At the end of the active vertical scan, the camera enters an erase cycle of 0.64 sec to prepare the target for the next exposure. The four P cameras are sequentially scanned and erased, so that while one is being scanned the remaining three are in various portions of the erase cycle. A 40-msec pulse is used to separate each sequence of the four-P-type cameras. Therefore, the total time period per sequence is 0.84 sec.

b. Camera and control sequencer. The sequencer consists of separate links for the two channels. Each link contains a video combiner, control programmer, camera sequencer, and sequencer power supply. The group generates synchronizing signals for the individual cameras, controls camera exposure and read-out, combines the video from the individual cameras with sync and tone code signals (camera F_b video is identified by a 144-kc tone burst) and applies the composite video signal to the respective RF transmitter channel modulator.

c. Telecommunications. The communications equipment consists of two transmitting channels and an RF combining section. Each channel contains an L-band FM transmitter, intermediate power amplifier, 60-w power amplifier, telemetry processor, and transmitter power supply. A four-port hybrid ring in the RF section combines the outputs of the two transmitting channels, the combined output being fed to an RF directional coupler and thence to the high-gain antenna. Each transmitter contains a modulator, two frequency multipliers, and an intermediate power amplifier. Each transmitter operates within a bandwidth of approximately 900 kc. A 160-kc band between the transmitter output frequencies was reserved for the spacecraft bus transponder transmitter.

Two commutated telemetry signals are provided. Fifteen-point telemetry, sampling at one point per second, carries critical temperatures and voltages and the backup clock position during the cruise and terminal phases. Output of the 15-point sampling switch drives a channel 8 IRIG subcarrier oscillator connected via an amplifier and transformer with the spacecraft Data Encoder.

The 90-point telemetry, sampling at three points per second, affords detailed diagnostic data from TV-warmup initiation through impact. It has two redundant outputs: one drives a 225-kc VCO whose output is mixed with the P-channel video for transmission; the other goes to the channel 8 3-kc VCO for transmission by the spacecraft bus, replacing the 15-point data (which is mixed with F-channel video).

d. Electrical power. The power assembly for each channel includes an individual battery and high-current voltage regulator for supplying unregulated and regulated power to the operating assemblies. Each battery consists of 22 series-connected silver—zinc-oxide cells, having a capacity of 40 amp-hr. The high-current voltage regulators supply current at 27.5 ± 0.5 vdc, as well as the unregulated battery voltage between 30.5 and 36 vdc; each regulator has an SCR turn-on device to switch on prime power to the system. A low-current voltage

regulator on the P battery provides power to the cruise-mode telemetry.

e. Command and control. The command control unit (CCU) contains control circuits to accomplish the following functions:

1. Circuits for turn-off of Channels F and P, when triggered by RTC-5.
2. Transfer of clock-start command to the distribution control unit (DCU).
3. Circuits to inhibit:
   a. Clock turn-on of Channel F before separation plus 32 hours.
   b. Clock turn-off via RTC-5 before separation plus 32 hours.
4. Cruise mode telemetry "on" prior to launch.
5. Isolation diodes to control and allow redundant powering of telemetry assembly by either F or P regulated voltage outputs.

f. TV backup clock. The backup clock is a solid-state timer with an accuracy of ± 5 min. It is designed to initiate Channel F warmup at a preset interval after *Agena*-spacecraft separation, when it is activated. It backs up turn-on commands from the spacecraft CC&S and the ground. In the *Ranger VII* mission, its setting ($67\frac{3}{4}$ hr) and the corrected trajectory (see Sect. VI, below) were such that its impulse came first and initiated TV operations. The clock is so mechanized that it can be disabled by an RTC-5 after separation plus 32 hours.

g. Structure and thermal control. Subsystem external structure is that of the frustum of a right circular cone topped by a cylindrical section. The primary strength of the structure is provided by an internal box span consisting of stiffened panel sections supported by eight longerons; the electrical assemblies are mounted on structural decks supported by the longerons. The cameras mount on a solid machined camera bracket housing within the top cylindrical section, with a view port cut in the external thermal shroud.

The thermal control is entirely passive, with a thermal shield (mounted outside the structure body) and fins used to control the radiative exchange of energy between the TV Subsystem and other sources (or links) of thermal energy. The thermal mass of the structure was the primary heat sink during the terminal mode of operation.

2. Subsystem mission performance

Television Subsystem operation and performance were normal and satisfactory from prelaunch checkout through mission termination at lunar impact. Critical mission events for the subsystem are given in Table 5.

A prelaunch TV test at reduced power and prelaunch cruise-telemetry turn-on (at L-15 min) indicated subsystem launch readiness. From launch to separation, telemetry indicated normal operation.

At spacecraft/*Agena* separation, the TV backup clock (preprogrammed to turn on Channel F video operations in 67 hr 45 min) was initiated, as shown by a telemetry change. Clock turn-on of the system (or clock disable via ground command RTC-5) was inhibited for 32 hr after separation. Thirty minutes after separation, the spacecraft hydraulic timer (Sect. IV.L above) commanded "ground enable" for the SCR turn-on circuit and other critical TV command lines; the critical ground circuits had been held open during the boost phase to ensure that the Subsystem could not be inadvertently powered in the critical-pressure region of the atmosphere. A backup "ground enable" was provided via a microswitch actuated by deployment of the $-X$ solar panel.

In the cruise mode, the TV furnishes 15 commutated points of battery, backup-clock, and temperature measurements to the Data Encoder's Channel 8 subcarrier (see Sect. IV.E above). During the midcourse maneuver this telemetry was switched off for the period of the motor burn, about 14 min. Also during the maneuver TV temperatures fluctuated somewhat (as did bus temperatures) owing to the attitude change.

The terminal mode commenced when the TV backup clock initiated warmup of Channel F. The CC&S backed up this action and initiated P-channel warmup via the TV-2 command. An additional backup, ground command RTC-7, was available but unnecessary.

In each channel, the warm-up signal applied the battery output to the high-current regulator; regulated 27.5-v dc was applied to the camera and sequencer electronics and transmitter modulator, and unregulated battery output was supplied to the telemetry (via the low-current regulator) and communications equipment. After an 80-sec warmup, each channel was switched by its sequencer to the full-power mode, and a relay in the transmitter power supply gave high voltage to the intermediate and final power amplifiers. CC&S signal TV-3 backed up the full-power signal, five minutes after TV-2.

Channel F, centered at 959.52 Mc, contains composite video signals (0 to 177 kc video baseband) from the two full-scan cameras, F_a and F_b, and 225-kc telemetry data (15 points). Channel P, centered at 960.58 Mc, contains composite video signals (0 to 144 kc video baseband) from the four partial scan cameras, P_1, P_2, P_3, and P_4, and 225-kc telemetry data (90 points). The 90-point telemetry is also transmitted via the bus Channel 8 subcarrier in place of the 15-point data during this mode.

The appearance of 90-point telemetry on Channel 8 (Table 5) was the first indication on the ground of TV initiation. The telemetry indicated normal operation and verified that battery capacity and drain and thermal conditions (Fig. 31) would permit video operations at least until impact.

Normal RF and video were observed at the two receiving stations, DSIF 11 and 12, at Goldstone. Polaroid prints further verified normal operations and pictorial quality. The telemetry, A-scope presentation, and photographs indicated a slightly higher video level than anticipated (see Sect. VII.A below).

Table 5. Television Subsystems critical events

Description	Predicted mission time	Actual time, GMT
July 28		
Prelaunch reduced power test	L − 115 min	1344:45
Start of cruise-mode telemetry	L − 15 min	1625:25
Launch	Launch	1650:08
Backup clock start on signal	Separation	1722:36
TV enable via hydraulic timer	S + 30 min	Not telemetered
TV enable backup via microswitch on −X solar panel	L + 61 min	1751:17
July 29		
8-hr clock pulse	S + 8 hr	0122:40[a]
16-hr clock pulse	S + 16 hr	0922:40[a]
TV Channel 8 removed from bus carrier	Midcourse (Telemode II)	1016:41 to 1030:39
24-hr clock pulse	S + 24 hr	1722:40[a]
July 30		
32-hr clock pulse	S + 32 hr	0122:37[a]
48-hr clock pulse	S + 48 hr	1722:31[a]
July 31		
64-hr clock pulse	S + 64 hr	0922:23[a]
Warmup of F channel via backup clock	S + 67 hr 45 min	1307:15
Full power of F channel via internal sequencer	I − 17 min	1308:35
Warmup of P channel via CC&S	I − 15 min	1310:49
Full power of P channel via internal sequencer	I − 13 min 40 sec	1312:09
CC&S and backup full-power command	I − 10 min	1315:48
Impact	I	1325:49

[a]Accuracy: −0, +15 sec

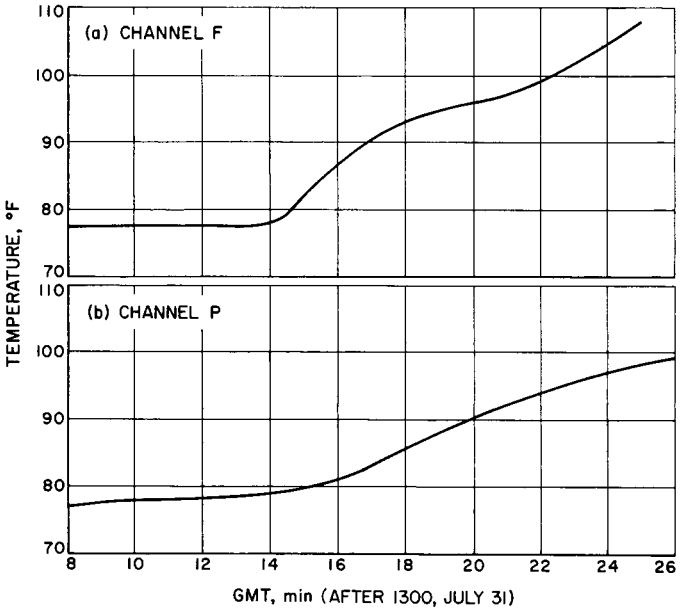

Fig. 31. Channel F and P heat-sink temperatures during terminal operations

At lunar impact all signals were lost. Channel F had operated in full power for 17 min 14 sec, Channel P for 13 min 40 sec. Telemetry analysis of battery capacity and thermal conditions (Fig. 31) indicated that at least 22 min of additional TV operation was feasible.

Temperature profiles of the mission for five TV-Subsystem regions are given in Fig. 32.

The *Ranger VII* television performance was well within what was anticipated from the test history of the system, with few exceptions. There were no failures of any kind and the mission was completely successful from a photographic point of view. Those factors which could not be completely determined experimentally, such

as camera focus, temperatures, the effects of gravity, and lunar surface brightness, were predicted accurately enough to accomplish the mission objectives perfectly.

The only anomalies in camera performance noted to date are due to variations in exposure time on the P_1 and P_4 shutters. These variations were apparently due to the change in gravity but were not serious enough to degrade the picture quality. The difference between the predicted and actual lunar surface brightness did not affect the performance significantly. Some aspects of camera performance such as resolution are difficult to evaluate quantitatively from the mission photographs; however, it is apparent from a qualitative evaluation that no major loss in performance was incurred.

During the mission, the Channel 8 VCO shifted slowly about 1–2 cps; this was within tolerance (±2 cps) and did not affect results.

In the P transmitter, a minor center-frequency shift of about 8 kc between the preflight calibration and the mission was noted. This shift is within the specified range and again had no effect on the mission results.

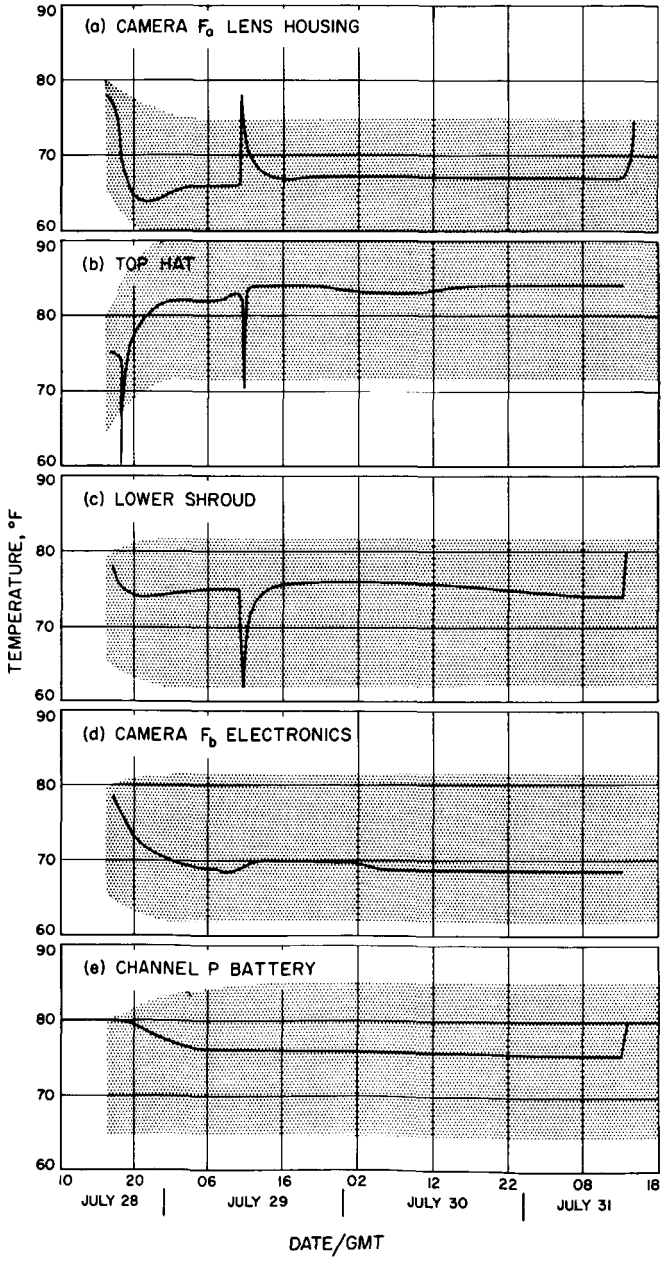

Fig. 32. Television Subsystem flight temperatures

V. DEEP SPACE NETWORK SYSTEM

The Deep Space Network (DSN) is a NASA facility managed by JPL. It consists of the Deep Space Instrumentation Facility, the Space Flight Operations Facility and the Ground Communications System.

A. DSIF Subsystem

The DSIF is a precision tracking and communications system capable of providing command, control, tracking, and data acquisition for deep-space flight missions. Continuous coverage during missions is provided by locating antennas approximately 120 deg apart in longitude; accordingly, stations are located in Australia and South Africa, as well as in Southern California; the foreign stations are maintained and operated by personnel of cooperating agencies in these countries. A block diagram of the Goldstone Echo Station (DSIF 12), in *Ranger VII* configuration, is given in Fig. 33.

The DSIF support for *Ranger VII* consisted of permanent stations located at Goldstone, California (DSIF 11 and 12), Woomera, Australia (DSIF 41), and Johannesburg, South Africa (DSIF 51); a Spacecraft Monitoring Station (DSIF 71) at Cape Kennedy, Florida; and the Mobile Tracking Station (DSIF 59), located near DSIF 51, used for initial acquisition and tracking. Equipment of the six stations is listed in Table 6.

Table 6. DSIF L-band master equipment list

Equipment	DSIF Stations					
	Goldstone		Australia	South Africa		Cape
	11	12	41	51	59	71
Antennas:						
85-ft paraboloid HA-DEC	○	○	○	○		
10-ft paraboloid AZ-EL					○	
6-ft paraboloid AZ-EL						○
Low noise amplifiers:						
Maser	○	○				
Paramp	○	○	○	○		
Feeds and diplexers:						
Tracking feed			○	○	○	
Horn feed	○	○				
Acquisition aid			○	○		
Dipole						○
Diplexer		○	○	○	○	○
Receiver:						
960 mc GSDS modified					○	○
960 mc GSDS	○	○	○	○		
Transmitter:						
50 w backup		○				
10 kw (operated 200 w for *Ranger* Block III)		○	○	○		
25 w					○	○[a]
Rubidium standard		○				
Synthesizer		○				
Doppler:						
One-way		○	○	○	○	○
Two-way		○	○	○	○	
Two-way two-station noncoherent		○	○	○	○	

Equipment	DSIF Stations					
	Goldstone		Australia	South Africa		Cape
	11	12	41	51	59	71
Recording:						
7 Ch magnetic tape	2	2	2	2	2	2
Strip chart:						
36 Ch ultraviolet	○	○	○	○	○	○
8 Ch hot stylus	○	○	○	○	○	
Acquisition aids:						
10-cps modulator		○	○	○		
Mission-oriented equipment:						
Command system		○	○	○		
Command interrupt		○				
Telemetry decommutator/ encoder		○	○	○		
Telemetry discriminator		10	10	10	10	
Prime RCA TV GSE		○				
Secondary RCA TV GSE	○					
JPL TV GSE		○[b]	○	○		
Prime test equipment:						
Test transponder	○	○	○	○	○	○
Closed-loop RF system	○	○	○	○	○	○
Bit error checker		○				
Optical star tracker		○				
Miscellaneous:						
Intersite microwave	○	○				
Coordinate converter	○	○				

[a]Transmitter used for prelaunch only.

[b]Redundant system backup mag tape converter/FR-800.

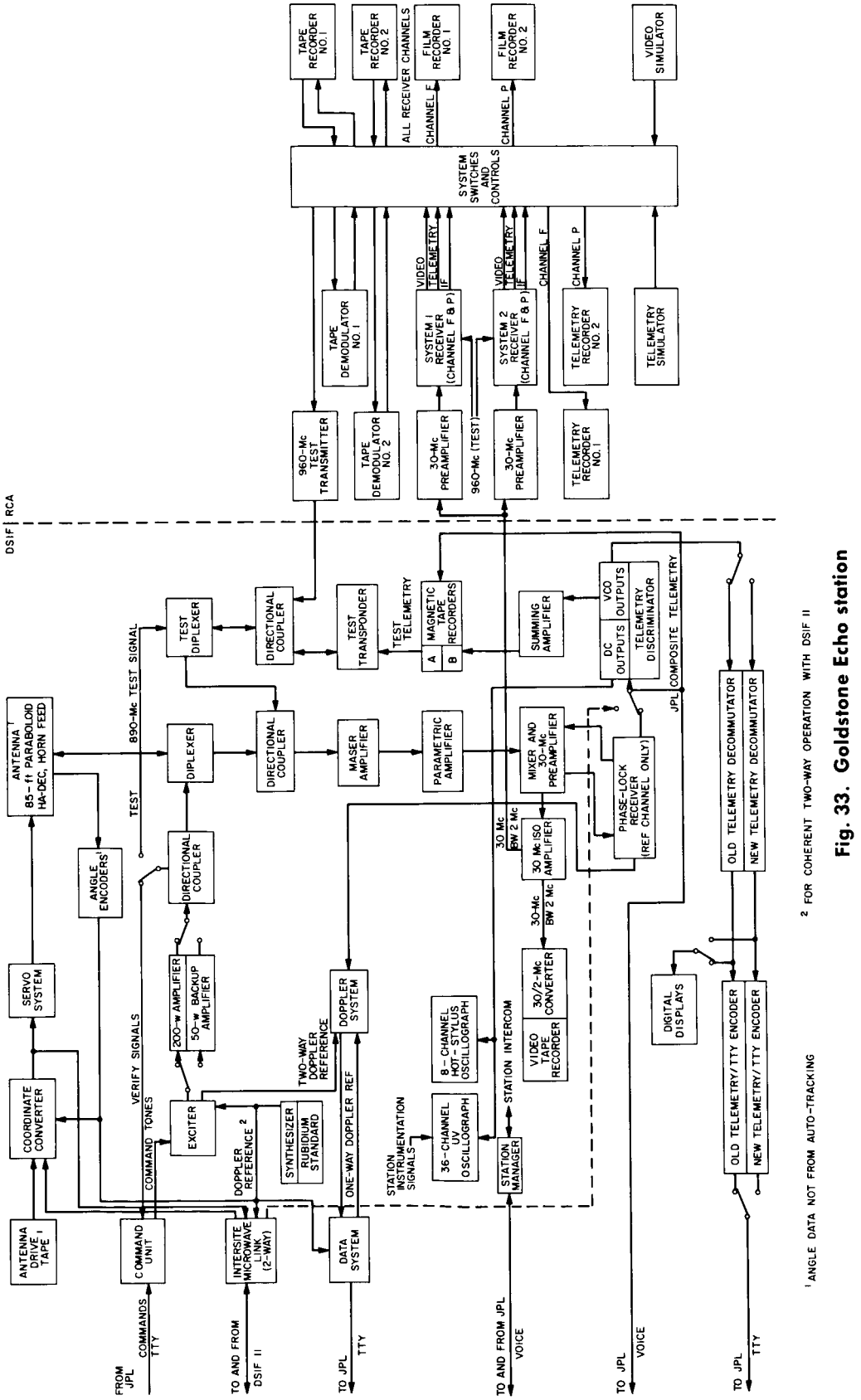

1 ANGLE DATA NOT FROM AUTO-TRACKING

2 FOR COHERENT TWO-WAY OPERATION WITH DSIF 11

Fig. 33. Goldstone Echo station

1. Mission Preparation

Prior to the *Ranger VII* mission and its associated operational readiness testing, a series of calibration and checkout tests were performed at each station. These tests consisted of comprehensive system and subsystem checks to ensure compatibility, reliability, and operator proficiency. Premission tests, designed to exercise the station configuration after modifications associated with the *Mariner* Mars missions and this mission, were performed at the overseas stations. A series of operational readiness tests to exercise components of the entire Space Flight System was concluded just prior to launch.

In general, the only difficulties experienced were in the area of procedures and in test data simulation. One problem of considerable concern that appeared in the few days prior to launch involved receiver difficulties in DSIF 51; however, the nature of the failure was discovered and the necessary repairs were made prior to launch. No such problems were experienced during the mission.

2. Launch to Injection

DSIF 71 (Spacecraft Monitor Station at Cape Kennedy) obtained two-way lock with the spacecraft 50 min before launch on July 28, 1964. Because the decision had been made to launch with the station and the spacecraft in two-way lock, the transmitter was left on until the spacecraft was lost over the horizon. The countdown proceeded normally to 1650 GMT with only minor holds of a few seconds duration. Launch occurred at 1650:08 and liftoff was normal. The ground receiver at DSIF 71 lost lock at L + 31.5 sec. The station receiver was again locked at L + 148 sec, but unfortunately on a sideband. Lock was maintained to the horizon and was lost at L + 462 sec. However, the 890-mc up-link (that being transmitted from the ground to the spacecraft) did not unlock at any time.

3. Injection to Midcourse

The injection of the spacecraft into a lunar transfer orbit occurred at 1720:01. *Agena*/spacecraft separation appeared normal and *Ranger VII* continued on a lunar trajectory. DSIF 59 acquired the spacecraft at 1721:01 and DSIF 51 at 1721:38. Considerable difficulty, of a nature yet to be determined, caused DSIF 59 to go in and out of a two-way lock during this period of time, reducing the number of satisfactory tracking data points to eight.

DSIF 41 acquired the spacecraft in one-way lock at 1735:22 and established two-way lock at 1737:57. The following events were observed: solar panel extension, initiation of the solar-acquisition sequence, solar acquisition, initiation of Earth-acquisition sequence, and Earth acquisition. DSIF 41 (Woomera) transmitted a series of commands to initiate spacecraft antenna transfer with the antenna switchover (RTC-3) being initiated at 2119:00. This was the first time DSIF 41 had performed this function.

4. Midcourse to Impact

Corrective midcourse maneuver commands were sent to the *Ranger VII* spacecraft by DSIF 12 (Goldstone). The midcourse maneuver was initiated at 1000:00 on July 29, 1964.

As discussed elsewhere in this report it was decided to send an RTC-6 (terminal maneuver) and an RTC-8 (attitude control disconnect) to provide an additional backup turn-on command for the TV subsystem. The RTC-6 was transmitted to the spacecraft at 1225:08 on July 31, 1964 by DSIF 12.

DSIF 12 was prepared to transmit RTC-7 backup turn-on commands in the event of failure in the timing systems in the spacecraft. Both F and P channel video came on with full power as scheduled, but the RTC-7 was retained in the command system until impact, in the event that the television should turn off for some reason. Reception of video at both DSIF 12 (Echo) and DSIF 11 (Pioneer) was of excellent quality with all systems functioning properly.

Station tracking periods, together with nominal view periods, may be seen in Table 7. The ground commands sent to the spacecraft by the DSIF stations are presented in Table 2.

5. Tracking Performance

In general, DSIF station operations were effectively implemented. After the first pass over DSIF Stations 59, 51 and 41, the spacecraft was in two-way lock at all times and a minimum of good data was lost during station transfers. During the first pass over DSIF 59, 51 and 41, however, several difficulties were encountered. Although both DSIF 51 and 59 acquired the spacecraft quite soon after injection, neither was very successful in obtaining good two-way data during the pass. Both stations were unable to maintain their receivers in continuous lock,

Table 7. Nominal view periods and actual tracking at DSIF stations

Date	DSIF station	Nominal rise, GMT	Nominal set, GMT	Nominal view period, hr:min:sec	Acquisition by station, GMT	Loss of signal by station, GMT	Actual view period, hr:min:sec
July 28	51	1721:17	1732:00	00:10:43	1721:38	1732:55	00:11:17
	59	1721:17	1732:00	00:10:43	1720:50	1737:53	00:17:03
	41	1736:54	0046:21[a]	07:09:27	1735:24	0117:00[a]	07:41:36
	51	2042:52	0828:04[a]	11:45:12	2045:50	0854:29[a]	11:68:39
July 29	12	0711:54	1836:01	11:24:07	0644:10	1845:35	12:01:25
	41	1438:45	0124:04[a]	10:45:19	1413:55	0149:00[a]	11:35:05
	51	2200:10	0848:32[a]	10:48:22	2202:45	0912:03[a]	11:09:18
July 30	12	0720:28	1859:03	11:38:35	0655:30	1859:49	12:04:19
	41	1459:08	0131:08[a]	10:32:00	1436:03	0159:00[a]	11:22:57
	51	2214:05	0853:41[a]	10:39:36	2213:17	0914:37[a]	11:01:20
July 31	12	0722:02	1325:50[b]	06:03:48	0700:56	1325:50[b]	06:24:54

[a]Next day
[b]Lunar impact

with DSIF 59, particularly, evidencing trouble in locating and following the spacecraft. Moreover, both DSIF 51 and 59 indicated certain data as being good with their Data Condition Code, when in fact the data were unusable. From the period 1728:41 to 1729:06, July 28, 1964, *both* DSIF 51 and 59 reported good two-way lock with the spacecraft transponder at the same time. At this time, the problems appear to be at least partially due to the high angular rates encountered during the pass.

During the first-pass transfer from DSIF 51 to DSIF 41, a gap occurred from 1735:11 until 1738:02 in which neither station had the spacecraft in two-way lock. When DSIF 41 acquired two-way lock at 1738:02, it was unable to obtain good two-way doppler until 1754:02. This problem appeared to be due to a load imposed by a counter in the doppler system at DSIF 41. No further trouble was encountered after this load was removed at approximately 1753:00.

During the remainder of the mission, two minor problems arose at DSIF 41. On occasion, 100- to 200-cycle dropouts occurred in the doppler when the last two digits of the doppler were zero. This was evidently a purely electrical problem in one of the counters. During the third pass, a gradual reduction in signal strength occurred, dropping from about -119 dbm at the beginning of the pass to about -126 dbm at the end of the pass. At present, this problem appears to have been caused by a marginal power supply at DSIF 41.

6. Ground Telemetry Operations

The DSIF ground telemetry subsystem performed the function of demodulating and decommutating the spacecraft telemetry signal. The composite signal from the station RF receiver was utilized for the input to the phase-lock-loop discriminators. The discriminators then separated the composite signal into the ten channels assigned to the *Ranger* telemetry system. The decommutator sampled and identified the data, and the TTY encoder prepared the signal for transmission.

There was one minor failure in the ground telemetry equipment during the flight which was promptly corrected. There were no data losses during the flight and all equipment operation was at near optimum design levels.

Real-time recovery and display of spacecraft telemetry during the *Ranger VII* mission greatly exceeded that of previous *Rangers* in both quantity and quality. The increased performance can be attributed to the perfect performance of the spacecraft elements in the data system, the high degree of performance of the DSIF ground telemetry recovery and encoding equipment and crews, and the improved communications subsystem.

Two real-time telemetry ground recovery systems were operational at each DSIF station and were utilized throughout the entire mission. The primary system dis-

criminated the various subcarriers, decommutated and encoded the data into teletype language, and then transmitted the encoded telemetry data to the SFOF via teletype circuits. The secondary system merely transmitted the spacecraft "raw" or composite analog signal to the SFOF via voice communications circuits. The Spacecraft Data Analysis Team (SDAT) chose to monitor and evaluate the data supplied by the telemetry secondary ground system during both DSIF 12 and DSIF 41's tracking periods in order that the television (15-point cruise data) information telemetered on Channel 8 could be processed and displayed in real time. The primary telemetry ground recovery system, employing teletype transmission of data, was used satisfactorily for determining spacecraft bus performance.

B. Space Flight Operations Facility (SFOF)

The SFOF is located at JPL, Pasadena, California. The *Ranger VII* mission was the first flight activity to be completely controlled and operated from the new facility. The SFOF utilizes operations control consoles, status and operations displays, computers, and data processing equipment as tools in the analysis of spacecraft performance and space science experiments, and communication facilities to control space flight operations.

1. Facility

The SFOF included a display system, a gallery for observers, television output of certain cameras with an audio status line for an internal/external laboratory information system, access control and facility security, standby maintenance personnel support, standby room for operations personnel, bunkroom, technical area assistants support for the Spacecraft Data Analysis Team (SDAT) and the Flight Path Analysis and Command (FPAC) group, and the necessary capability for the correction of any facility housekeeping failures or problems.

One facility failure occurred during the mission. This was an internal power failure which occurred at 0025, July 31, affecting only the data processing system. The power failure was corrected and all SFOF data processing equipment was operating by 0049. The difficulty was traced to a power switch which had arced to ground. The fix during the mission was a temporary one, and steps have been taken to prevent a recurrence of similar failures.

Several minor display equipment failures occurred and were fixed in near-real time during the mission.

The SFOF provided a secure area for the analysis of the Lunar television pictures by the Space Science Analysis and Command (SSAC) group and experimenters for two weeks after the conclusion of the flight.

2. Central Computing Complex

This complex consisted of two IBM 7094 computers, three IBM 1401 computers, an SC-4020 plotter, a PDP-1 computer, the Telemetry Processing Station, and the personnel required to operate and maintain the equipment.

During the last three days prior to the *Ranger VII* launch, the complex executed a launch-checkout sequence of events which included testing and shakedown of both software and hardware. The completion of this checkout indicated a state of mission readiness for the complex.

In general, all computer programs performed well during the missions. The orbit determination and trajectory computation effort was very satisfactory and all scheduled tasks were completed. The computation of the midcourse and terminal maneuver commands proved to be excellent. Real-time display of raw and converted engineering telemetry data, including television subsystem data, was supplied to the Spacecraft Performance Analysis Area by the PDP-1 computer and the Telemetry Processing Station. Bulk processing, in the form of printed listings and plots, of engineering telemetry data on the IBM 7094's was satisfactory although more computer time was consumed than had been anticipated.

The computers and associated equipment had a good record of reliability during the course of the mission. The few equipment problems which occurred were minor and caused little or no delay to the operations due to quick repair and/or duplicate or backup hardware capabilities which were available.

Post-flight processing of tracking and telemetry data began immediately upon completion of the mission.

3. Communications Center

The performance of the Communications Center during the flight was quite effective. The communications failures experienced within the SFOF were due to terminating apparatus only, and were of a type and quantity well within normal expectations. Mechanical failures of teletype equipment, tube and semiconductor failures, plus minor technical adjustment problems constituted all of these failures. In one instance the teletype switching

system apparently locked up for approximately three minutes. This problem was experienced during system tests and is currently under engineering evaluation. The momentary lockup caused a short loss of teletype data and was cleared by emergency operational procedures. There is presently no explanation for the cause of the lockup.

C. Ground Communications System (GCS)

The DSN Ground Communications System consisted of: voice, normal and high data rate teletype circuits provided by the NASA world-wide communications network between each overseas DSIF station and the SFOF; and teletype and voice circuits between the SFOF, Goldstone stations and Cape Kennedy, and a microwave link between the SFOF and Goldstone. The ground communications net configuration for the *Ranger VII* mission is shown in Fig. 34.

1. Lines to Woomera

Teletype, analog data and voice communications to DSIF 41 were generally excellent and much improved over *Ranger VI*. This was the result of using the new submarine cable in place of the high frequency radio. The high frequency radio from Hawaii to Sydney (used as a backup in this mission) was not operationally acceptable during the flight, probably because of lack of adequate time for exercising this configuration after switching the main communications to the cable.

2. Lines to Johannesburg

The circuits to Johannesburg continue to provide the most difficult communications problem. In addition to the Sydney-Pretoria "back-door" circuit installed prior to *Ranger VI*, another radio teletype circuit was implemented just prior to *Ranger VII* in an attempt to correct deficiencies in teletype and voice communication. The new circuit was made available through the cooperation of ETR. The late installation of this circuit left some unsolved problems on switching and data transfer at ETR station 13, Cape Kennedy and Goddard Space Flight Center.

3. Goldstone Link

Between *Ranger VI* and *VII*, Goldstone communications services were transferred to the new microwave system between JPL and Goldstone. This system worked very well.

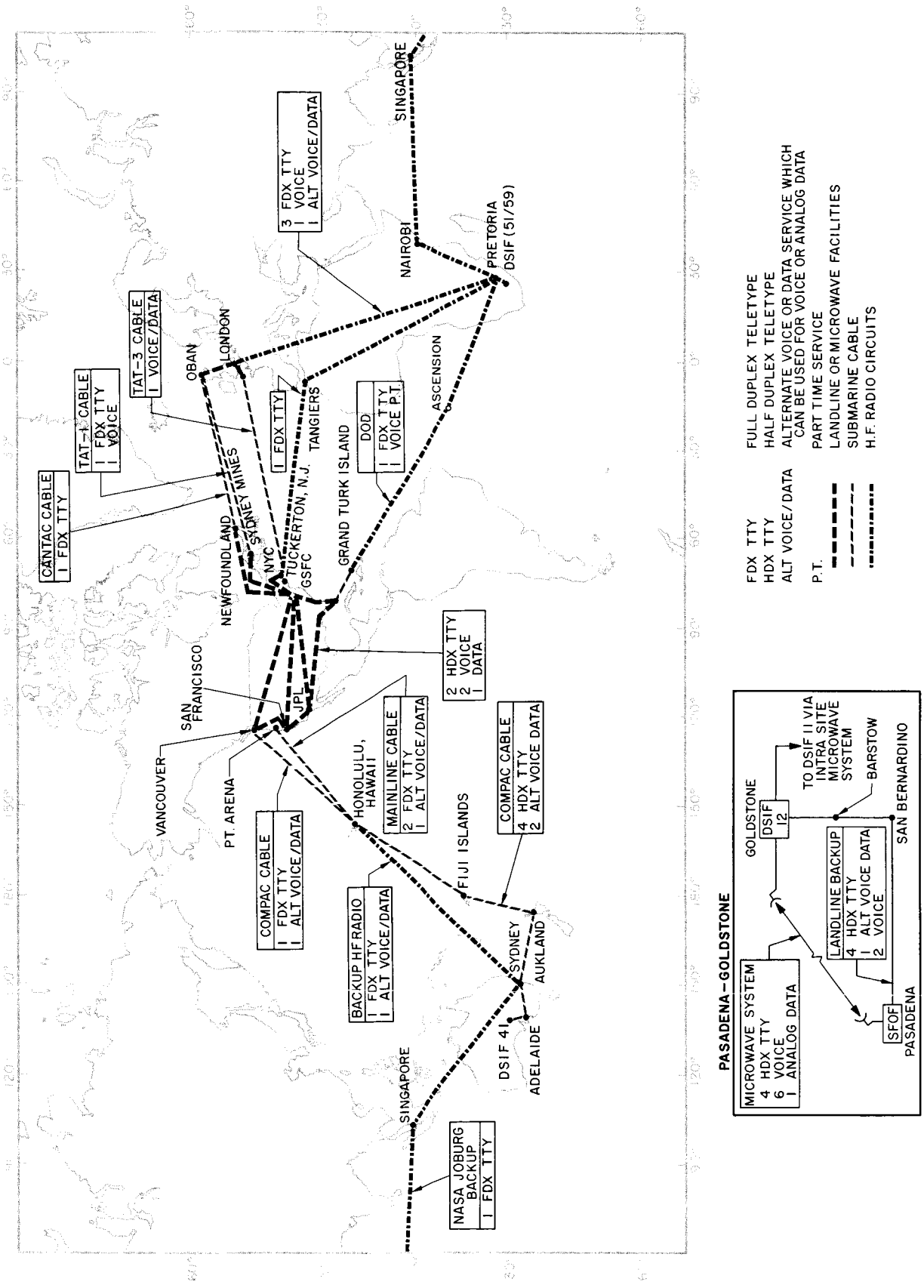

Fig. 34. DSN Ground Communications Subsystem

VI. SPACE FLIGHT OPERATIONS SYSTEM

The function of the Space Flight Operations System is to perform those functions during the flight that are required to achieve the mission objectives. These functions include determining the trajectory of the spacecraft, defining and performing corrections to the trajectory, obtaining and evaluating telemetry from the spacecraft, transmitting required command functions to the spacecraft, and receiving and recording the spacecraft video signals. To fulfill these functions the Space Flight Operations System makes use of the operational groups required to direct the mission, the tracking nets (ETR and DSIF) required to obtain tracking and telemetry data from the spacecraft and to transmit commands to the spacecraft, the Earth-based communications between all the groups, and the data processing and computing facilities required to support the operation.

A. Spacecraft Data Analysis Team (SDAT)

It is the responsibility of this group to monitor and analyze the operation of the spacecraft. This group would also recommend corrective action to be taken in the event of nonstandard spacecraft performance. Fortunately, the very nominal spacecraft performance precluded the necessity for a full exercising of SDAT capabilities.

B. Flight Path Analysis and Command Group (FPAC)

It is the responsibility of this group to determine the trajectory of the spacecraft and to determine the required spacecraft midcourse and terminal maneuvers. The earliest orbit determination was not attained on schedule, due primarily to a lack of early tracking data from the DSIF. The problem was recognized early, and was not considered critical because of the nominal appearance of the tracking data from AFETR indicating a very good spacecraft injection. A difference in terminology between the SDAT and FPAC groups caused a time of flight error of 80 sec in the midcourse maneuver calculation. Although this problem was discovered early enough to correct, it was not felt to be significant enough to repeat the calculations. The functions required of this group were all executed satisfactorily.

C. Space Science Analysis and Command Group (SSAC)

It is the responsibility of this group to recommend the aiming points and evaluate the picture quality expected under the mission conditions. No problems were encountered in executing this function.

VII. FLIGHT PATH

A. Launch Phase

Ranger VII was launched from the Eastern Test Range (ETR) at Cape Kennedy, Florida, at 1650:07.873 GMT on Tuesday, July 28, 1964 using the *Atlas D/Agena B* launch vehicle. After liftoff, the booster rolled to an azimuth of 97.1 deg and performed a programmed pitch maneuver until booster cutoff. During sustainer and vernier stages, adjustments in vehicle attitude and engine cutoff times were commanded as required by the ground guidance computer to adjust the altitude and velocity at *Atlas* vernier engine cutoff. After *Atlas/Agena* separation, there was a short coast period prior to the first ignition of the *Agena* engine. At a preset value of sensed velocity increase, the *Agena* engine was cut off. At this time the *Agena*/spacecraft combination was coasting in a nearly circular parking orbit in a southeasterly direction at an altitude of 188 km and an inertial speed of 7.80 km/sec. After an orbit coast time of 19.97 min, determined by the ground guidance computer and transmitted to the *Agena* during the *Atlas* vernier stage, a second ignition of the *Agena* engine occurred. Eighty-nine seconds later the *Agena* was cut off with the *Agena*/spacecraft combination in a nominal Earth–Moon transfer orbit.

B. Cruise Phase

Injection occurred at 1720:01 GMT, over the western coast of South Africa at a geocentric latitude and longitude of −12.89 and 15.07 deg respectively. The *Agena* and spacecraft were at an altitude of 192 km and traveling at an inertial speed of 10.949 km/sec. One minute 32 sec after injection the *Agena*/spacecraft combination entered the Earth's shadow. The *Agena* separated from the spacecraft 2 min 35 sec after injection, then performed a programmed 180-deg yaw maneuver and ignited its retro rocket. The retro rocket impulse was designed to eliminate interference with the spacecraft operation and reduce the chance of the *Agena* impacting the Moon. Tracking data indicated that the *Agena* passed the upper trailing edge of the Moon at an altitude of 4170 km about 3 hr after *Ranger VII* impact.

The spacecraft left the Earth's shadow 40 min 5 sec after injection, after a total shadow duration of 38 min 33 sec. Sun acquisition had been initiated 9 min 58 sec prior to leaving the Earth's shadow. Five minutes after leaving the Earth's shadow the Sun was acquired. Within an hour after injection, the spacecraft was receding from the Earth in almost a radial direction with decreasing speed. This reduced the geocentric angular rate of the spacecraft (in inertial coordinates) until, at 1.4 hr after injection, the angular rate of the Earth's rotation exceeded that of the spacecraft. This caused the Earth track of the spacecraft (Fig. 35) to reverse its direction from increasing to decreasing Earth longitude.

C. Midcourse Maneuver

Three gross factors bound a midcourse maneuver: target location, time of flight, and spacecraft capability.

Prior to the flight, *Ranger VII*'s selected impact site had been designated as the "most desirable" target for the launch day of July 28. Several of the factors leading to this choice are presented in Fig. 36, which presents the portion of the Moon available to impact in terms of the initial flight conditions[1].

The criterion of solar illumination of the impact site led to the choice of the zone between 50 deg and 80 deg from the subsolar point. In order to avoid loss of Earth-lock by the Earth sensor, the Earth/probe/near-limb angle was limited to a minimum of 15 deg, which selected a region within 75 deg of the sub-Earth point. The intersection of these two regions, for the July 31, 1964 encounter, determined the general desirable impact area for that date.

In addition, the mission reliability would be increased if a terminal maneuver was not required to change the camera-pointing directions from the cruise-mode orientation. This was the case for much of the desired impact were made for the other days of the period.

Within that general area, a number of specific sites were identified as of particular combined interest to the *Ranger* Experimenters and the *Apollo* project, and one site—that eventually chosen—as best. Similar selections were made for the other days of the period.

[1] For convenience, these parameters are presented in a plane defined by the miss parameter **B**. This parameter is nearly a linear function of changes at injection conditions and is defined as the vector from the target's center of mass normal to the incoming asymptote of the osculating conic at closest approach to the target body. $\mathbf{S}_t$ is defined as a unit vector in the direction of the incoming asymptote. In the plane normal to $\mathbf{S}_t$, referred to as the **B**-plane, the unit vector **T** is parallel to the plane of the true lunar equator, and **R** completes a right-hand orthogonal system to describe **B**. This technique is rigorously described in JPL External Publication No. 674 (August, 1957), by W. Kizner.

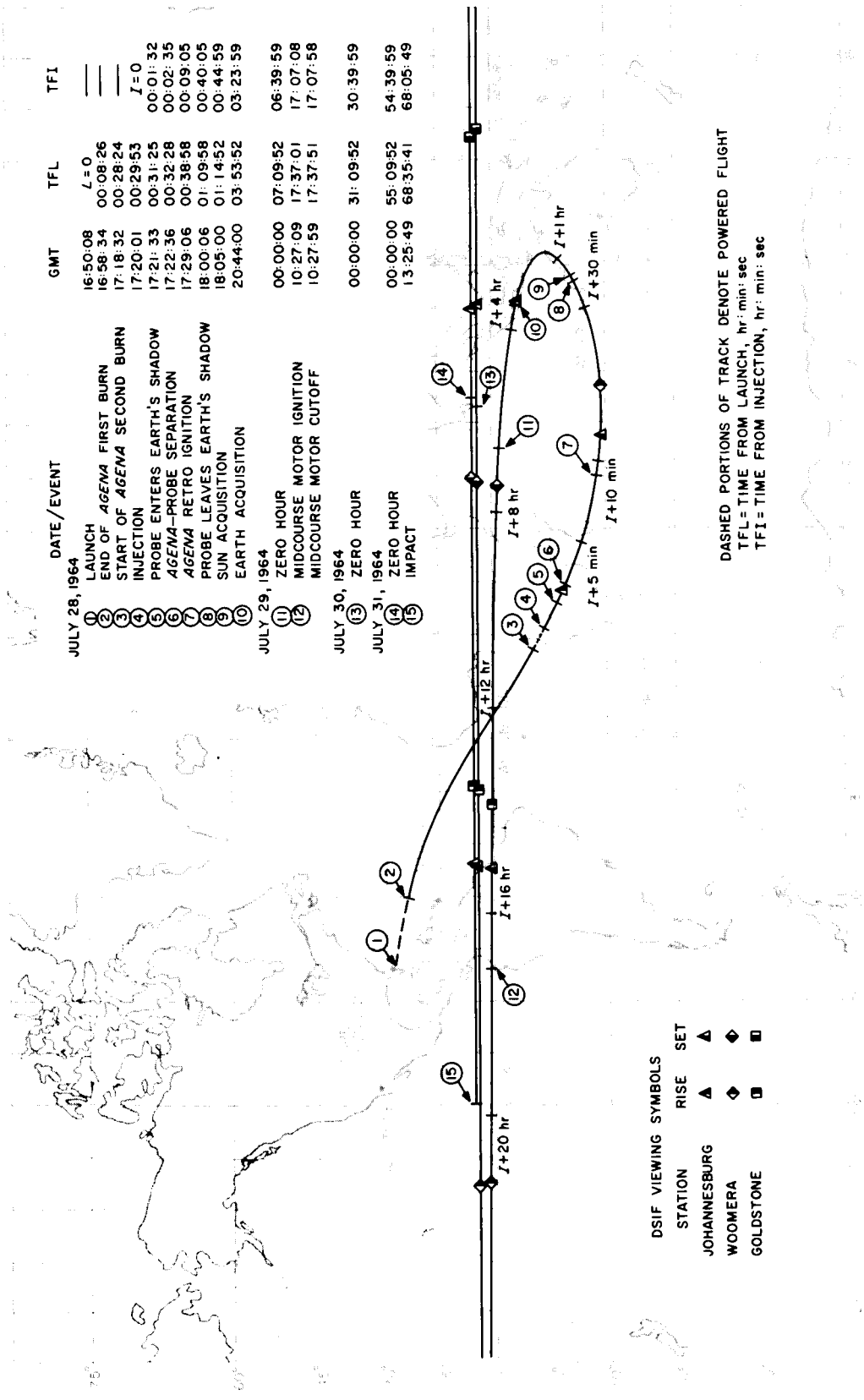

Fig. 35. *Ranger VII* trajectory Earth track

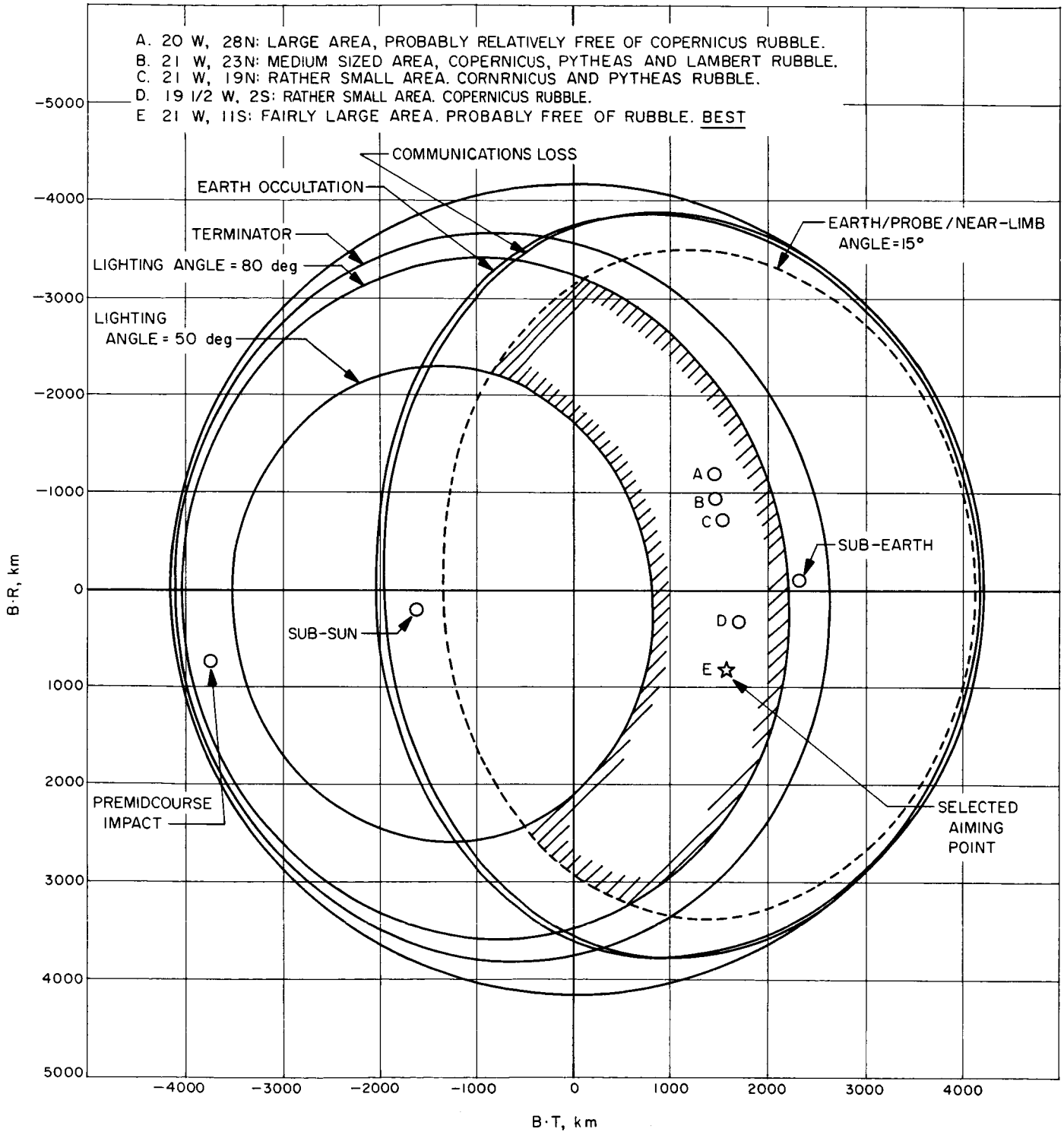

Fig. 36. Midcourse maneuver and site selection factors

Orbit determinations early in the course of the mission identified the uncorrected lunar impact site at 12.3 deg latitude and 204.0 deg east longitude, well within the midcourse correction capability to reach the desired area, particularly, including the best site. In addition, analysis of the probable dispersion resulting from orbit determination and midcourse execution errors indicated a low risk in reaching the near vicinity of the best site.

Transit time from injection to impact on the uncorrected trajectory was 67.391 hr. The TV camera backup clock had been set prior to launch to turn on the F cameras 67.793 hr after injection, and the use of this mechanism was considered desirable to enhance mission reliability.

The preferred clock turn-on time was to be between 10 and 30 min prior to impact. Flight-time corrections to

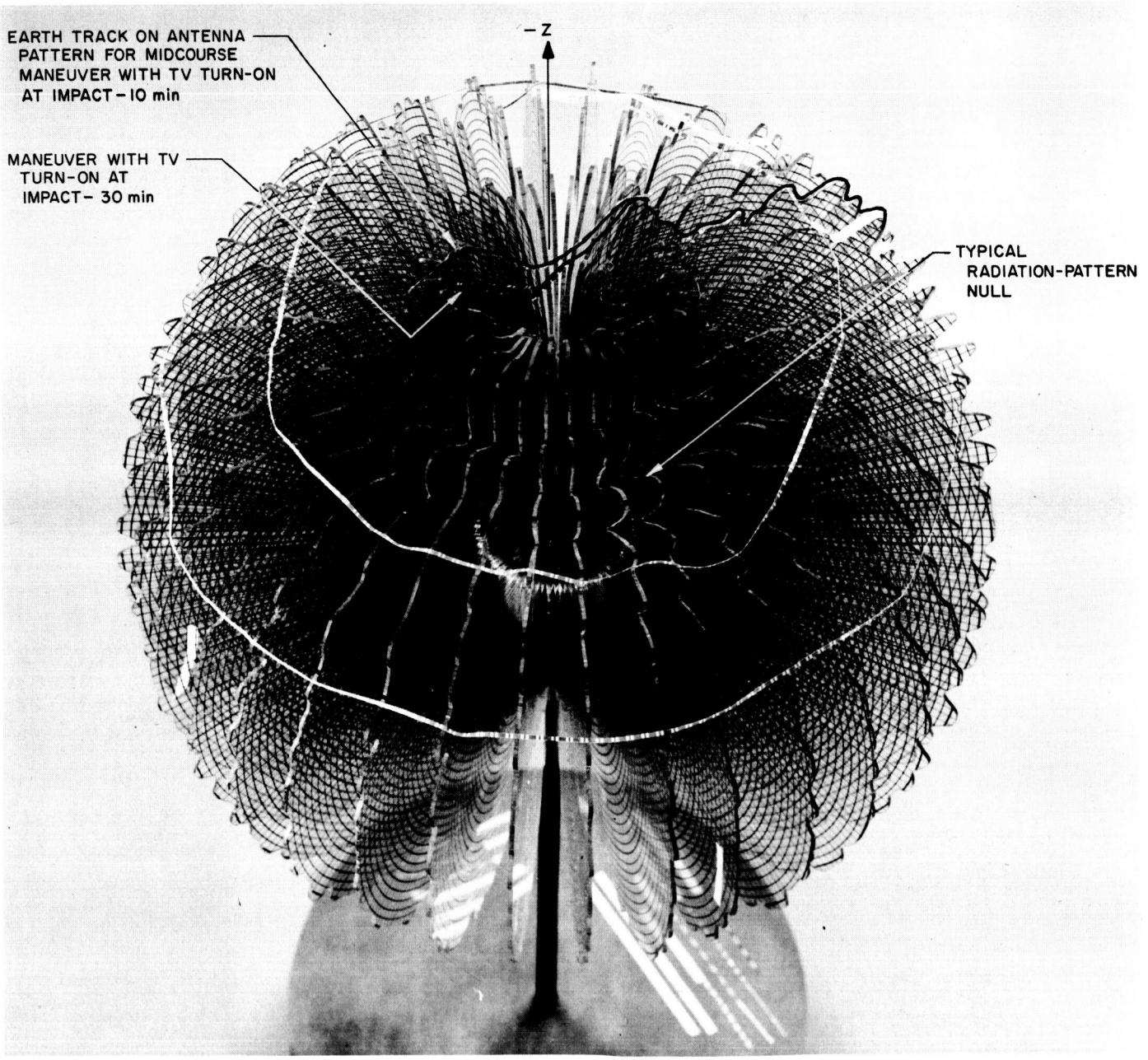

Fig. 37. Midcourse maneuver and omni antenna pattern model

realize these turn-on times required midcourse maneuver roll and pitch sequences which would at times cause loss of some telemetry channels due to the tracking stations passing through or near the nulls in the omnidirectional antenna radiation pattern (Fig. 37). Further analysis determined that the loss in telemetry was less serious for the maneuvers resulting in turn-on times less than 30 min prior to impact. However, early turn-on times yield a larger picture coverage due to the greater distance between the spacecraft and the lunar surface. A compromise between loss in telemetry and over-all picture coverage was made. The flight time was to be increased by 0.708 hr in order that the F camera backup turn-on time be 18 min prior to impact.

The selected midcourse maneuver required the spacecraft to roll 5.56 deg, pitch −86.80 deg, and then burn its motor to slow down the spacecraft by 29.89 m/sec (the maximum velocity change capability of the motor was 59.8 msec).

The pre- and post-midcourse trajectories near the Moon and the impact sites are shown in Fig. 38.

The midcourse motor was ignited at 1027:09 GMT on July 29, 1964 at which time the spacecraft was at a geocentric distance of 169,000 km and traveling with an inertial speed of 1.786 km/sec relative to Earth. At the end of a 50-sec burn duration of the midcourse motor the geocentric distance had increased to 169,075 km and the inertial speed relative to Earth had decreased to 1.756 km/sec. Telemetry data received at the Goldstone Tracking Station and relayed to the Operations Facility at JPL gave positive indication that the midcourse maneuver and motor burn had been executed precisely. This was further verified by the observed doppler data being essentially the same as predicted.

D. Post-Midcourse Cruise

Following the midcourse maneuver, the spacecraft reacquired the Sun and Earth, thus returning to the cruise mode. At about 63 hr from injection and at a geocentric distance of 355,300 km the spacecraft inertial speed relative to the Earth reached a minimum value of 0.850 km/sec. At this point the spacecraft was about 28,300 km from the lunar surface with an inertial speed of 1.36 km/sec relative to the Moon. Because of the lunar gravitational field the spacecraft velocity then began to increase.

Post-midcourse tracking data up to within ½ hr before impact were analyzed and resolved the lunar encounter conditions to a high degree of accuracy with the lunar impact to occur at 10.68 deg S latitude and 20.68 deg W longitude with a flight time from injection of 68.097 hr. The encounter conditions along with the corresponding post-midcourse initial conditions are presented in Table 8. The space trace of the trajectory from injection to impact is given in Fig. 39.

E. Terminal Maneuver

The terminal maneuver study was begun some 4 hr after the midcourse maneuver. The camera orientation with the spacecraft in the cruise mode gave desirable results in that the surface viewed covered the region from the terminator (edge of camera B and right corner of camera A) to nearly 50 deg from the terminator; thus giving observation of a wide luminance range. Additionally, the field of the A camera viewed the impact point all the way down. At impact the velocity vector was approximately 7 deg from the central axis of the camera system and would give about 0.7 m/rms image motion over the last P-camera frame. With the predicted last frame resolution from the P_{1-2} cameras of 0.3 m and from the P_{3-4} cameras of 1.0 m (based on a 15-deg crater slope), the image motion would not become important until the last frame and then only for the P_{1-2} cameras. The image motion quoted is an rms average over an entire frame. Of course, all other factors equal, one desires to minimize image motion in all the cameras as is done in performing the nominal maneuver.

One degrading factor in the cruise mode orientation, as indicated by the experimenters, was the inclination of the surface to the cameras, that inclination being approximately 23, 32, and 37 deg from the local surface normal for the F_a, P, and F_b cameras, respectively, at impact.

Alternate terminal orientations were then studied that would reduce the image motion and the surface inclination to the cameras. In all, six orientations including the nominal maneuver cases were analyzed. Each of these maneuvers had one overriding factor eliminating them from contention—that factor being the surface-area coverage. In no case could one obtain reduced motion and reduced inclination and still view the terminator region with both the F_a and F_b cameras. Conversely, performing a maneuver to increase the terminator coverage also would increase the image motion above tolerable limits.

Thus, the cruise-mode orientation resulted in the most desirable camera orientation for the *Ranger VII* picture sequence.

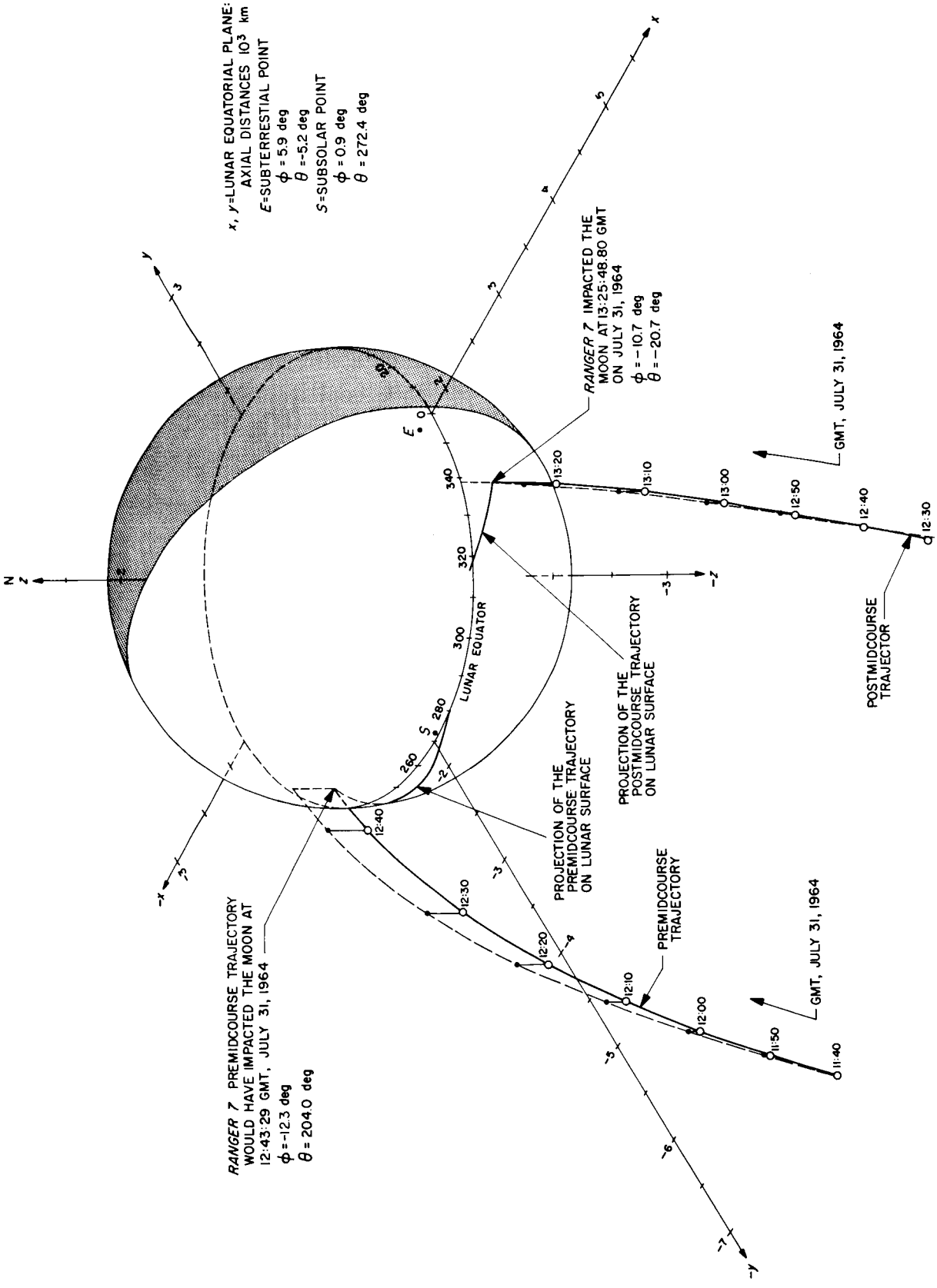

Fig. 38. Premidcourse and actual lunar encounters

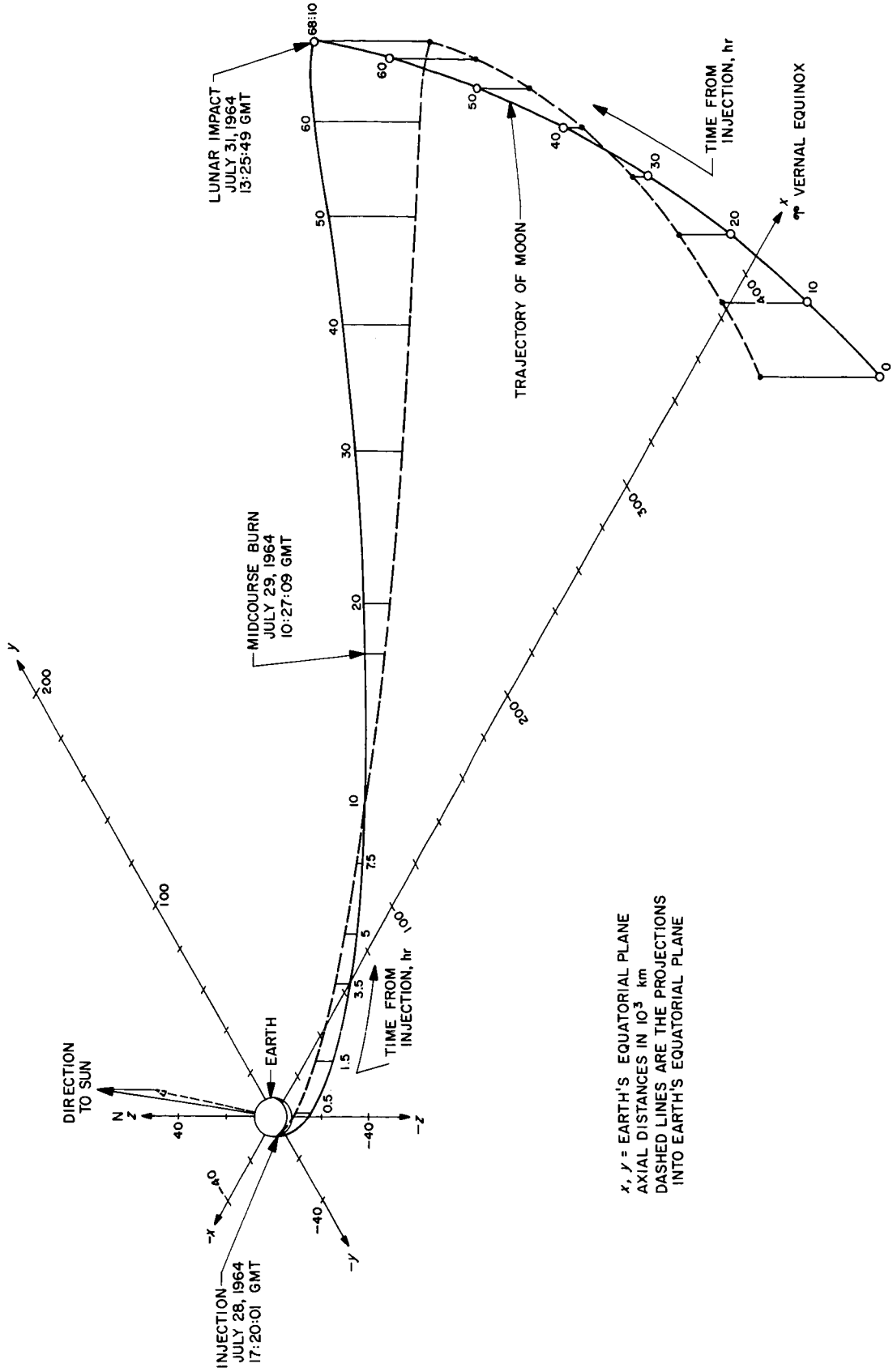

Fig. 39. *Ranger VII* trajectory in space

Table 8. Orbit used for maneuver determination and last postmidcourse orbit

Parameter	Premidcourse[a]	Postmidcourse[a]
Epoch	July 28, 1964; 1719:56 GMT	July 29, 1964; 1027:58 GMT
Earth-fixed sphericals		
R	6567.6350 km	169075.11 km
ϕ	−12.676075 deg	2.7386728 deg
θ	14.647727 deg	277.82452 deg
V	10.533237 km/sec	12.070902 km/sec
γ	1.3798852 deg	8.1207532 deg
σ	117.37931 deg	270.95860 deg
Inertial Cartesian		
x	−4833.6829 km	156674.78 km
y	−4206.2223 km	63040.835 km
z	−1441.1942 km	8078.5225 km
$\dot{x}$	7.0598554 km/sec	1.4342630 km/sec
$\dot{y}$	−6.8711888 km/sec	0.97256602 km/sec
$\dot{z}$	−4.7802415	0.28116494 km/sec
Orbital elements		
a	269557.90 km	244087.41 km
e	0.97564876	0.97401678
i	28.957643 deg	28.706807 deg
Ω	17.045773 deg	16.907167 deg
ω	204.26350 deg	203.78348 deg
ν	2.6878172 deg	161.92545 deg
Impact parameters		
Impact epoch	July 31, 1964; 1243:29.17 GMT	July 31, 1964; 1325:48.50 GMT
Selenocentric latitude	−12.344962	−10.671182 deg
Selenocentric longitude	203.95135	−20.68303 deg
Time of flight from injection	67.391 hr[b]	68.0965 hr[e]
$\lvert B \rvert$	3869.9779[c]	1811.2719 km[f]
$B \cdot T$[d]	−3794.9573	1623.8932 km
$B \cdot R$[d]	758.30590	802.29478 km

Definition of terms

R	Probe radius distance, km
ϕ	Probe geocentric latitude, deg
θ	Probe east longitude, deg
V	Probe Earth-fixed velocity, km/sec
γ	Path angle of the probe Earth-fixed velocity vector with respect to the local horizontal, deg
σ	Azimuth angle of the probe Earth-fixed velocity vector measured east of true north, deg
x,y,z	Vernal equinox Cartesian coordinates in a geocentric equatorial system. The origin is the center of the central body. The principal direction (x) is the vernal equinox direction of date, and the principal plane (x,y) is the Earth equatorial plane of date. z is along the direction of the Earth's spin axis of date, km.
$\dot{x},\dot{y},\dot{z}$	First time derivatives of x, y, and z, respectively: i.e Cartesian components of the probe space-fixed velocity vector, km/sec.
a	Semi-major axis, km
e	Eccentricity
i	Inclination, deg
Ω	Longitude of the ascending node, deg
ω	Argument of pericenter, deg
ν	True anomaly, deg

[a]See definition of terms.
[b]1σ uncertainty of 5.2 sec.
[c]1σ uncertainty of 15.9 km.
[d]$B \cdot T$ and $B \cdot R$ are referenced to the true lunar equator.
[e]1σ uncertainty of 1.0 sec.
[f]1σ uncertainty of 14.7 km.

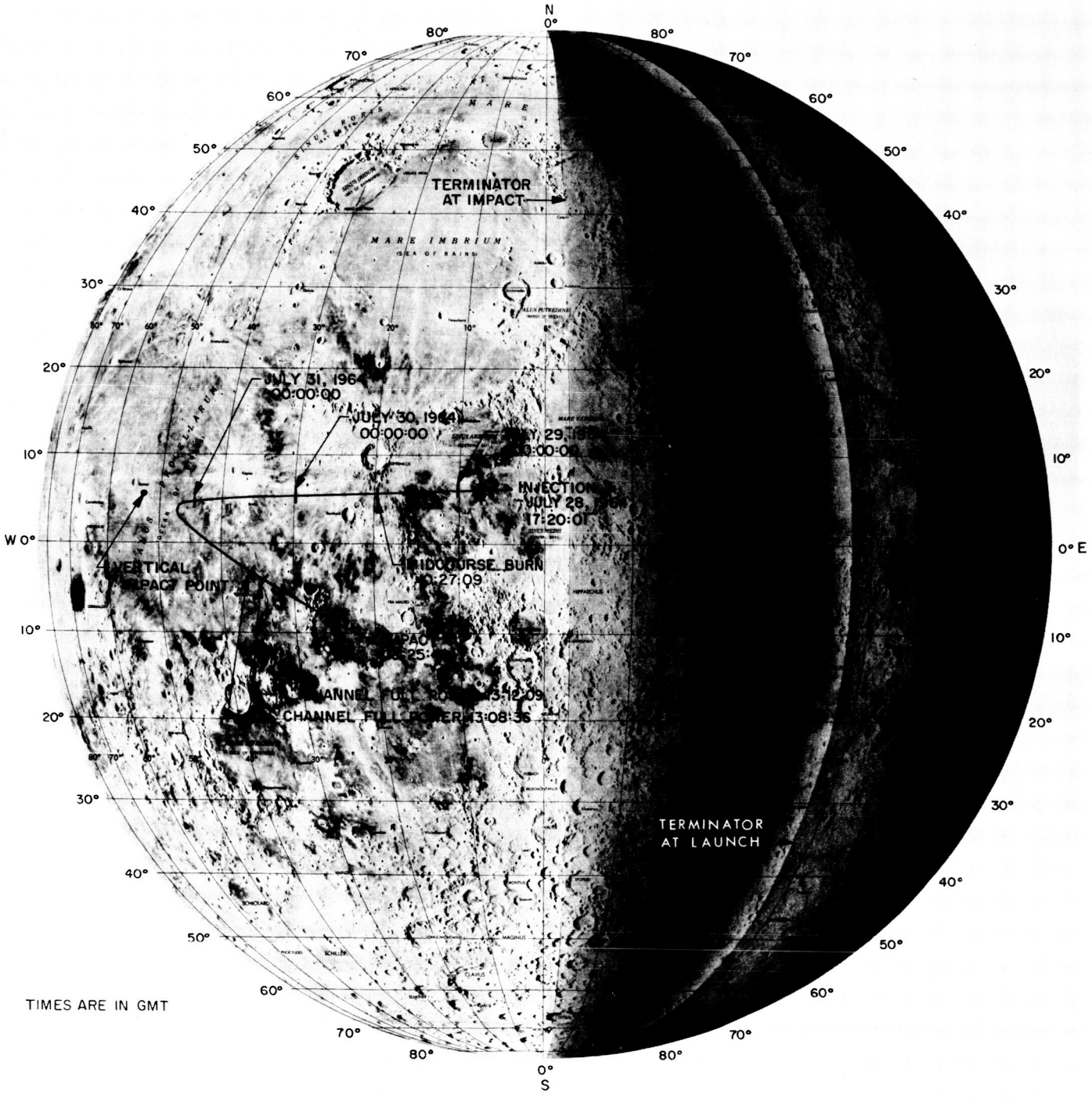

Fig. 40. *Ranger VII* trajectory Moon track

F. Encounter

During the encounter the spacecraft was subjected to increasing acceleration due to the pull of the lunar gravity field.

At an hour before impact, the speed of the probe relative to the Moon had increased to 1.551 km/sec and was at a lunar altitude of 6390 km.

The spacecraft approached the Moon in direct motion along a hyperbolic trajectory with the incoming asymptote direction at an angle of −5.57 deg to the lunar equator and with the orbit plane inclined 26.84 deg to the lunar equator. About 45.5 min before impact, the spacecraft crossed the lunar equator at an altitude of 4933 km. At 1308:36 GMT while at an altitude of 2126 km above the lunar surface, "F" channel full power was verified. At 1312:09 GMT and at an altitude of 1723 km, "P" channel full power was also verified. At 1325:49 GMT on July 31, 1964 *Ranger VII* crashed onto what was to be named the lunar *Mare Cognitum* at an impact speed of 2.616 km/sec and at a path angle of −64.1 deg.

The trace of the trajectory on the lunar surface from injection to impact is given in Fig. 40, while the traces of the lunar approach portions of the pre-midcourse and post-midcourse orbits are illustrated in Fig. 38.

VIII. PREFLIGHT CALIBRATION AND DATA ENHANCEMENT

A. Photometric Studies

The photometric calibration of the television cameras served two fundamental purposes: to verify the predicted surface brightness (used for camera gain adjustment), and to provide information for surface slope measurements in conjunction with the known photometric characteristics of the Moon. This section presents preliminary results of the surface-brightness verification.

On the P_3 and P_4 cameras, calibration curves were obtained for two small regions, each consisting of 32 picture elements, one-third and two-thirds of the way from top to bottom of the picture raster. The four resulting curves are given in Fig. 41 and 42. These curves, called light-transfer characteristics, represent the camera output as a function of the incident illumination.

The data were obtained by exposing the cameras to known light levels and recording the system output on magnetic tape. Illumination was adjusted in 12 steps with neutral density filters to cover the entire dynamic range. The magnetic tapes were demodulated and the information was digitally encoded to provide a computer input; the computer provided camera output in relative amplitude units. Incident illumination was plotted in

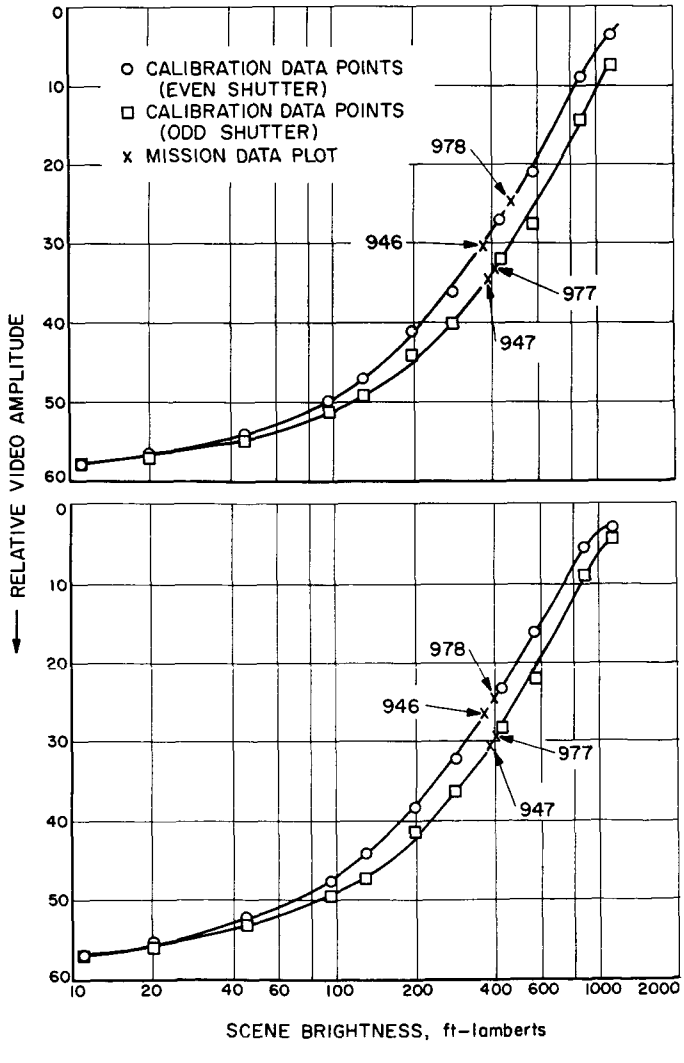

Fig. 41. Light-transfer characteristics, camera P_3

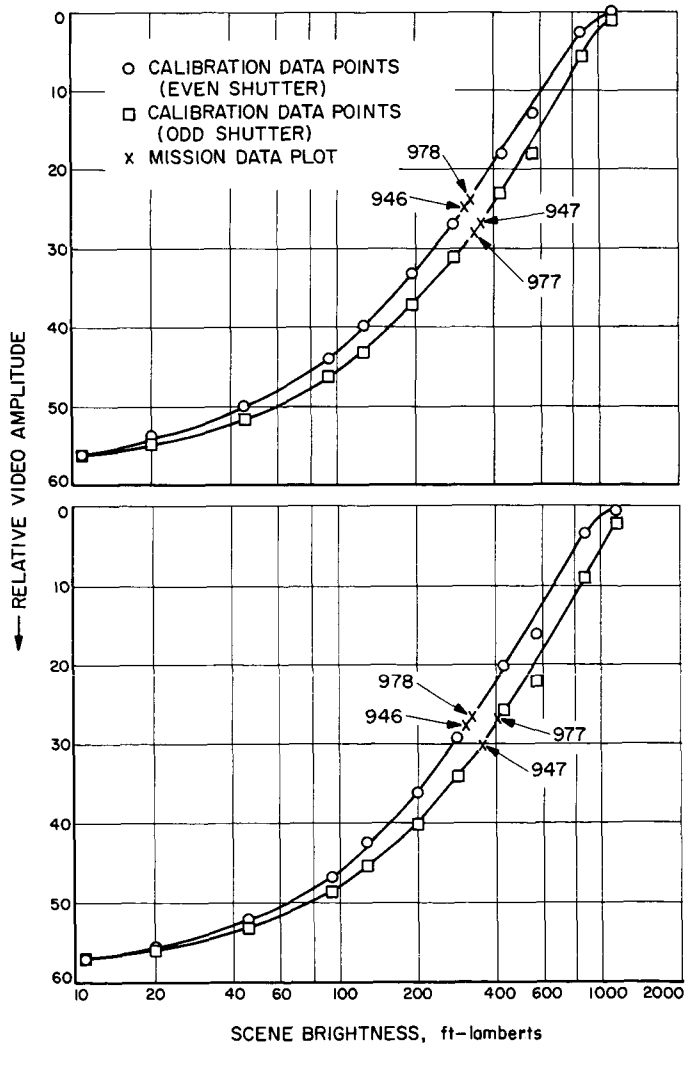

Fig. 42. Light-transfer characteristics, camera P_4

terms of scene brightness, after application of a spectral correction factor to account for differences in the spectral emission characteristics of the calibration sources and the reflected solar energy from the Moon. Due to the alternating operation of the shutter, small exposure-time variations are noted between "even" and "odd" pictures. Therefore, two curves are presented in each Figure: one corresponds to even-numbered mission frames and the other to odd-numbered mission frames. Surface brightness measurements could then be obtained by plotting camera outputs from pictures taken during the *Ranger VII* mission. The curves show the results from a total of eight photographs taken with the P_3 and P_4 cameras. Two pictures from each camera of the area close to the impact point (frames 977 and 978), and a second set of four pictures of an area photographed 27 sec before impact (frames 946 and 947), were used. The brightness measurements were taken at exactly the same two locations on the vidicons as had been calibrated, since the vidicon transfer curves vary from spot to spot. In frames 978 and 979 the area photographed is very rough and changing from one frame to the next. As a result, the measured brightness varies from frame to frame and within a picture. On frames 946 and 947, however, the area is fairly uniform and changing slowly so that the measured values should be consistent from frame to frame and between the two cameras.

The values from the curves are tabulated in Table 9. The values from P_3 on 946 and 947 are in very good agreement. The values taken from P_4, however, are not consistent from 946 to 947, although the top and bottom of each picture are in good agreement. Frame 947 on P_4 is about 20 ft-lamberts below the average of the P_3 readings, while 946 on P_4 is 60 ft-lamberts below P_3 average. This difference could easily be explained by a slight exposure change (from that observed before flight) in one direction of the P_4 shutter.

Table 9. Preliminary surface-brightness measurements

Frame	Brightness, ft-lamberts			
	P_3 Camera		P_4 Camera	
	Upper	Lower	Upper	Lower
946	360	360	300	310
947	375	370	340	350
977	400	400	400	330
978	460	395	315	320
(Ref. Fig.)	41a	41b	42a	42b

Based on the two cameras evaluated, the surface brightness is higher than expected in the region covered by frames 946 and 947. The average for these two frames is 345 ft-lamberts; predicted value was 245 ft-lamberts.

B. Figure of Merit Verification

The figure of merit is a mathematical tool for predicting the TV subsystem performance in terms of the minimum surface element that can be detected on the lunar surface by an observer viewing the output film of the *Ranger* system. The mathematical model includes an empirical lunar photometric model, a simplified mathematical description of the TV system, and a low-pass filtering model for the human observer. With the many approximations involved, it is desirable to verify the accuracy of the model by use of the *Ranger VII* data. Owing to the nature of the human-observer model, a subjective verification is required. Further the model employs many "idealizing" assumptions (for example, white noise): the ideal system of the mathematical model represents the ultimate in picture resolution.

As has been discussed, the preliminary luminance value obtained from the P_3 and P_4 cameras on *Ranger VII* in the region of impact was approximately 345 ft-lamberts, although the photometric model had predicted a luminance value of 245 ft-lamberts for the P cameras. The observed value was about 43% greater than the predicted value.

A number of factors may account for the difference. For example, the photometric function is an average of all lunar marial surfaces into one function. The original data scatter for the observational geometry involved in the *Ranger* encounter is $+35\%$ to -20% about the average. A spherical moon is assumed for the luminance calculations, and the luminance curve (again for the *Ranger VII* observation geometry) has a slope of 7 ft-lamberts per degree of surface inclination. Thus, if the local surface is "out of round" some luminance error will occur.

The combination of possible local surface slope variations with the original data scatter then places the observed luminance value within the expected accuracy of the photometric model. However, it should be noted that the quoted slope of the luminance curve applies only over a short region and that an inclination of nearly 20 deg would be required to explain the observed luminance by use of this hypothesis alone. The general reflectivity characteristic of *Mare Cognitum* is that of an

average mare surface; it cannot be said that the impact region, at least for the frames used to obtain the measured luminance values, is brighter than most other mare surfaces.

An appropriate figure-of-merit calculation for verification of the general model should include the observed higher luminance value and the actual frame time before impact for each of the last camera exposures. The increase in luminance is obtained by simply increasing the reflectivity of the mare surface (in the computer program). A last-picture frame time of 0.187 sec was assumed for camera P_3.

Two separate calculations are made in the figure of merit: one, the rms image motion over the entire frame; the other, the minimum detectable element through the camera system, considering surface luminance and contrast as generated by a feature of 5, 15, and 30-deg slope. For the last P_3 frame, image motion is calculated to be 0.8 m, based on actual altitude, while element sizes of 0.57 and 0.22 m respectively are found for a 5 and 30-deg slope feature. The observable resolution (or minimum detectable element) for the last P_3 frame is seen subjectively to be bounded by the 0.8 and 0.22-m values, thus indicating that the figure of merit is a reasonable predictor of system performance for this particular case.

C. Video Retrieval

The removal of distortion and noise from video data, desirable in itself, is particularly important in the case of the last few *Ranger VII* lunar pictures, inasmuch as the increase in photographic resolution of lunar-surface detail was a prime mission objective.

The effect of noise on visual resolution is direct. The noisier the data, the greater the number of adjacent picture elements must be averaged to establish correct intensity for a given point; hence, the larger, and fewer, are the individual resolution elements.

The upper bound on *Ranger VII* video resolution was based on a combination of the optical system and the size of the video scanning beam (as well as spacecraft position during exposure). A large number of distortion sources were present, and the preflight possibilities were very broad.

The first step in processing the video data for distortion removal is to digitize it for manipulation and analysis. A facility has been established for this processing. It uses the magnetic-tape data as source, in order to recover the initial film-recorder losses, and outputs a processed signal to a high-precision film recorder.

The processing facility can take the received video signal along with appropriate calibration data and perform the following operations:

1. Locate line sync in weak signal recovered directly from magnetic tape.
2. Correct for photometric distortion caused by nonuniformity in camera sensitivity.
3. Correct for geometric distortion caused by nonlinear sweep deflection in the camera.
4. Remove random noise by superposition of pictures containing the same lunar area.
5. Make linear geometric transformations of photographs to correct for pictures not taken normal to the surface.
6. Remove structured noise:
   a. Mesh noise detectable in calibration photos.
   b. Ghosting noise caused by retention of previous image on the vidicon.
   c. Periodic noise caused by stray electronic coupling to oscillators on board the spacecraft.
   d. Clamp-error noise causing shift of intensity for whole video line.
   e. Fiducial marks.

Enhancement of signal becomes automatic as more noise is removed. But more effective visually is the ability to use the computer to increase the contrast of the picture as desired, in the digital output tape which goes to the film recorder.

In addition, the retrieval facility is capable of pattern extraction. The cross-correlation program used in filtering can also be used to establish the magnitude of any described objects, its geographic distribution, and its frequency of occurrence. It is also possible to perform statistical transformations, tabulations, and calculations which serve as powerful tools for analysis of various specific problems. A program which is under development and almost complete will convert brightness to slope and integrate these slopes along the Sun line to derive altitudes which can then be contoured.

Under detailed examination, the unenhanced *Ranger VII* photographs exhibited many forms of distortion. A

number of these, intrinsic to the film recorder, were eliminated initially by digitizing from the magnetic tape. In conjunction with a computer program which reassembles digitized data for the digital film recorder, digitized photographs, with resolution improved over those initially recorded, were prepared.

Figures 43–45 present the digitizing and noise-extracting process. The original film record of the last A frame is given in Fig. 43a, with enlargements of the "rock" feature and the impact area in Fig. 43b and 43c. The stages of the retrieval process are given in Fig. 44 and 45: 44a represents the data of Fig. 43b digitized, and 45a similarly corresponds to 43c.

As a result of the improved resolution, certain noises became much more prominent. An example is the 15-kc erase signal which was on during part of the video cycle. This oscillator was involved with erasing the already transmitted video image from the F cameras. While this erasing was taking place, pictures from other cameras were being transmitted and some noise signal was superimposed on the desired signal. Through interaction with the line level clamp, a moiré pattern appears in the final signal.

A two-dimensional digital filter was programmed and the magnitude of the unwanted frequency was determined at each point in the picture (see Fig. 44b and 45b). The noise was then subtracted from the picture to give the results seen in Fig. 44c and 45c. Enhancement of contrast brings out more detail (Fig. 44d and 45d). Enhancement without noise removal is shown for comparison in Fig. 45e.

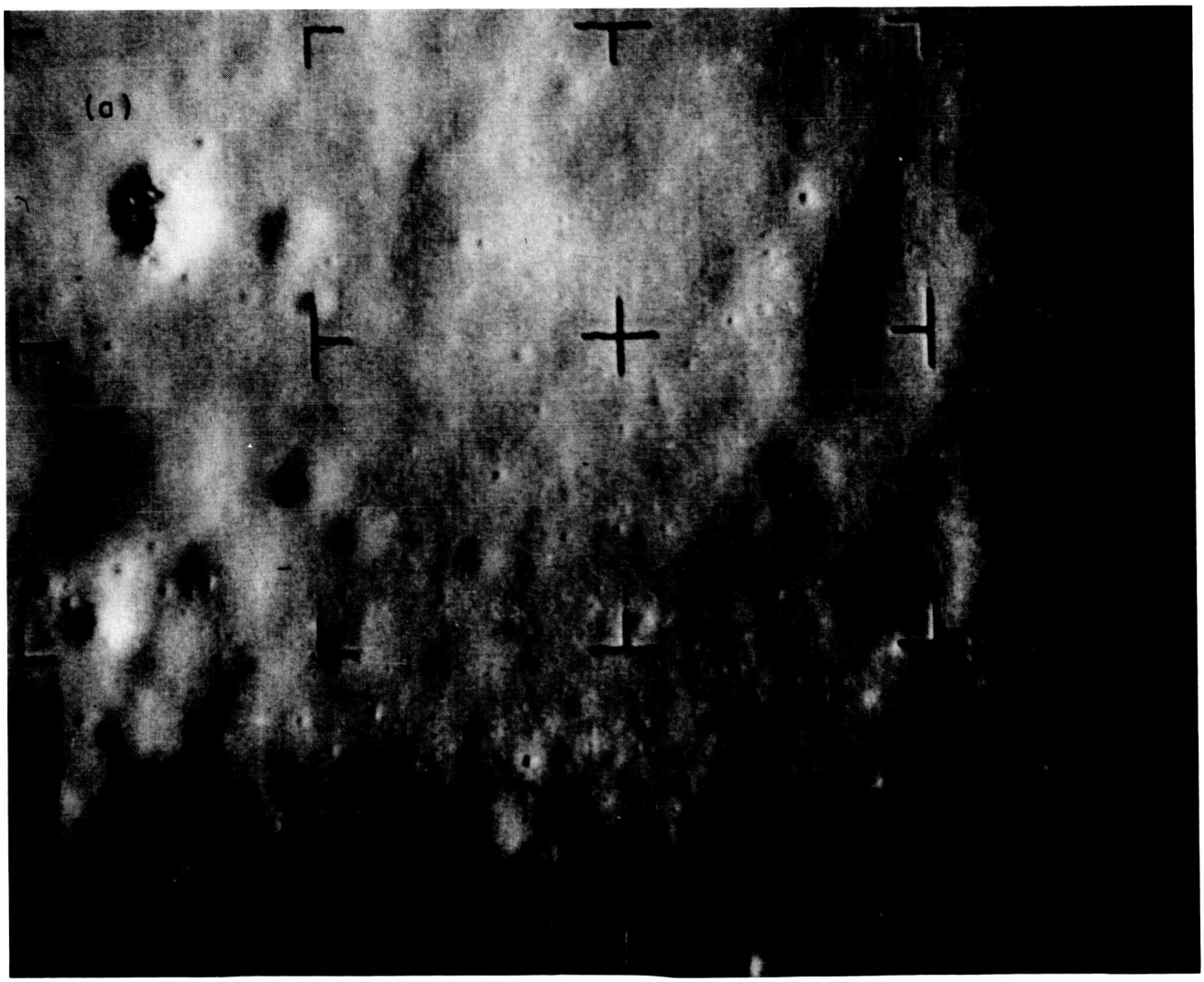

Fig. 43. Original recording, last photograph from camera F_a

Another source of distortion appears as streaks across the picture arising from improper line clamping and/or drift of line level (for example, the last P_3 frame, shown in Fig. 46a). Another digital filter was applied and contrast increased to give the results in Fig. 46b. The operations performed by the computer as illustrated in this section are only a brief sample of the capability of this tool as it serves to aid in the analysis of the data. Planning is now in progress for continued development of this capability for use in the general data analysis program with particular emphasis on supporting the Experimenters' requirements.

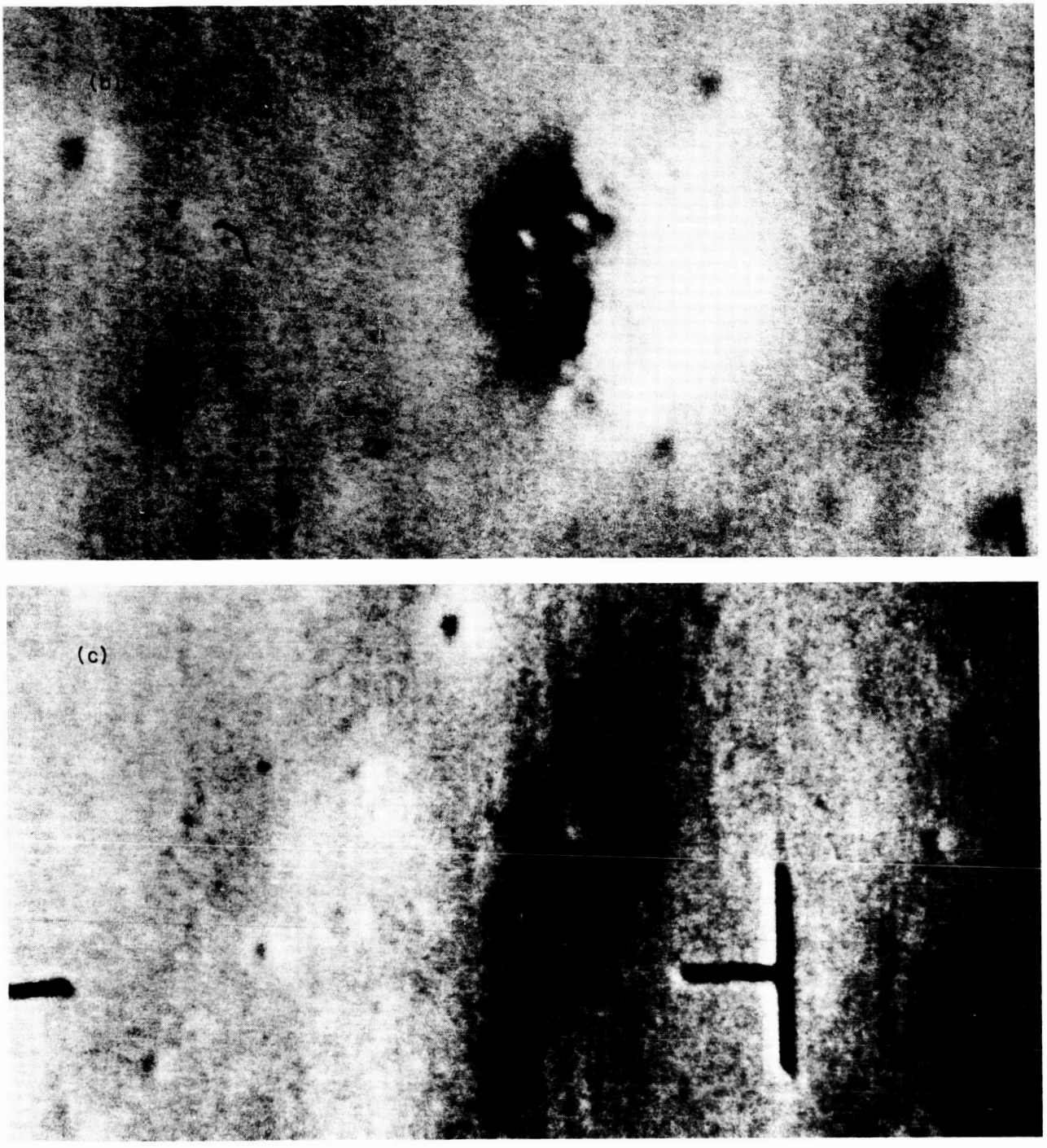

Fig. 43. Original recording, last photograph from camera F_a (Cont'd)

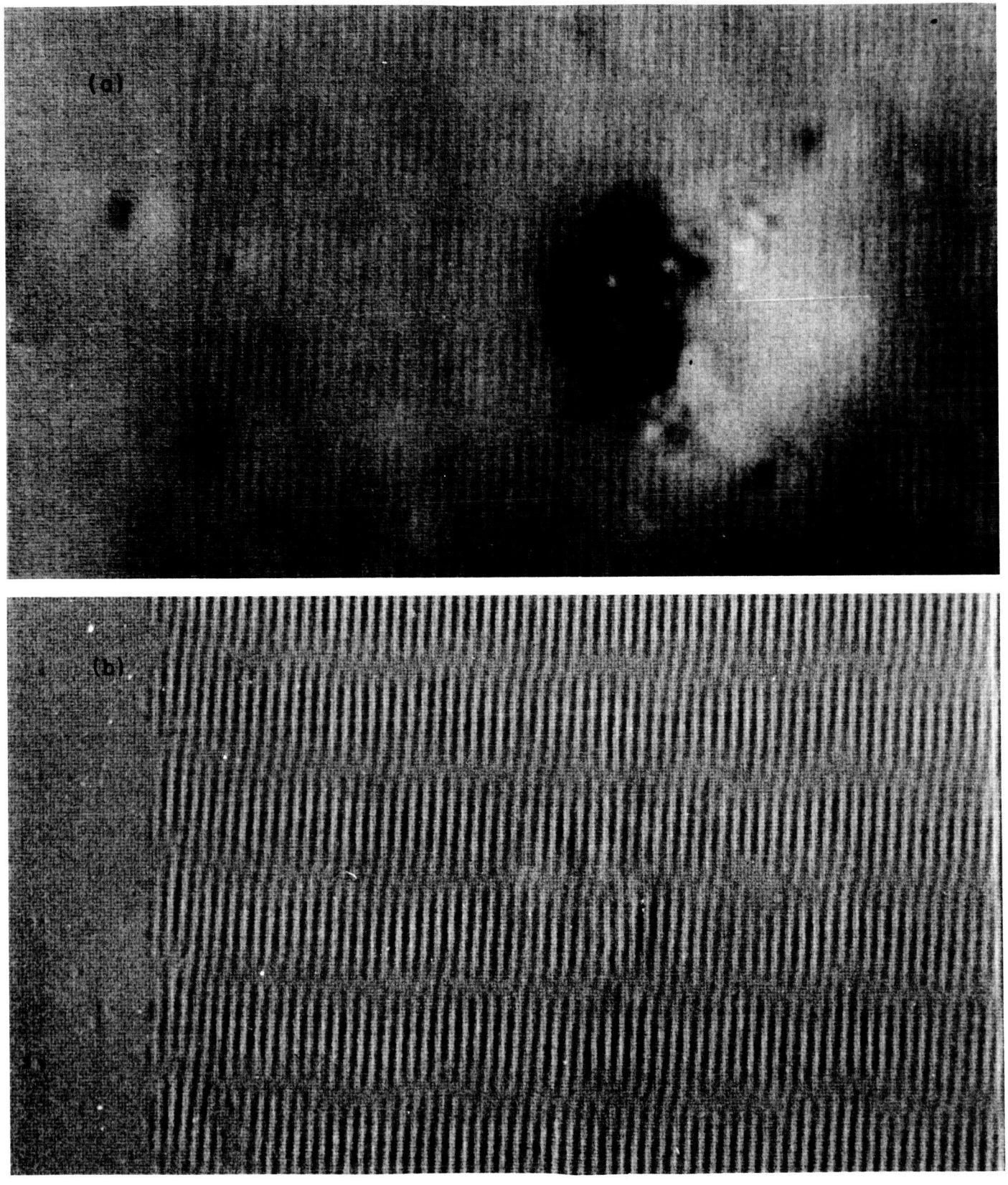

Fig. 44. Noise removal and contrast enhancement, Fig. 43b

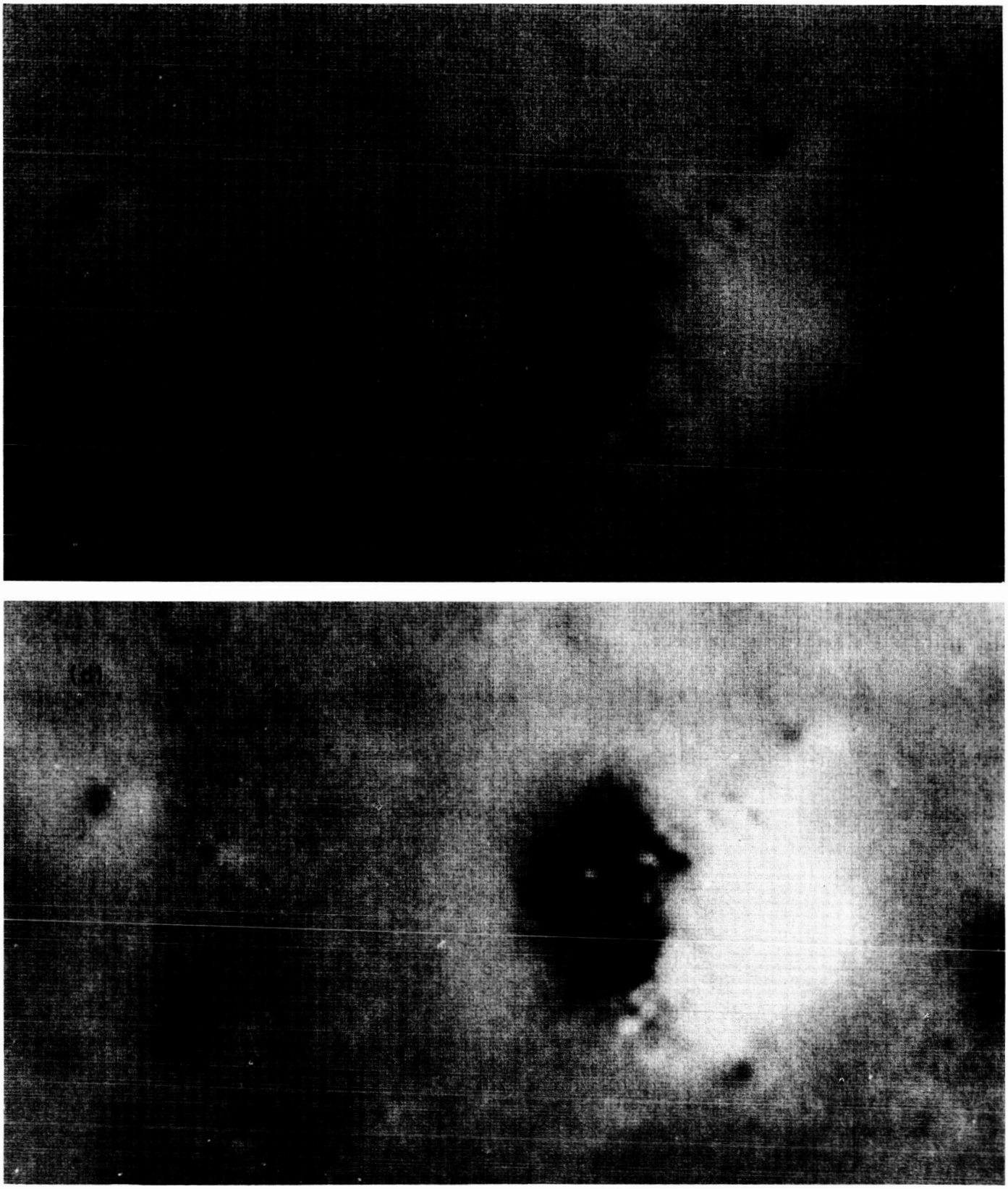

Fig. 44. Noise removal and contrast enhancement, Fig. 43b (Cont'd)

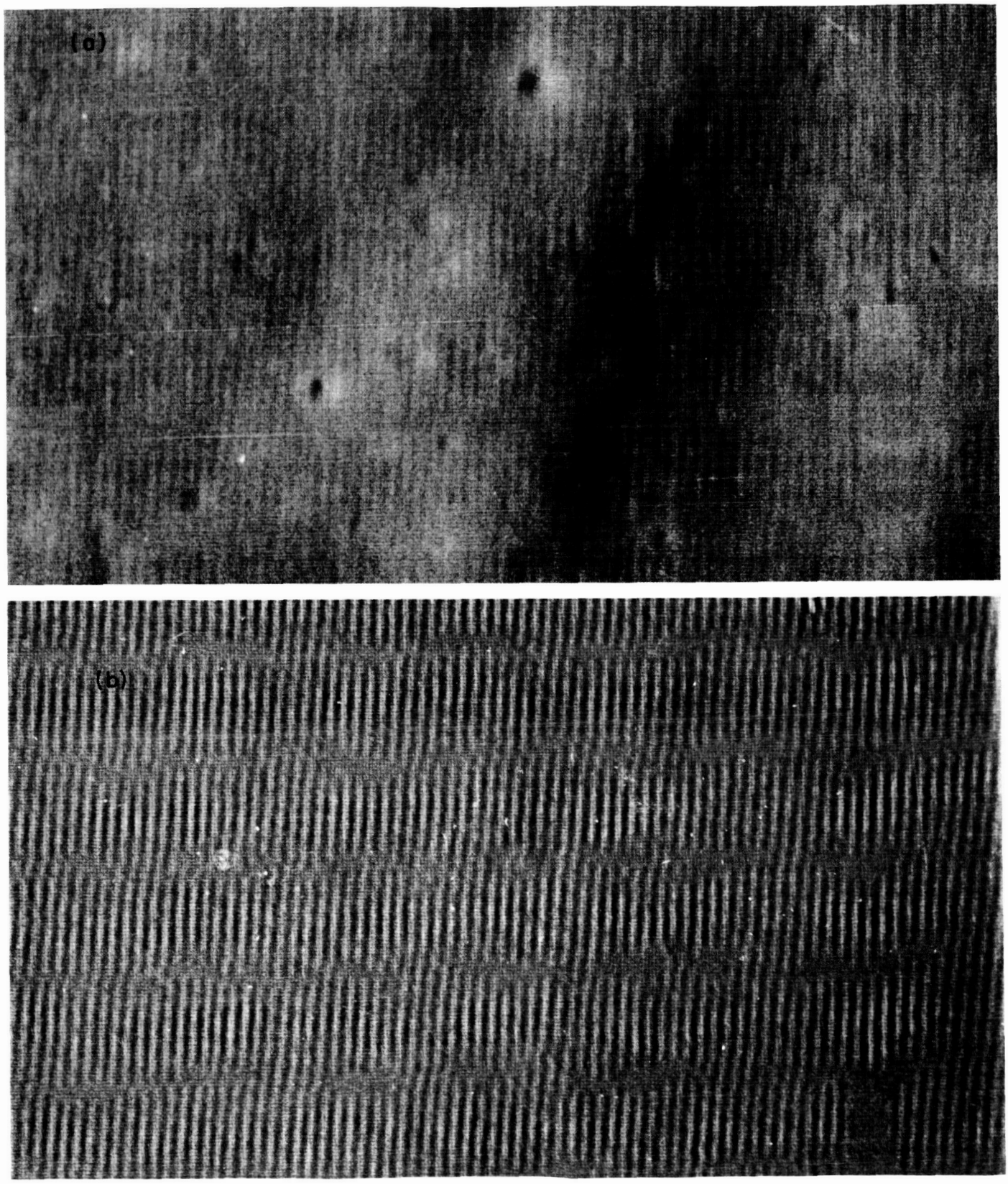

Fig. 45. Noise removal and contrast enhancement, Fig. 43c

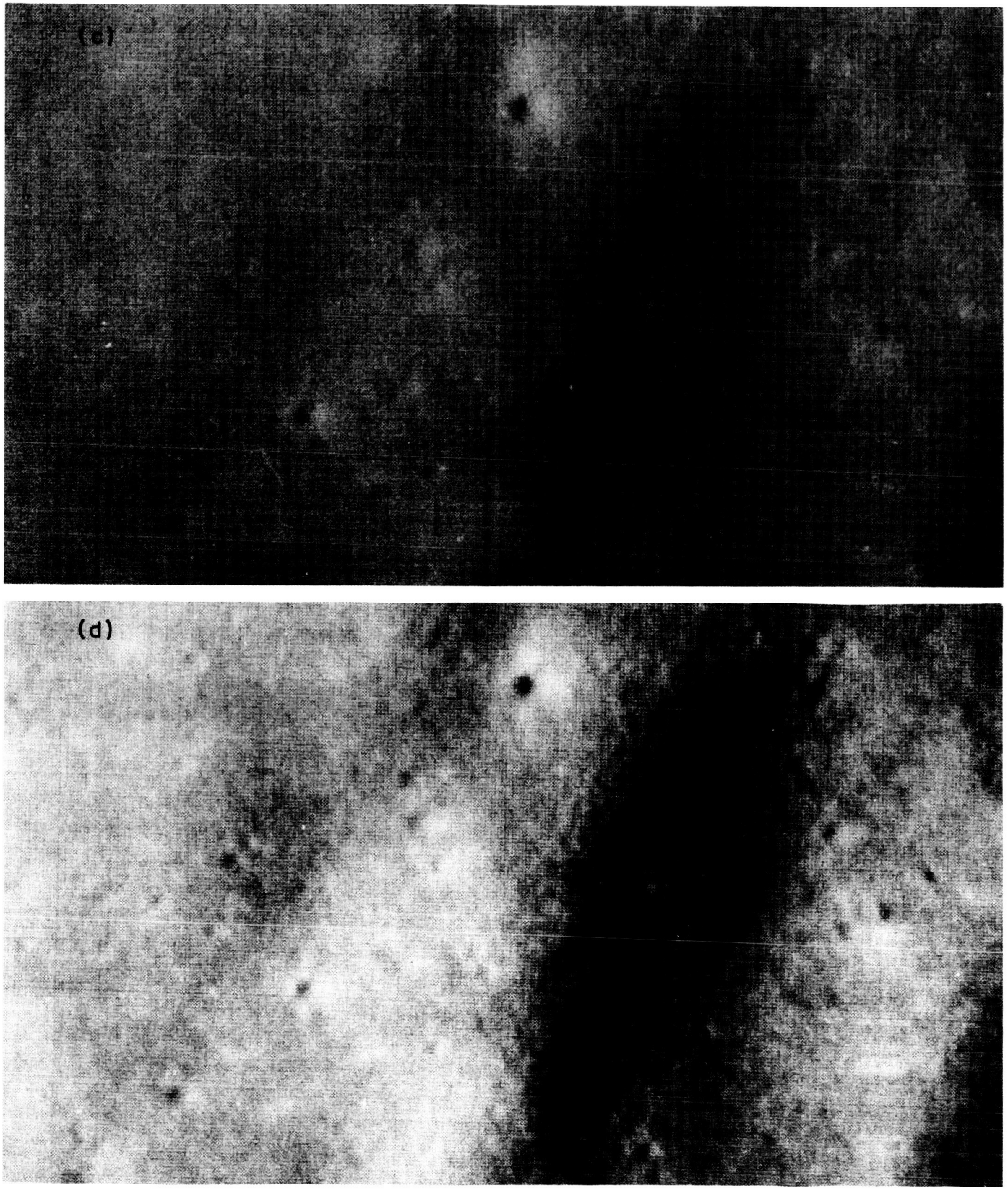

Fig. 45. Noise removal and contrast enhancement, Fig. 43c (Cont'd)

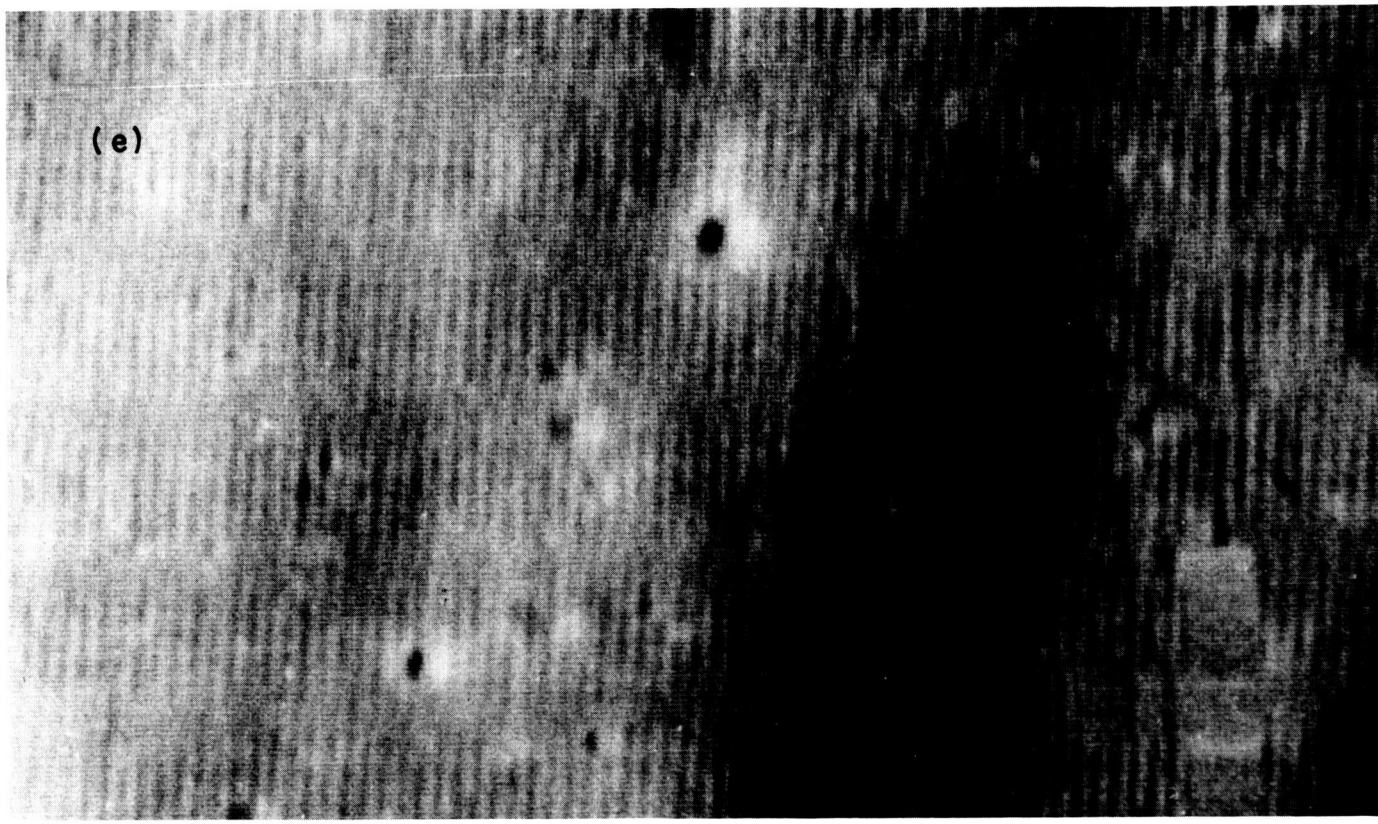

Fig. 45. Noise removal and contrast enhancement, Fig. 43c (Cont'd)

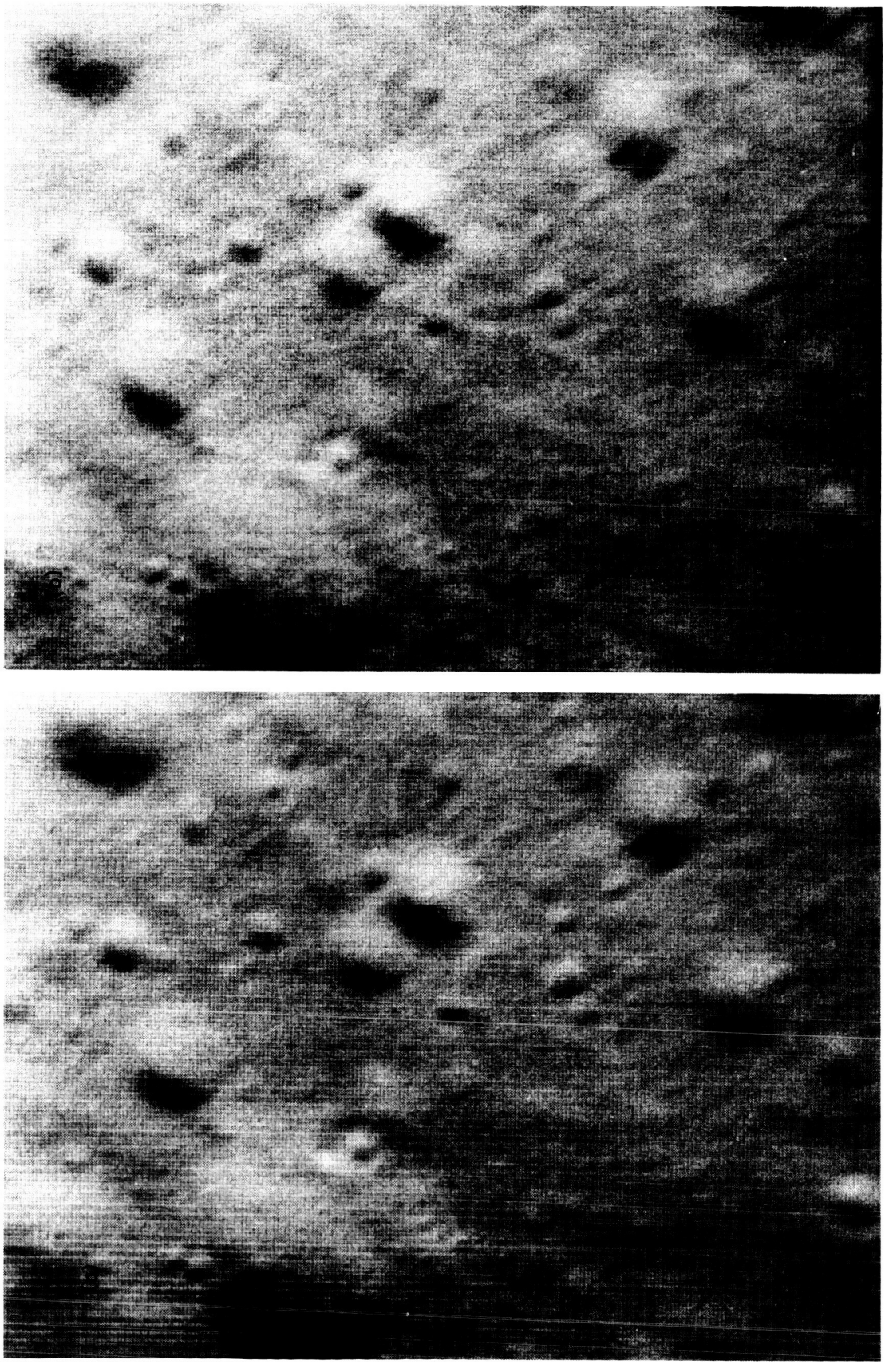

Fig. 46. Line distortion removal

APPENDIX A

Ranger VII Spacecraft Flight Events

Spacecraft flight events	Nominal mission time	Predicted GMT	Actual GMT
Prelaunch Events, July 28, 1964 (Day 210)			
1. Spacecraft power turned on	T − 210 min	—	1210
2. Transmission of 2 RTC-2 commands	T − 126 min	—	1334
a. Antenna preset hinge angle—122 deg			
3. Start TV low-power-mode checks	T − 116 min	—	1344
4. Stop TV low-power-mode checks	T − 106 min	—	1354
5. Programmed hold	T − 60 min	—	1440
6. Resuming countdown	T − 60 min	—	1540
7. TV cruise-mode telemetry turned on	T − 15 min	—	1625
8. Programmed hold	T − 07 min	—	1633
9. ETR reports H9 sync end at 1633:36	—	—	1642
10. Resuming countdown	T − 07 min	—	1643
11. Spacecraft on internal power	T − 05 min	1645:00[a]	1645:00
12. CC&S inhibit released	T − 02 min	1648:00[a]	1648:00
13. CC&S clear relays event (B-2-1)	T − 01 min	1649:00[a]	1649:00
Flight Events			
14. Liftoff	T − L	1650:00[a]	1650:08
15. Spacecraft squib-firing assemblies armed	L + 10 sec	1650:10[a]	—
16. Mark 1	—	—	1652:23.2
17. Mark 2	—	—	1652:26.1
18. Mark 3	—	—	1654:53.8
19. Mark 4	—	—	1655:12.0
20. Mark 5: nose fairing ejection	—	—	1655:13.1
21. Mark 6: *Atlas/Agena* separation	—	—	1655:16.8
22. Mark 7	—	—	1655:57.8
23. DSIF 71 loses lock (spacecraft over horizon)	—	—	1657:49
24. Mark 8	—	—	1658:34.4
25. CC&S commands transmitter power up (B-2-1)	L + 23 min	1713:00[b]	1713:00
26. Mark 9	—	—	1718:32.1
27. Mark 10: injection	—	—	1720:01.0
28. Spacecraft enters Earth's shadow	L + 31 min	1721:00[c]	—
29. DSIF 59 acquires spacecraft	—	—	1721:01
30. DSIF 51 acquires spacecraft	—	—	1721:38
31. Mark 11: fire payload interface connectors	—	—	Not known
32. Mark 12: Spacecraft/*Agena* separation	S	—	1722:36.1
a. Start TV backup clock (F-chain)	S + 00 sec	1722:36[c]	—
b. Start backup command timer (BUCT)	S + 00 sec	1722:36[c]	—
c. Remove CC&S relay clamp	S + 00 sec	1722:36[c]	—
d. TV enable via hydraulic timer (BUCT)	S + 30 min	1752:36	—
33. Mark 13: *Agena* retro maneuver	—	—	1729:06.3
34. DSIF 51, 59 lose lock (spacecraft over horizon)	—	—	1732
35. DSIF 41 acquires spacecraft (one-way lock)	—	—	1735:22
a. Establishes two-way lock	—	—	1737:57
36. CC&S commands solar panel extension (B-2-1)	L + 60 min	1750:00[b]	1750:00
a. Squib-firing assemblies fired	L + 60 min	1750:00[b]	—
b. B-2-2 event (SFA "A" had fired)	—	1750:04[b]	1750:04
c. B-2-3 event (SFA "B" had fired)	—	1750:08[b]	1750:08
d. B-2-4 microswitch closure (panels extended)	—	1752:22[d]	1751:17
e. TV subsystem "armed" by −X solar panel microswitch	S + 46 min	1751:17[e]	—

[a] Times are based on launch plan announced at T − 7 min.
[b] Predicted times derived from CC&S inhibit-release time of 1648:00.
[c] Times based on a nominal spacecraft trajectory for launch azimuth of 97 deg.
[d] Predicted slowing of actuator-response time due to spacecraft being in Earth's shadow.
[e] After B-2-4 event had occurred. This observed time became the best time prediction for this event.

Spacecraft flight events	Nominal mission time	Predicted GMT	Actual GMT
Flight Events			
37. CC&S commands Sun-acquisition sequence (B-2-1)	L + 63 min	1753:00[b]	1753:00
38. Spacecraft exists from Earth's shadow	L + 70 min	1800:00[c]	—
39. Spacecraft acquires Sun	L + 100 min	—	1806:52
40. CC&S commands Earth-acquisition sequence (B-2-1)	L + 211 min	2021:00[b]	2021:00
41. Spacecraft acquires Earth	L + 241 min	—	2045:02
42. DSIF 41 transmits spacecraft antenna-transfer command	L + 265 min	2115:00[f]	—
a. 1st RTC-0 initiated	—	2115:00	2115:00
b. 1st RTC-0 verified	—	2115:38	2115:38
c. 2nd RTC-0 initiated	—	2117:00	2116:00
d. 2nd RTC-0 verified	—	2117:38	2116:38
e. RTC-3 initiated	—	2119:00	2119:00
f. RTC-3 verified	—	2119:38	2119:38
g. B-20 event: spacecraft on high-gain antenna	—	2119:38	2119:38
July 29, 1964 (Day 211)			
43. TV backup clock 8-hr pulse (Rdg to −15 sec)	S + 08 hr	0122:36[g]	0122:40
44. DSIF 12 transmits midcourse stored commands	M − 70 min	0850:00[f]	—
a. 1st RTC-0 initiated	—	0850:00	0850:00
b. 1st RTC-0 verified	—	0850:39	0850:39
c. 2nd RTC-0 initiated	—	0852:00	0852:00
d. 2nd RTC-0 verified	—	0852:39	0852:39
e. SC-1 initiated (25-1645-1) + 5.56 deg	—	0854:00	0854:00
f. SC-1 verified (24-sec positive roll)	—	0854:39	0854:40
g. B-2-1 event: capacitor cycling pulse	—	—	0854:44
h. SC-2 initiated (35-2251-0) −86.80 deg	—	0856:00	0856:00
i. SC-2 verified (392-sec negative pitch)	—	0856:39	0856:41
j. SC-3 initiated (03-2440-1) 29.89 m/sec	—	0858:00	0858:00
k. SC-3 verified (49-sec burn)	—	0858:39	0858:41
45. TV backup clock 16-hr pulse (Rdg to −15 sec)	S + 16 hr	0922:36[g]	0922:40
46. DSIF 12 transmits spacecraft antenna-transfer command	M − 20 min	0940:00[f]	—
a. 1st RTC-0 initiated	—	0936:00	0936:00
b. 1st RTC-0 verified	—	0936:39	0936:38
c. 2nd RTC-0 initiated	—	0938:00	0938:00
d. 2nd RTC-0 verified	—	0938:39	0938:39
e. RTC-3 initiated	—	0940:00	0940:00
f. RTC-3 verified	—	0940:39	0940:39
g. B-20 event: spacecraft on low-gain antenna	—	—	0940:41
47. DSIF 12 initiates midcourse maneuver sequence	—	—	1000:00
a. RTC-4 initiated	—	1000:00[f]	1000:00
b. RTC-4 verified	—	1000:39	1000:38
48. B-20 event: B-counter counting	M	1000:39[h]	1000:39
a. CC&S commands start roll maneuver (B-2-1)	M + 05 sec	1000:44	1000:44
b. CC&S commands stop roll maneuver (B-2-1)	Item 48a + 24 sec	1001:08	1001:08
c. CC&S commands start pitch maneuver (B-2-1)	M + 9.5 min	1010:09	1010:09
d. CC&S commands stop pitch maneuver (B-2-1)	Item 48c + 329 sec	1016:41	1016:41
e. Telemetry mode II (accelerometer data on channel 8)	—	1016:41	1016:41
f. CC&S commands midcourse motor ignition (B-2-1)	M + 26.5 min	1027:09	1027:09
f-1. Squib-firing assemblies fired	M + 26.5 min	1027:09	1027:09
f-2. B-2-2 event	—	1027:13	1027:13
f-3. B-2-3 event	—	1027:17	1027:17
g. CC&S commands midcourse-motor shutoff (B-2-1)	Item 48f + 49 sec	1027:58	1027:59
g-1. Squib-firing assemblies fired	Item 48f + 49 sec	1027:58	1027:59

[b] Predicted times derived from CC&S inhibit-release time of 1648:00.
[c] Times based on a nominal spacecraft trajectory for launch azimuth of 97 deg.
[f] Times are based on command message sent to the DSIF initiating this sequence.
[g] Times are based upon observed spacecraft/Agena separation time.
[h] Predicted times in the midcourse sequence are based on CC&S design and stored commands entered by ground command.

Spacecraft flight events	Nominal mission time	Predicted GMT	Actual GMT
Flight Events			
g-2. B-2-2 event	—	1028:03	1028:03
g-3. B-2-3 event	—	1028:07	1028:07
49. CC&S commands Sun reacquisition sequence (B-2-1)	M + 30 min	1030:39	1030:39
a. Telemetry mode III (15-pt TV data on channel 8)	M + 30 min	1030:39	1030:39
50. Spacecraft reacquires Sun	≤ M + 60 min	—	1036
51. CC&S commands Earth reacquisition sequence (B-2-1)	M + 58 min	1058:39	1058:39
52. Spacecraft reacquires Earth	≤ M + 88 min	—	1058:39
53. DSIF 12 transmits spacecraft antenna transfer command	M + 80 min	1120[f]	—
a. 1st RTC-0 initiated	—	1121:00	1121:00
b. 1st RTC-0 verified	—	1121:39	1121:38
c. 2nd RTC-0 initiated	—	1123:00	1123:00
d. 2nd RTC-0 verified	—	1123:39	1123:39
e. RTC-3 initiated	—	1125:00	1125:00
f. RTC-3 verified	—	1125:39	1125:39
g. B-20 event: spacecraft on high-gain antenna	—	—	1125:43
54. TV backup clock 24-hr pulse (Rdg to +5 sec)	S + 24 hr	1722:36[g]	1722:40
July 30, 1964 (Day 212)			
55. TV backup clock 32-hr pulse (Rdg to −15 sec)	S + 32 hr	0122:36[g]	0122:37
56. TV backup clock 48-hr pulse (Rdg to −15 sec)	S + 48 hr	1722:36[g]	1722:31
July 31, 1964 (Day 213)			
57. TV backup clock 64-hr pulse (Rdg to −15 sec)	S + 64 hr	0922:36[g]	0922:23
58. DSIF 11 transmits terminal stored commands	C − 70 min	1115[f]	—
a. 1st RTC-0 initiated	—	1115:30	1115:30
b. 1st RTC-0 verified	—	1116:09	1116:08
c. 2nd RTC-0 initiated	—	1117:30	1117:30
d. 2nd RTC-0 verified	—	1118:09	1118:09
e. SC-4 initiated (23-1771-1)	—	1119:30	1119:30
f. SC-4 verified (1-sec positive pitch)	—	1120:09	1120:10
g. B-2-1 event: capacitor cycling pulse	—	—	1120:16
h. SC-5 initiated (13-1771-1)	—	1121:30	1121:30
i. SC-5 verified (1-sec positive yaw)	—	1122:09	1122:10
j. SC-6 initiated (33-1771-1)	—	1123:30	1123:30
k. SC-6 verified (1-sec positive pitch)	—	1124:09	1124:10
59. DSIF 12 transmits maneuver override command	C − 25 min	1150[f]	—
a. 1st RTC-0 initiated	—	1151:00	1151:00
b. 1st RTC-0 verified	—	1151:39	1151:38
c. 2nd RTC-0 initiated	—	1153:00	1153:00
d. 2nd RTC-0 verified	—	1153:39	1153:39
e. RTC-8 initiated	—	1155:00	1155:00
f. RTC-8 verified	—	1155:39	1155:38
g. B-20 event: CC&S "disconnected" from Attitude-Control Subsystem	—	—	1155:41
60. DSIF 12 initiates terminal maneuver sequence	C − 39 sec	1225:08[f]	—
a. RTC-6 initiated	—	1225:08	1225:08
b. RTC-6 verified	—	1225:47	1225:47
61. B-20 event: C counter counting	C	1225:47[l]	1225:49
a. CC&S commands start 1st pitch maneuver (B-2-1)	C + 05 sec	1225:54	1225:54
b. CC&S commands stop 1st pitch maneuver	Item 61a + 1 sec	1225:55	—
c. CC&S commands start yaw maneuver (B-2-1)	C + 9.5 min	1235:19	1235:19

[f] Times are based on command message sent to the DSIF initiating this sequence.

[K] Times are based upon observed spacecraft/Agena separation time.

[l] Predicted times in the terminal sequence are based on CC&S design and stored commands entered by ground command. Mechanization of the event coder does not permit the readout of a B-2-1 event occurring 1 sec after a first B-2-1 event.

[J] Based on fourth postmidcourse orbit computed about 4 hr before impact.

Spacecraft flight events	Nominal mission time	Predicted GMT	Actual GMT
Flight Events			
d. CC&S commands stop yaw maneuver	Item 61c + 1 sec	1235:20	—
e. CC&S commands start 2nd pitch maneuver (B-2-1)	C + 26.5 min	1252:19	1252:19
f. CC&S commands stop 2nd pitch maneuver	Item 61e + 1 sec	1252:20	—
g. Telemetry mode IV	Item 61e + 1 sec	1252:20	—
62. TV clock commands F-chain warmup	S + 67¾ hr	1307:36[K]	1307:15
63. F-chain on full power	Item 62 + 80 sec	1308:35	1308:35
64. CC&S commands TV on (warmup)	C + 45 min	1310:49	1310:49
a. P-chain in warmup	C + 45 min	1310:49	1310:49
65. P-chain on full power	Item 64 + 80 sec	1312:09	1312:09
66. CC&S commands TV on full power (backup)	C + 50 min	1315:49	1315:48
67. Spacecraft impacts Moon	—	1325:49[J]	1325:49

APPENDIX B

Summary of Redesign Following *Ranger VI*

I. SPACECRAFT BUS

Design changes approved for the spacecraft were limited to those which provided a significant reliability improvement. The most significant changes were those required to interface with the TV Subsystem.

A. TV Interface

1. Rewire hydraulic timer to provide TV-enable function at separation + 30 min.
2. Rewire solar-panel actuation microswitch to provide redundant enabling to TV subsystem.
3. Modify spacecraft wiring to accommodate enabling functions.
4. Rewire RTC-7 relay to use separate sets of contacts for the two sides of the TV subsystem.

B. Launch Complex and System-Test Complex: TV Interface

1. Separate full-power inhibit for each side of TV to umbilical J-box.
2. Transfer wire in System Test J-box to provide spacecraft/TV-OSE compatibility.
3. Add isolation resistors to OSE power-monitor J-box.

C. Non-TV-Related Spacecraft Bus Items

1. Add Earth-sensor thermal shield.
2. Delete midcourse motor chamber temperature sensor (to protect eight other temperature measurements).
3. Reconnect CC&S to provide reset capability so that midcourse maneuver can be re-initiated after being inhibited by RTC-8.

II. TV SUBSYSTEM

The following areas were affected during the redesign cycle:

A. Command and Control Circuits and Umbilical Functions.

B. Telemetry—Mode of Operation and Data Points.

C. Control Programmer and Camera Sequencer.

D. Communications.

E. Harness.

F. Thermal Control.

G. Packaging.

The general philosophy for the design changes was to optimize in the allotted time schedule certain areas to increase the probability of mission success. The basic approach was to:

1. Simplify the command and control circuitry;
2. Isolate the two channels, P and F, where feasible;
3. Optimize telemetry mechanization and data information;
4. Incorporate means of preventing premature system turn-on, i.e., during launch phase and reduce susceptibility of system to transients;
5. Eliminate all unnecessary hardline umbilical wiring;
6. Change thermal control as a result of *Ranger VI* high temperature profile;
7. Coat any remaining exposed terminals and pins, and improve mechanical integrity of overall system package;
8. Review system assembly venting characteristics.

A. Command and Control Circuitry—Interface Aspects

1. Eliminated command switch and power control unit. Functions combined in one unit: command control unit (CCU). Eliminated emergency mode operation. Change commands to single function only:

a. RTC-7 utilized only to turn system on. Utilizes separate contacts on bus RTC-7 relay to turn on P and F channels separately.

b. RTC-5 utilized only to turn system off. Channels F and P diode-isolated. A secondary function of

RTC-5 is to turn off the backup clock; this function cannot be employed until after separation + 32 hr has occurred, due to an inhibit function circuit.

2. *SCR gate ground.* The SCR gate ground path for SCR turn-on has been routed through relay contacts in the bus. The contacts (two redundant functions) are held open until separation + 30 min (BUCT) and/or Launch + 61 min (solar panel microswitch). These functions also redundantly turn on cruise mode, if cruise mode became disabled during launch phase.

3. Reduced-power functions are split, so that each channel is separately tied to ground in the J-box.

4. Eliminated hardline umbilical command functions. Remaining functions are:

a. Battery monitor line and return (3 wires) have 10K resistors in series.

b. Reduced-power P and F lines (2 wires).

c. Cruise-mode telemetry on and off (2 wires).

d. TV-on enable.

5. CC&S warmup and full-power commands remain the same, except latching aspect removed via circuits in HCVR circuits, so that system can be turned off (RTC-5) if failure occurs in CC&S functions.

6. *Clock output.* The clock output is now inhibited via self-inhibit function until separation + 32 hr and cannot be turned off by RTC-5 before that time. RTC-5 can therefore be used for its original function of data-mode change backup or for turning off the TV after an inadvertent turn-on without disabling the clock function.

7. Clock-start remains unchanged with turn-on occurring at separation.

8. *Desensitized SCR switches.* In order to minimize an inadvertent turn-on of either channel of the subsystem:

a. A 0.1-μf capacitor has been connected from gate to cathode on the SCR's to permit the cathode and gate to vary in unison to rapid external stimuli in the event of transients.

b. Normally closed contacts of relays K1 and K2 in the HCVR's are connected in series between the gate and the cathode of the SCR's. With this arrangement, the cathode and gate are permitted to vary in unison at low frequencies without causing SCR turn-on: The relay contacts are opened when RTC-7 or CC&S warm-up or clock-on (F only) is given.

c. A 0.1-μf capacitor and 47-ohm resistor in series shunts the SCR cathode to anode, decreasing transients across the SCR. Also, 30K resistor in series from the battery dampens transients.

d. Components of the SCR desensitizing circuits have been located in close proximity to the SCR's to increase the reliability of this circuit and decrease susceptibility to transients.

B. Telemetry

1. Change mechanization of operation so that:

a. Cruise-mode telemetry is activated prior to launch and remains on through the launch phase, energized through the umbilical leads.

b. Whenever the system is changed from the cruise mode to the warmup mode, the 90-point telemetry is transmitted over the bus Channel 8 system. The 15-point cruise telemetry is then transmitted over Channel F when the system goes to full power.

2. Add Current Sensor Unit to monitor the F and P battery currents.

3. Changed scale factor on significant telemetry points in HCVR and LCVR, i.e., battery voltages, HCVR-regulated voltage output.

4. Changed measurement circuit to give more meaningful data, i.e., Video Combiner, Clock Increments, Sequencer.

5. Interchange points between 15- and 90-point commutators to give more operational data.

6. Better overall telemetry calibration procedures.

C. Control Programmer and Camera Sequencer

1. Changed 5 min warmup to 80 sec in sequencer counter output chain.

2. Telemetry change per item B.4 above.

3. Changed manual reset function from flip-flop reset to full-power relay inhibit. Flip-flops were susceptible to noise.

4. Redundantized full-power command relay contacts.

D. Communications

1. Removed K1 (emergency-mode relay) from modulator circuits.

2. Added insulation in critical areas, such as between transistor and chassis in the transmitter power supply.

3. Added regulator circuit to telemetry chassis to permit telemetry to run from either unregulated battery supply (diode-isolated).

E. Harness

1. General changes necessitated by previously discussed system design changes.

2. Eliminated or changed where feasible:

a. Unnecessary routing through boxes.

b. Connector wiring where signal pins were adjacent to ground pins and where the two channels, P and F, were adjacent.

c. Dependence of both channels, P and F, on the same wire or path.

F. Thermal Control

1. Changed overall thermal pattern to give low temperature profile in cruise and during terminal based on *Ranger VI* mission temperature profile.

G. Packaging

1. Conformal coated exposed terminals.

2. Spot-bonded elements subject to vibration effects such as relays, cable routing in assemblies, etc.

3. Potted connector pins on the assemblies.

4. Pin retention techniques.

5. Mechanical design.

6. Review of assembly venting.

APPENDIX C

Ranger Spacecraft Configuration and Interfaces

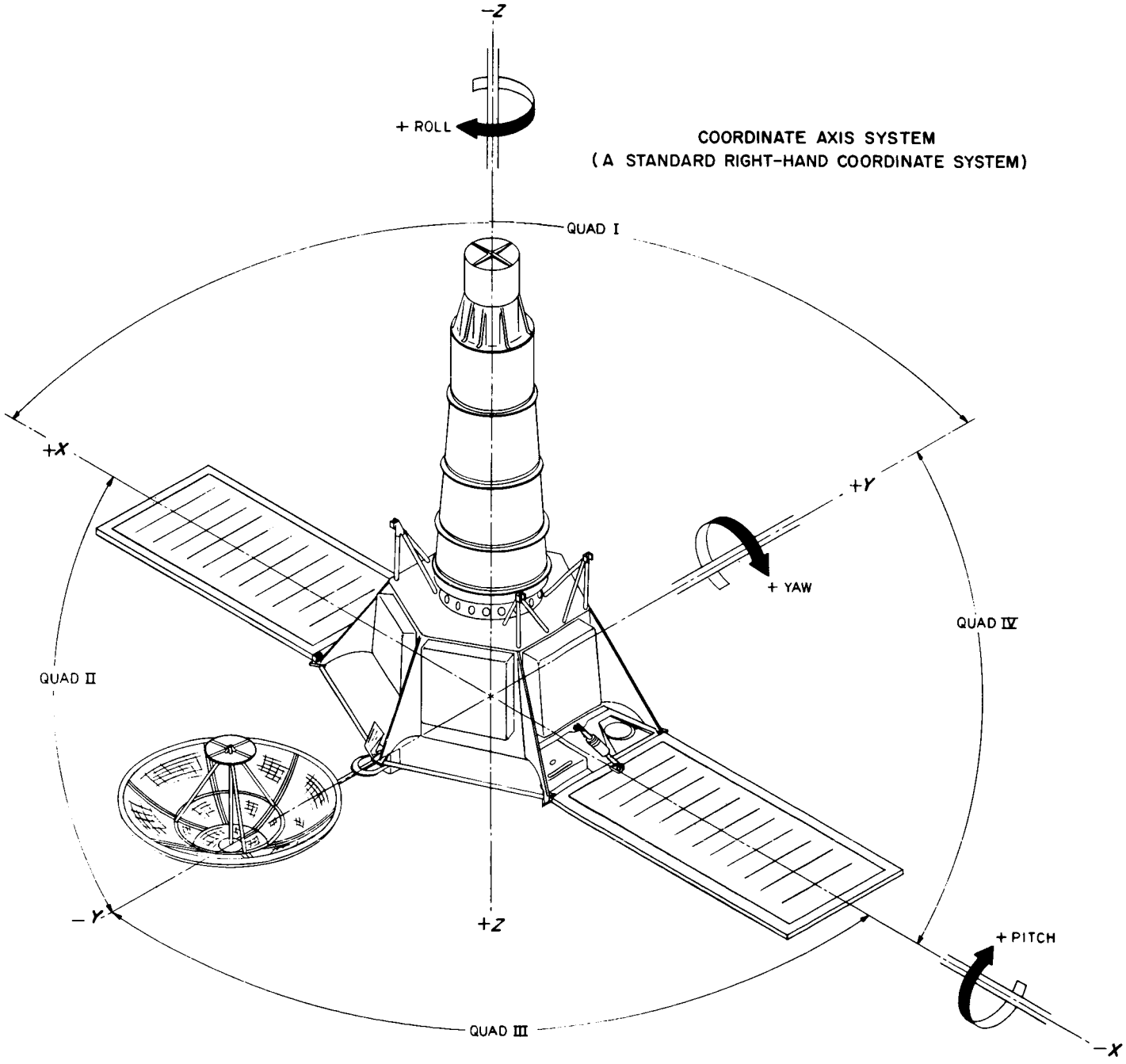

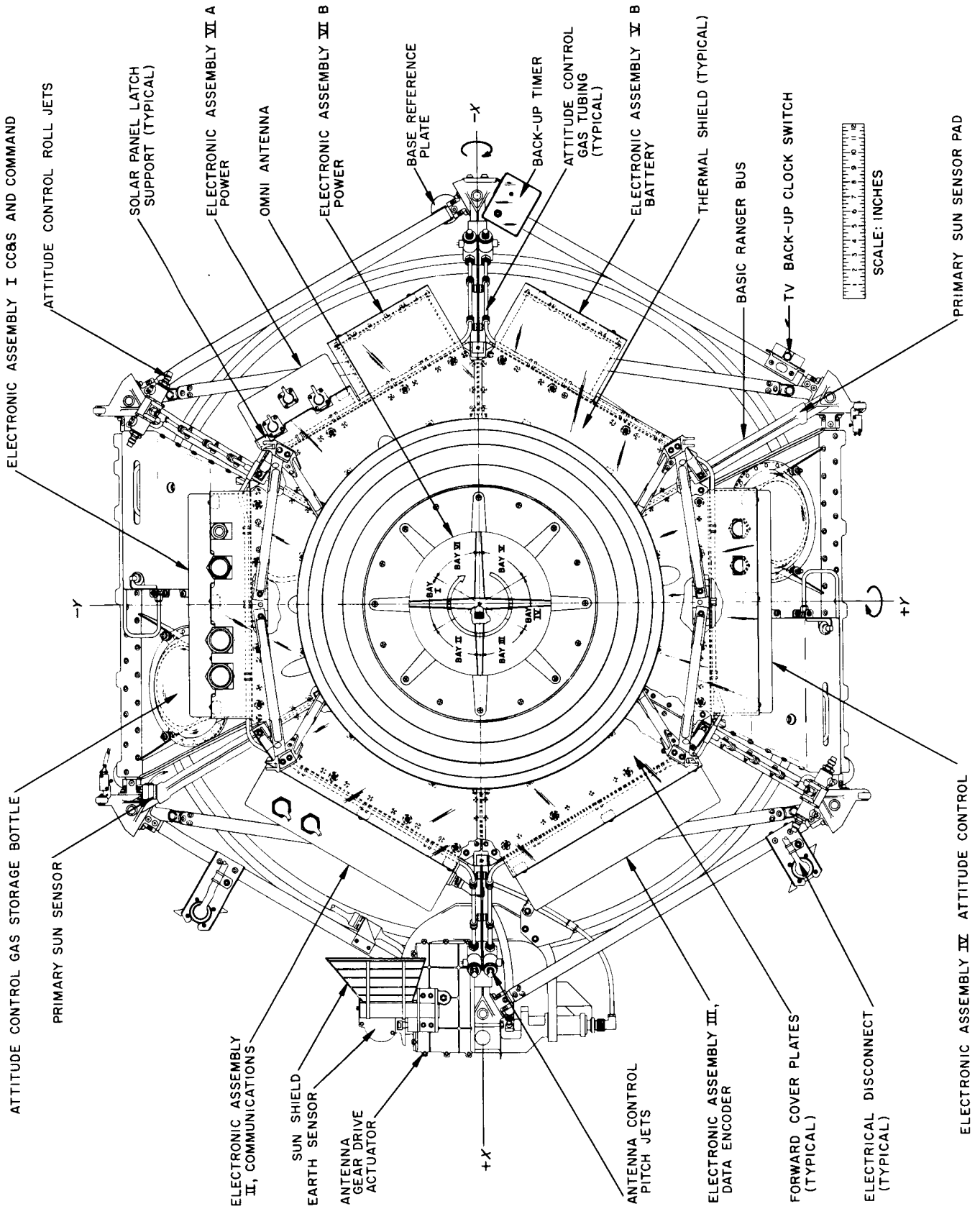
ELECTRONIC ASSEMBLY I CC&S AND COMMAND
ATTITUDE CONTROL ROLL JETS
SOLAR PANEL LATCH SUPPORT (TYPICAL)
ELECTRONIC ASSEMBLY VI A POWER
OMNI ANTENNA
ELECTRONIC ASSEMBLY VI B POWER
BASE REFERENCE PLATE
BACK-UP TIMER
ATTITUDE CONTROL GAS TUBING (TYPICAL)
ELECTRONIC ASSEMBLY V B BATTERY
THERMAL SHIELD (TYPICAL)
BASIC RANGER BUS
TV BACK-UP CLOCK SWITCH
SCALE: INCHES
PRIMARY SUN SENSOR PAD
ATTITUDE CONTROL GAS STORAGE BOTTLE
PRIMARY SUN SENSOR
ELECTRONIC ASSEMBLY II, COMMUNICATIONS
SUN SHIELD
EARTH SENSOR
ANTENNA GEAR DRIVE ACTUATOR
ANTENNA CONTROL PITCH JETS
ELECTRONIC ASSEMBLY III, DATA ENCODER
FORWARD COVER PLATES (TYPICAL)
ELECTRICAL DISCONNECT (TYPICAL)
ELECTRONIC ASSEMBLY IV ATTITUDE CONTROL
BAY I
BAY II
BAY III
BAY IV
BAY V
BAY VI
-Y
+Y
-X
+X

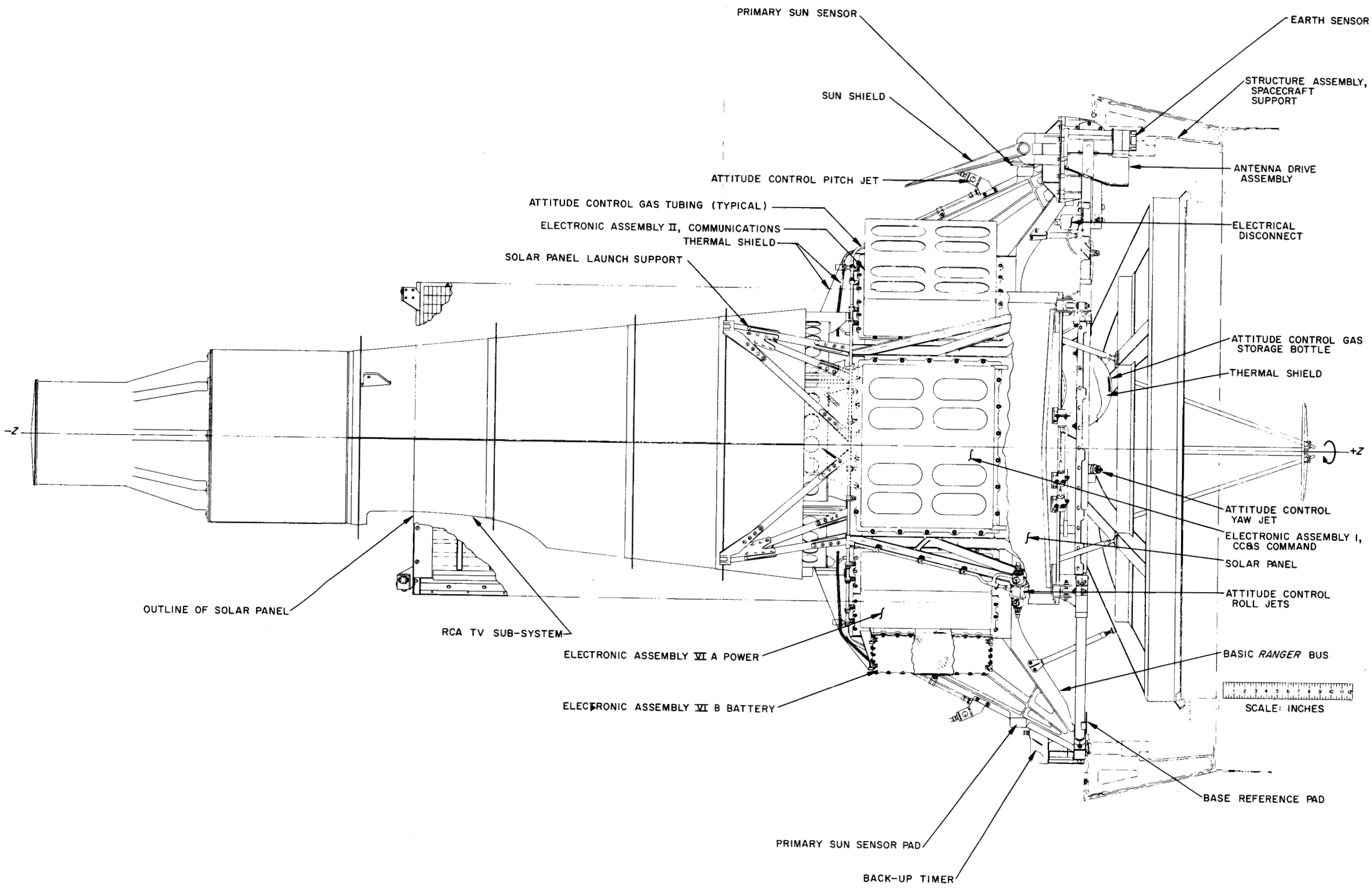
PRIMARY SUN SENSOR
EARTH SENSOR
SUN SHIELD
STRUCTURE ASSEMBLY, SPACECRAFT SUPPORT
ATTITUDE CONTROL PITCH JET
ANTENNA DRIVE ASSEMBLY
ATTITUDE CONTROL GAS TUBING (TYPICAL)
ELECTRONIC ASSEMBLY II, COMMUNICATIONS
THERMAL SHIELD
ELECTRICAL DISCONNECT
SOLAR PANEL LAUNCH SUPPORT
ATTITUDE CONTROL GAS STORAGE BOTTLE
THERMAL SHIELD
-Z
+Z
ATTITUDE CONTROL YAW JET
ELECTRONIC ASSEMBLY I, CC&S COMMAND
SOLAR PANEL
ATTITUDE CONTROL ROLL JETS
OUTLINE OF SOLAR PANEL
RCA TV SUB-SYSTEM
ELECTRONIC ASSEMBLY VI A POWER
BASIC RANGER BUS
ELECTRONIC ASSEMBLY VI B BATTERY
SCALE: INCHES
BASE REFERENCE PAD
PRIMARY SUN SENSOR PAD
BACK-UP TIMER

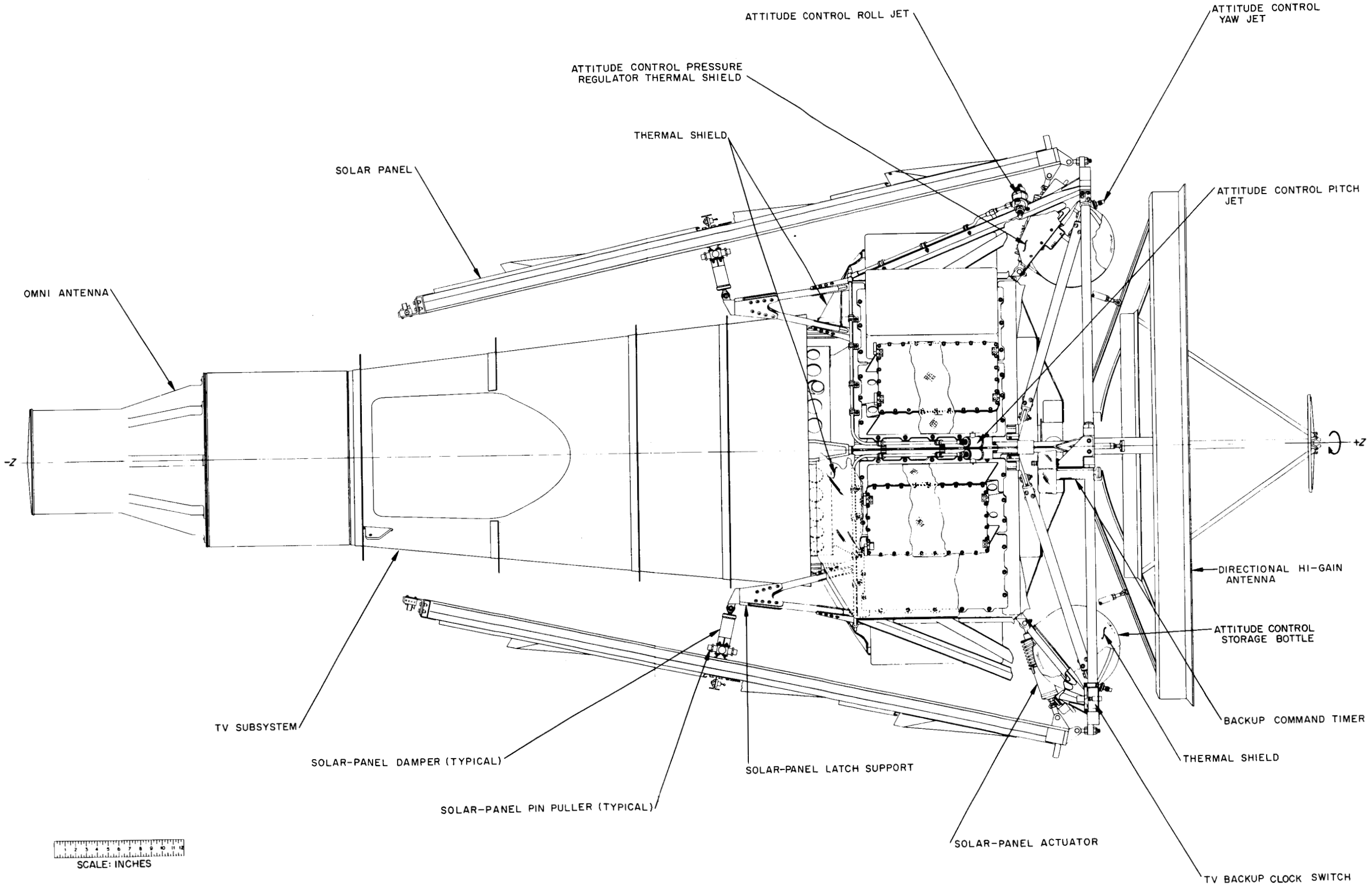
ATTITUDE CONTROL ROLL JET
ATTITUDE CONTROL YAW JET
ATTITUDE CONTROL PRESSURE REGULATOR THERMAL SHIELD
THERMAL SHIELD
SOLAR PANEL
ATTITUDE CONTROL PITCH JET
OMNI ANTENNA
-Z
+Z
DIRECTIONAL HI-GAIN ANTENNA
ATTITUDE CONTROL STORAGE BOTTLE
BACKUP COMMAND TIMER
THERMAL SHIELD
TV SUBSYSTEM
SOLAR-PANEL DAMPER (TYPICAL)
SOLAR-PANEL LATCH SUPPORT
SOLAR-PANEL PIN PULLER (TYPICAL)
SOLAR-PANEL ACTUATOR
TV BACKUP CLOCK SWITCH
SCALE: INCHES

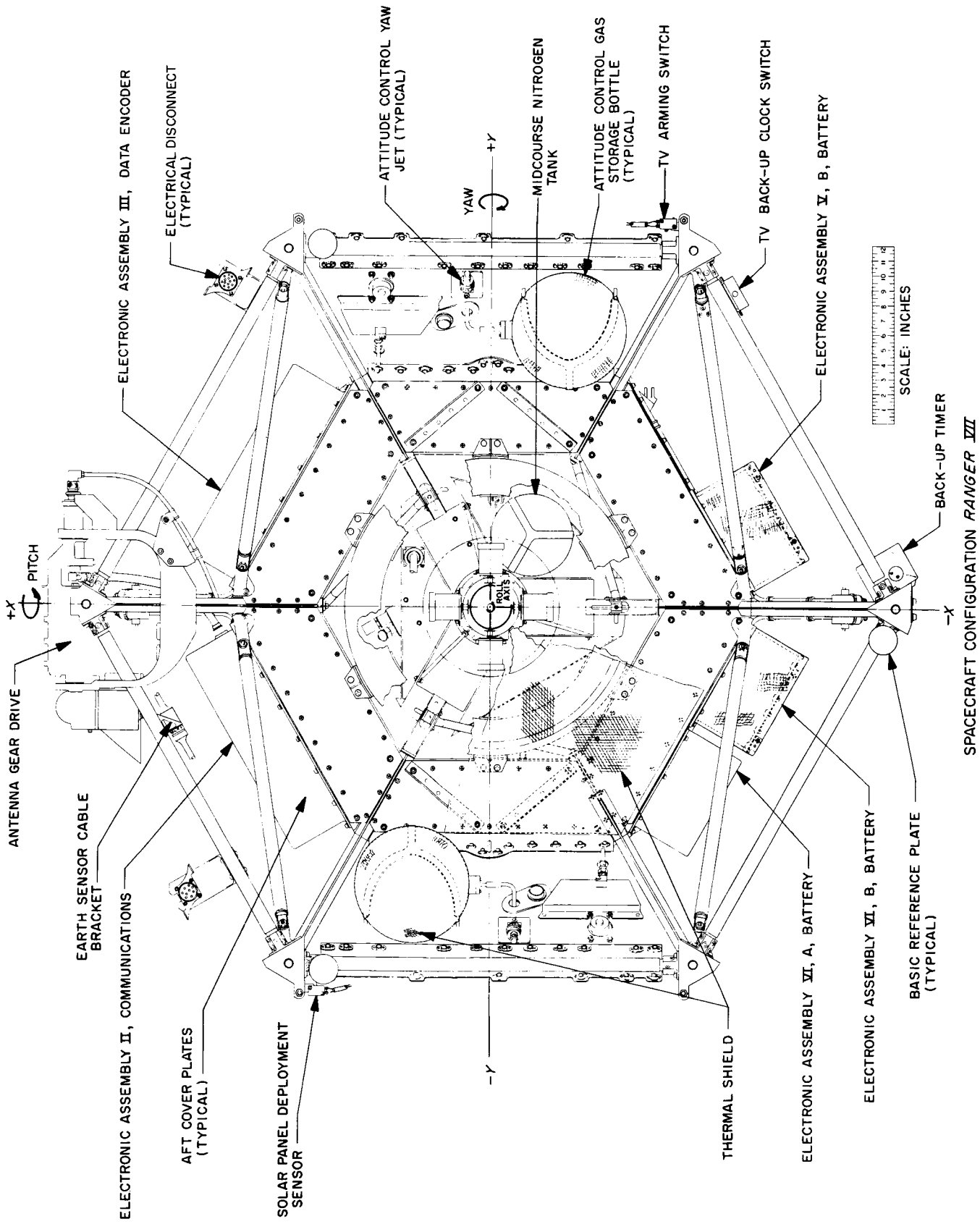

SPACECRAFT CONFIGURATION *RANGER VIII*

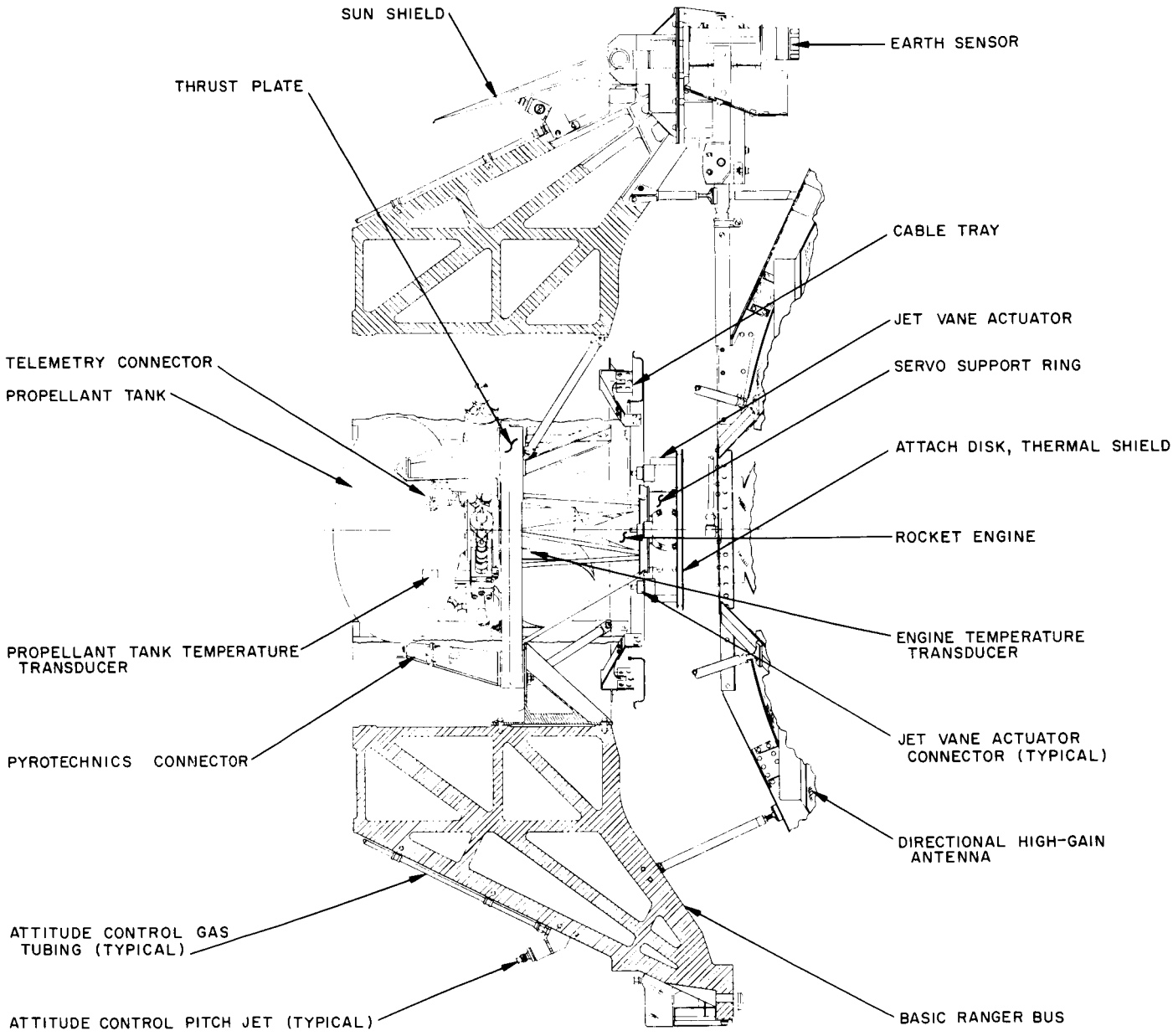
SUN SHIELD
EARTH SENSOR
THRUST PLATE
CABLE TRAY
JET VANE ACTUATOR
TELEMETRY CONNECTOR
SERVO SUPPORT RING
PROPELLANT TANK
ATTACH DISK, THERMAL SHIELD
ROCKET ENGINE
ENGINE TEMPERATURE TRANSDUCER
PROPELLANT TANK TEMPERATURE TRANSDUCER
JET VANE ACTUATOR CONNECTOR (TYPICAL)
PYROTECHNICS CONNECTOR
DIRECTIONAL HIGH-GAIN ANTENNA
ATTITUDE CONTROL GAS TUBING (TYPICAL)
ATTITUDE CONTROL PITCH JET (TYPICAL)
BASIC RANGER BUS

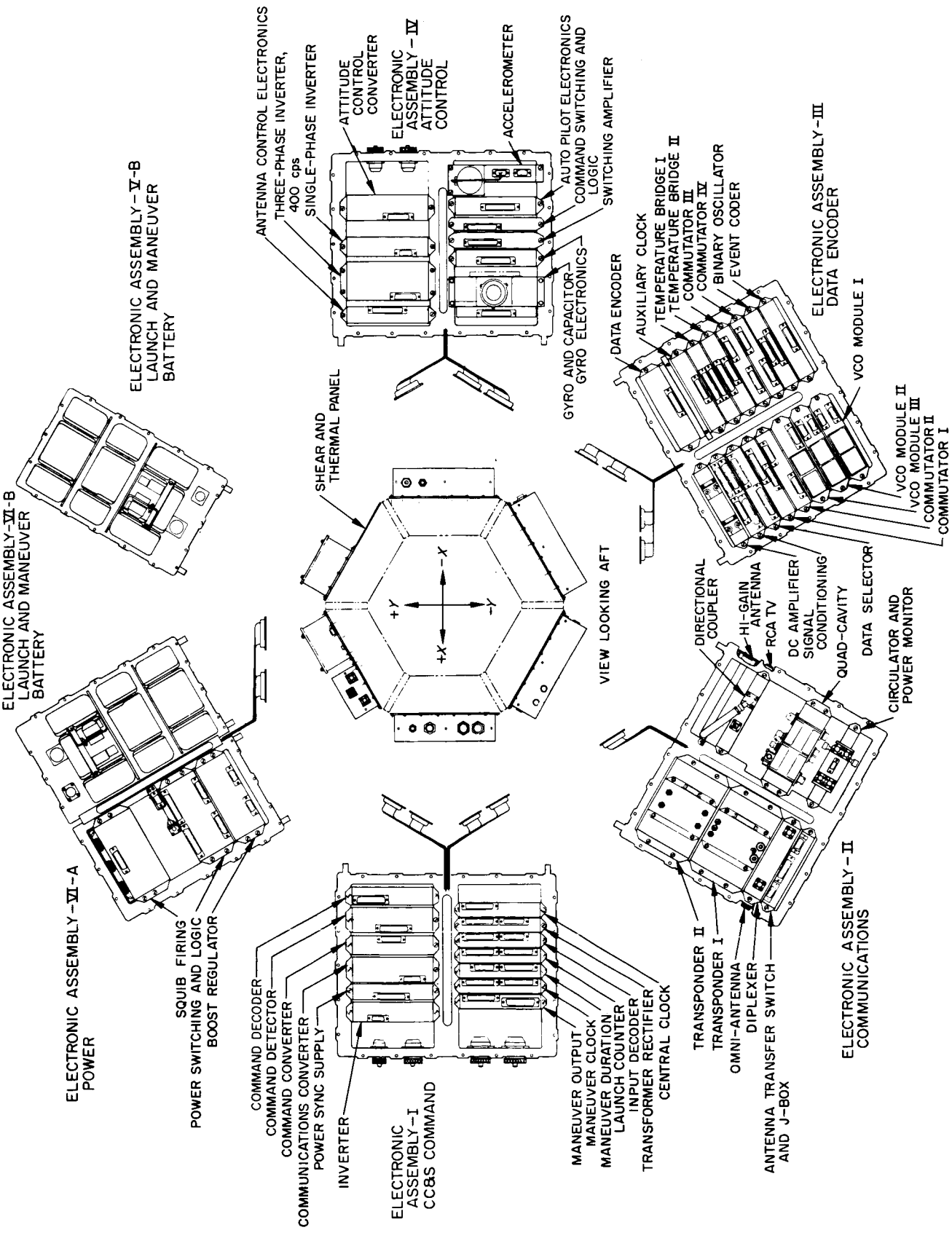
ELECTRONIC ASSEMBLY-VI-A
POWER
SQUIB FIRING
POWER SWITCHING AND LOGIC
BOOST REGULATOR
ELECTRONIC ASSEMBLY-VI-B
LAUNCH AND MANEUVER
BATTERY
ELECTRONIC ASSEMBLY-V-B
LAUNCH AND MANEUVER
BATTERY
ANTENNA CONTROL ELECTRONICS
THREE-PHASE INVERTER, 400 cps
SINGLE-PHASE INVERTER
ATTITUDE CONTROL CONVERTER
ELECTRONIC ASSEMBLY-IV
ATTITUDE CONTROL
ACCELEROMETER
AUTO PILOT ELECTRONICS
COMMAND SWITCHING AND LOGIC
SWITCHING AMPLIFIER
GYRO AND CAPACITOR GYRO ELECTRONICS
SHEAR AND THERMAL PANEL
VIEW LOOKING AFT
+Y
-Y
+X
-X
DATA ENCODER
AUXILIARY CLOCK
TEMPERATURE BRIDGE I
TEMPERATURE BRIDGE II
COMMUTATOR III
COMMUTATOR IV
BINARY OSCILLATOR
EVENT CODER
ELECTRONIC ASSEMBLY-III
DATA ENCODER
VCO MODULE I
VCO MODULE II
VCO MODULE III
COMMUTATOR II
COMMUTATOR I
DIRECTIONAL COUPLER
HI-GAIN ANTENNA
RCA TV
DC AMPLIFIER
SIGNAL CONDITIONING
QUAD-CAVITY
DATA SELECTOR
CIRCULATOR AND POWER MONITOR
ELECTRONIC ASSEMBLY-II
COMMUNICATIONS
TRANSPONDER II
TRANSPONDER I
OMNI-ANTENNA
DIPLEXER
ANTENNA TRANSFER SWITCH AND J-BOX
ELECTRONIC ASSEMBLY-I
CC&S COMMAND
COMMAND DECODER
COMMAND DETECTOR
COMMAND CONVERTER
COMMUNICATIONS CONVERTER
POWER SYNC SUPPLY
INVERTER
MANEUVER OUTPUT
MANEUVER CLOCK
MANEUVER DURATION
LAUNCH COUNTER
INPUT DECODER
TRANSFORMER RECTIFIER
CENTRAL CLOCK

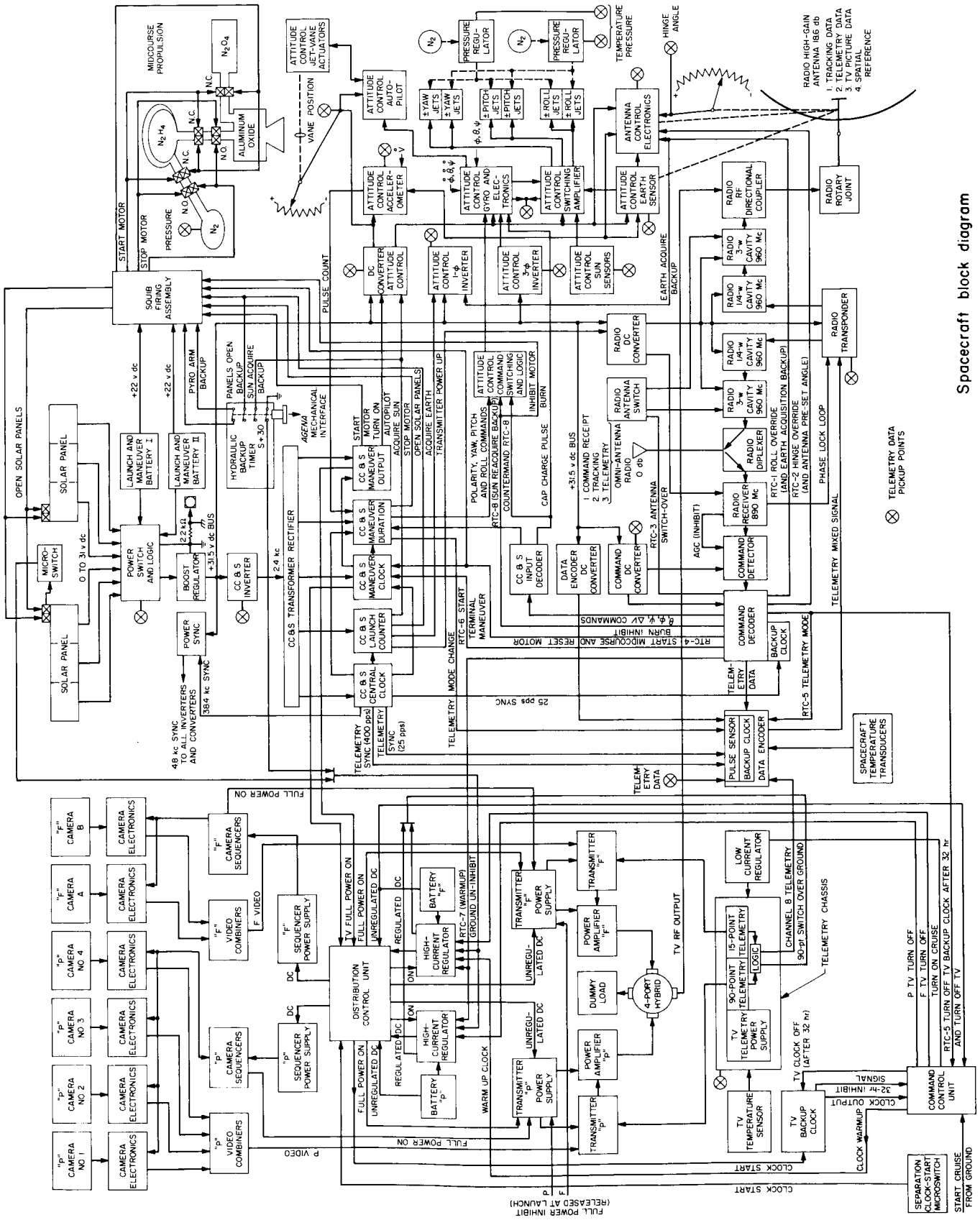
Spacecraft block diagram
TELEMETRY DATA PICKUP POINTS
MIDCOURSE PROPULSION
START MOTOR
STOP MOTOR
PRESSURE
ALUMINUM OXIDE
ATTITUDE CONTROL JET-VANE ACTUATORS
VANE POSITION
ATTITUDE CONTROL AUTO-PILOT
ATTITUDE CONTROL ACCELER-OMETER
ATTITUDE CONTROL GYRO AND ELEC-TRONICS
ATTITUDE CONTROL SWITCHING AMPLIFIER
PRESSURE REGU-LATOR
TEMPERATURE PRESSURE
HINGE ANGLE
ANTENNA CONTROL ELECTRONICS
ATTITUDE CONTROL EARTH SENSOR
RADIO HIGH-GAIN ANTENNA 186 db
1. TRACKING DATA
2. TELEMETRY DATA
3. TV PICTURE DATA
4. SPATIAL REFERENCE
RADIO ROTARY JOINT
RADIO RF DIRECTIONAL COUPLER
RADIO 3-w CAVITY 960 Mc
RADIO 1/4-w CAVITY 960 Mc
RADIO TRANSPONDER
RADIO DC CONVERTER
RADIO ANTENNA SWITCH
RADIO DIPLEXER
RADIO RECEIVER 890 Mc
COMMAND DETECTOR
COMMAND DECODER
BACKUP CLOCK
PULSE SENSOR
BACKUP CLOCK
DATA ENCODER
SPACECRAFT TEMPERATURE TRANSDUCERS
TELEMETRY MIXED SIGNAL
PHASE LOCK LOOP
RTC-1 ROLL OVERRIDE (AND EARTH ACQUISITION BACKUP)
RTC-2 HINGE OVERRIDE (AND ANTENNA PRE-SET ANGLE)
RTC-3 ANTENNA SWITCH-OVER
RTC-4 START MIDCOURSE AND RESET MOTOR BURN INHIBIT
RTC-5 TELEMETRY MODE
RTC-6 START TERMINAL MANEUVER
RTC-7 (WARMUP) GROUND UN-INHIBIT
RTC-8 (SUN REACQUIRE BACKUP) COUNTERMAND RTC-8
OMNI-ANTENNA RADIO 0 db
+31.5 v dc BUS
1. COMMAND RECEIPT
2. TRACKING
3. TELEMETRY
CAP CHARGE PULSE
INHIBIT MOTOR BURN
ATTITUDE CONTROL COMMAND SWITCHING AND LOGIC
POLARITY, YAW, PITCH AND ROLL COMMANDS
OPEN SOLAR PANELS
ACQUIRE EARTH
TRANSMITTER POWER UP
ACQUIRE SUN
STOP MOTOR
START MOTOR TURN ON
AUTOPILOT
CC & S MANEUVER OUTPUT
CC & S MANEUVER DURATION
CC & S MANEUVER CLOCK
CC & S LAUNCH COUNTER
CC & S CENTRAL CLOCK
CC & S INPUT DECODER
DATA ENCODER DC CONVERTER
COMMAND DC CONVERTER
CC & S INVERTER
CC & S TRANSFORMER RECTIFIER
POWER SYNC
BOOST REGULATOR
POWER SWITCH AND LOGIC
MICRO-SWITCH
SOLAR PANEL
LAUNCH AND MANEUVER BATTERY I
LAUNCH AND MANEUVER BATTERY II
HYDRAULIC BACKUP TIMER
PANELS OPEN BACKUP
SUN ACQUIRE BACKUP
PYRO ARM BACKUP
SQUIB FIRING ASSEMBLY
AGENA MECHANICAL INTERFACE
DC CONVERTER ATTITUDE CONTROL
ATTITUDE CONTROL 1-φ INVERTER
ATTITUDE CONTROL 2-φ INVERTER
ATTITUDE CONTROL SUN SENSORS
EARTH ACQUIRE BACKUP
PULSE COUNT
+22 v dc
0 TO 31 v dc
2.4 kc
2.2 kΩ
384 kc SYNC
48 kc SYNC TO ALL INVERTERS AND CONVERTERS
TELEMETRY SYNC (400 pps)
TELEMETRY SYNC (25 pps)
25 pps SYNC
TELEMETRY MODE CHANGE
TELEM-ETRY DATA
AGC (INHIBIT)
CHANNEL 8 TELEMETRY
90-pt SWITCH OVER GROUND
TELEMETRY CHASSIS
15-POINT TELEMETRY LOGIC
90-POINT TELEMETRY
TV TELEMETRY POWER SUPPLY
LOW CURRENT REGULATOR
TV RF OUTPUT
4-PORT HYBRID
DUMMY LOAD
TRANSMITTER "F"
TRANSMITTER "P"
TRANSMITTER "Pb"
TRANSMITTER "F" POWER SUPPLY
TRANSMITTER "P" POWER SUPPLY
POWER AMPLIFIER "F"
POWER AMPLIFIER "P"
HIGH-CURRENT REGULATOR
BATTERY "F"
BATTERY "P"
UNREGU-LATED DC
REGULATED DC
DISTRIBUTION CONTROL UNIT
FULL POWER ON
UNREGULATED DC
TV FULL POWER ON
WARM UP CLOCK
CAMERA SEQUENCERS
SEQUENCER POWER SUPPLY
VIDEO COMBINERS
F VIDEO
P VIDEO
CAMERA ELECTRONICS
CAMERA NO 1
CAMERA NO 2
CAMERA NO 3
CAMERA NO 4
CAMERA A
CAMERA B
TV TEMPERATURE SENSOR
TV BACKUP CLOCK
TV CLOCK OFF (AFTER 32 hr)
32-hr INHIBIT
CLOCK OUTPUT
SIGNAL
CLOCK WARMUP
CLOCK START
COMMAND CONTROL UNIT
P TV TURN OFF
F TV TURN OFF
TURN ON CRUISE
RTC-5 TURN OFF TV BACKUP CLOCK AFTER 32 hr AND TURN OFF TV
SEPARATION CLOCK-START MICROSWITCH
START CRUISE FROM GROUND
FULL POWER INHIBIT (RELEASED AT LAUNCH)

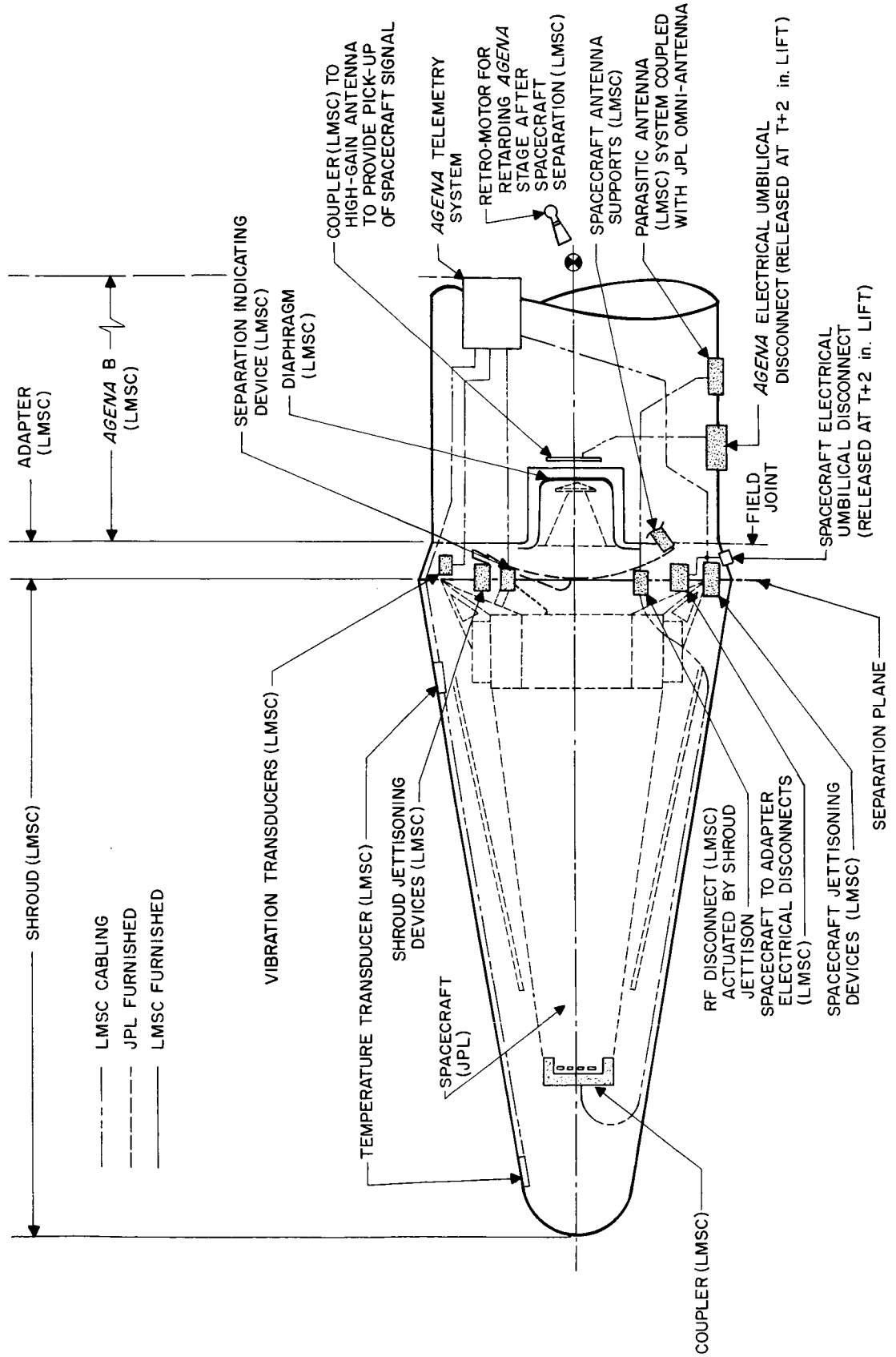

Spacecraft/*Agena* interface

BIBLIOGRAPHY

Project and Mission

Ranger Block III Project Development Plan. JPL Project Document No. 8, October 31, 1963.

(*Ranger* Block III) *Mission Operations Plan.* JPL PD-20, July 17, 1964.

Ranger Block III Project Policy and Requirements and Addendum No. 1. JPL EPD-65 Rev. 1, March 8, 1964.

Ranger VI Failure Analysis and Supporting Investigations. JPL EPD-205, March 27, 1964.

Ranger Block III Launch Constraints Planning Document. JPL Project Document No. 18, July 17, 1964.

Ranger 1964/1965. JPL, July 1964 (Brochure).

Ranger VII Photographs of the Moon: Part I, Camera A Series. NASA SP-61, September 1964.

Winneberger, R. A., *Postinjection Standard Trajectory, Ranger Block III, for June–July, July, August, 1964 Launch Periods.* JPL Project Document No. 16, June 15, 1964.

Hamilton, T., W. Wollenhaupt, R. Winneberger, A. Berman, E. Piaggi, and A. Liu, *Ranger 7 Flight Path and Its Determination from Tracking Data.* JPL Technical Report No. 32-694, in press.

Spacecraft System

(*Ranger* Block III) Spacecraft Design Specifications. JPL RO-64-69, June 6, 1963. Includes 30 specifications, revised, various dates.

Ranger Block III TV Subsystem Design Plan and Environmental Test Plan. RCA Astro-Electronics Division, AED-R-1910, May 15, 1963.

(Ranger VII) Test and Operations Plan. JPL TOP 3R001, April 6, 1964.

(Ranger VII) System Test and Operations Report. JPL STOR R7001, September 25, 1964.

(Ranger VII) Test Results Summary, and *Flight Environmental Dynamic and Acoustic Data Report.* (JPL Environmental Requirements Section).

Benson, M. A., and D. Williams, *Description and Flight Analysis of Ranger 7 TV Subsystem.* JPL Technical Report No. 32-680, December 1, 1964.

Turk, W., *Ranger Block III Attitude Control System.* JPL Technical Report No. 32-663, November 15, 1964.

Launch Vehicle System

See: *Medium Space Vehicle Programs Bibliography.* Lockheed A602037-A, June 30, 1964.

Project Agena/Ranger 7 Flash Flight Report, T+8 hr. NASA Goddard Launch Operations Branch GLOR-105, July 28, 1964 (SECRET)

BIBLIOGRAPHY (Cont'd)

Preliminary Flight Test Report—Mod III Guidance System. G. E./Burroughs ET-64-67072, July 28, 1964 (SECRET).

Ranger 7 Launch Report. Lockheed B040513, August 14, 1964 (SECRET).

(Ranger VII) Flight Test Evaluation Report. General Dynamics/Astronautics.

Ranger VII 30-Day Postflight Report. Space Technology Laboratories 8679-60051 -TC-000, August 25, 1964 (Confidential).

Evaluation Report of Mod III Radio Guidance and Instrumentation System with Launch Vehicle 250D, RA-7. General Electric GE-64H-200, August 28, 1964 (SECRET).

Flight Evaluation and Performance Analysis for Ranger VII Mission. Lockheed LMSC-A605114, September 10, 1964 (Confidential).

Deep Space Network

(Ranger VII) Tracking Instruction Manual. JPL EPD-202, May 4, 1964.

(Ranger VII) Tracking Systems Data Analysis Report. JPL, August 14, 1964.

(Ranger VII) Tracking Operations Memorandum. JPL EPD-219, September 14, 1964.

(Ranger VII) Operations Analysis Report. JPL EPD, to be published.

Space Flight Operations

(Ranger Block III) Space Flight Operations Plan. JPL EPD-78, Rev. 4, May 28, 1964.

(*Ranger VII* Space Flight Operations) *Capabilities and Procedures.* JPL EPD-143, July 20, 1964.

(Ranger VII) Space Flight Operations Memorandum. JPL EPD-242, October 12, 1964.